
[All ETDs from UAB](#)

[UAB Theses & Dissertations](#)

2015

Functional Role Of Mepe In Tooth Mineralization: Mediation By Tgf-Beta1

Angela Gullard
University of Alabama at Birmingham

Follow this and additional works at: <https://digitalcommons.library.uab.edu/etd-collection>

Recommended Citation

Gullard, Angela, "Functional Role Of Mepe In Tooth Mineralization: Mediation By Tgf-Beta1" (2015). *All ETDs from UAB*. 1808.
<https://digitalcommons.library.uab.edu/etd-collection/1808>

This content has been accepted for inclusion by an authorized administrator of the UAB Digital Commons, and is provided as a free open access item. All inquiries regarding this item or the UAB Digital Commons should be directed to the [UAB Libraries Office of Scholarly Communication](#).

FUNCTIONAL ROLE OF MEPE IN TOOTH MINERALIZATION: MEDIATION BY
TGF-BETA1

by

ANGELA GULLARD

SELVARANGAN PONNAZHAGAN, COMMITTEE CHAIR

XU FENG

MARY MACDOUGALL

DOBRAWA NAPIERALA

ROSA SERRA

A DISSERTATION

Submitted to the graduate faculty of The University of Alabama at Birmingham,
in partial fulfillment of the requirements for the degree of
Doctor of Philosophy

BIRMINGHAM, ALABAMA

2015

Copyright by
Angela Gullard
2015

FUNCTIONAL ROLE OF MEPE IN TOOTH MINERALIZATION: MEDIATION BY TGF-BETA1

ANGELA GULLARD

MOLECULAR AND CELLULAR PATHOLOGY

ABSTRACT

Transforming growth factor- β 1 (TGF- β 1) is one of the most abundant cytokines of the dentin-pulp complex that regulates a broad range of biological processes related to matrix synthesis and ultimately tooth formation, including secretion and mineralization of the dentin extracellular matrix (DECM). TGF- β 1 mediates odontoblast cytodifferentiation from precursor dental pulp cells, being up-regulated in odontoblasts and then incorporated into the DECM as a reservoir that can be utilized in times of mechanical, chemical, or bacterial insult. Formation of the DECM is modulated by the actions of small integrin-binding ligand N-linked glycoproteins (SIBLINGs), which include DMP-1, DSPP, BSP, SPP1, and MEPE, with MEPE being the least characterized member. Critical for phosphate regulation in the skeleton and dentition of mammals, MEPE has elevated expression during matrix mineralization. Transgenic *TGFB1* mice displaying the pathophysiology of Camurati-Engelmann disease (CED) demonstrated abnormal molar and incisor development. CED mouse molars displayed more profound defects with decreased mineralization and higher matrix porosity as compared to WT animal teeth. Analysis of CED primary dental pulp cell cultures revealed disrupted expression of TGF- β /BMP

signaling pathway and SIBLING genes. In an effort to define the events of tooth formation in which MEPE is critical, molars of *Mepe*^{-/-} mouse were assessed for DECM density and volume. Interestingly, *Mepe*^{-/-} mice exhibit increased bone mass with enhanced mineralization activity and increased dentin mineralization. A downstream target of TGF- β 1 signaling, MEPE is expressed during tooth formation by odontoblasts and is incorporated into the DECM. Immunohistochemical studies of dental tissues confirmed that MEPE is produced by incisor and molar odontoblasts. These data suggested that MEPE is secreted by mature odontoblasts during dentinogenesis. The molecular crosstalk between TGF- β 1 and SIBLING proteins, particularly MEPE, has been observed both *in vitro* and *in vivo*, including differentiation of odontoblasts, models of overexpression, and dental and skeletal mineralized tissue pathophysiology. Together, these data demonstrate that TGF- β 1 overexpression disrupts DECM formation, and that MEPE inhibits dentin mineralization. However, excessive TGF- β 1 levels may be mitigated by SIBLINGs and other TGF- β /BMP family members during tooth development. These studies provide insight into the mineralization defects associated with dentin dysplasia, dentinogenesis imperfecta, hypophosphatemia, and CED.

Keywords: TGF- β 1, Camurati-Engelmann disease, dentin extracellular matrix, MEPE, odontoblasts, dentin formation

DEDICATION

I dedicate this work to my mom, who has always been there for me since the beginning, cheering me on through both thick and thin, the strongest person I know, the most loyal advocate, the best friend I could ever hope for throughout all my endeavors in life. So much of me is made of what I learned from you!

“Let me tell you something you already know. The world ain't all sunshine and rainbows. It's a very mean and nasty place, and I don't care how tough you are it will beat you to your knees and keep you there permanently if you let it. You, me, or nobody is gonna hit as hard as life. But it ain't about how hard ya hit. It's about how hard you can get hit and keep moving forward. How much you can take and keep moving forward. That's how winning is done!” – Sylvester Stallone, *Rocky Balboa*, 2006

ACKNOWLEDGMENTS

First and foremost, I must thank my advisor, and director of the UAB DMD/PhD program, Dr. Mary MacDougall, for giving me a place in her laboratory and in the dual-degree program these past seven and a half years. I would like to thank my committee members for their guidance and patience with me as I completed my research studies concurrently with dental school. I am grateful for their invaluable advice on project direction and editing of my scientific writing. You all inspire me to do my best, and I am very appreciative of all the knowledge, time, and effort that you gave to me throughout my training: Dr. Selvarangan Ponnazhagan (Pons), Dr. Dobrawa Napierala, Dr. Rosa Serra, and Dr. Xu Feng. To my past committee members who either retired or departed UAB: Dr. Jay McDonald, Dr. Xu Cao, and Dr. Patricia DeVilliers – thank you for all of your wisdom and contributions to my education!

To Dr. Amjad Javed, for allowing me to shadow in his lab eight years ago and teaching me about Runx2 in mice, and for helping me retrieve my car one Saturday afternoon after it was towed from campus after a long day's work in the lab. To Dr. Scott Ballinger and my interview committee for believing in me and accepting me into the MCP Graduate Program despite my lack of research experience.

To all the members of Dr. Xu Cao's laboratory, my first research family, who trained me during a my first 3-month summer research experience, and then during a 6-month MCP rotation. I cherished each day I was able to spend working in your lab; your teachings of how to do science have never left me, and I hope one day our paths will

cross again. Special thanks are in order for Weiqi Lei, the Cao lab manager, who is one of the most loyal and best friends anyone could hope to have; to Dr. Xiangwei Wu who enabled me to participate in his studies via the “see one, teach one, do one” method and spent countless hours mentoring me in data interpretation and presentation; and to Dr. Xu Cao who met with me every Wednesday morning for six months to coach me along in my “CED mouse teeth studies,” which have recently been accepted for publication.

To all past and current members of the MacDougall lab – you made working 12-20 hour days in the 7th floor ice box (AKA lab) fun! I would like to especially recognize Dr. Olga Mamaeva – for your big heart, vast wisdom, and insightful answers to my many questions about how to do science - you were like my mom away from home. I wouldn’t be half as far in my journey if it weren’t for you! Dr. Ejvis Lamani, the first DMD/PhD student at UAB, I will always remember our days of working until the wee hours of the morning, only to drop each other off at our cars and meet in the lab again just five to seven hours later. Dr. Hope Amm, the determined post-doc, who will one day soon be running her own research lab. I will never forget our heart to heart conversations about life nor the laughter we created from the most trivial of topics. Dr. Stephen Greene, the sharp dentist from Howard, who somehow manages balancing family life with completing his own graduate research, I am always inspired by your collected aura and professional demeanor.

I also worked with many fine post-docs and visiting scholars, including Dr. Helena Rivera and Dr. Marina Gonçalves Diniz. I had the opportunity to mentor a number of summer research students, who taught me just as much about coaching as I

tried to teach them about molecular biology: Dr. Lauren Paul Dean, Dr. Susanna Pischek, Michael Guzelian, and Sam Huguley.

To Dr. Pons, who taught thirty-two of us budding scientists in the IBS course series in the fall of 2008 about hydrogen bonds in DNA helices, and throughout the past seven years, has been my mentor in the truest sense of the word.

To Dr. Jerome Higgs, Dr. Niroop Kaza, and Dr. Yanna Ding – thank you for all the laughs and words of encouragement we shared while trying to survive grad school. At last it is my turn to defend, and the last class of Pathology department graduate students ends their chapter.

To my fellow boneheads, Dr. Jason Ashley, Dr. Erin McCoy, Dr. Joel Jules, Dr. Helen Liu, and Dr. Angelina Ix-Ik' Londoño Joshi – how much I enjoyed and cherished our pumpkin-carving parties, Christmas parties, CMBD journal clubs, and MCP picnics. You shared with me your far-reaching knowledge, creativity, and generosity both inside and outside of the lab. I, the osteoblast, will forever be grateful for having met you!

I have been encouraged along the way for the past five years by my fellow dental classmates, members of the Class of 2014, Class of 2015, and now my soon-to-be graduating Class of 2016. Special thanks to fellow senior dental students Cherie Gu, Anny Su, Katie Bell, Jessie Chu, and Dane Grovenstein for your friendship throughout this incredible journey. To Dr. Mitra Adhami, my fellow DMD/PhD candidate in the dental Class of 2017, who experienced with me the ups and downs of the dual-degree program. Thank you for all the pep talks and lunch hours at Sitar.

I could not have achieved this milestone without the love, support, and guidance of my family, who kept me grounded and sane throughout all the sunny and rainy days.

Thank you for understanding all the holidays and family events I missed in the name of science. To my mom, one of the strongest people I know, who was a pillar of unwavering support, an open mind, and a keen ear when times were especially trying. To my brother who has given his constant support of my academic endeavors, despite his self-professed aversion to school. To all the cats, dogs, and guinea pigs in my life who stole my heart and reminded me about the simple, important things in life. To Marion, Mike, Paul, and Frances Avery for your enthusiasm and continuous support of my lengthy education. Last but certainly not least, to James Avery, my incredibly loving, supportive, and brilliant boyfriend of the past three and a half years who has witnessed both my joy and tears during this chapter in my life. Thank you for the tranquility you give me with your easy-going personality, words of wisdom, and for the seemingly endless supply of “brain food” in the form of high-quality dark chocolate bars.

Though scientific findings and theories may change, one thing remains certain – I would not be the same person if it weren’t for all of you, and many more whom I did not have space to mention. I am grateful for each and every one of you being in my life!

TABLE OF CONTENTS

<i>Figure</i>	<i>Page</i>
ABSTRACT.....	iii
DEDICATION.....	v
ACKNOWLEDGMENTS	vi
LIST OF FIGURES	xii
LIST OF ABBREVIATIONS.....	xiv
 CHAPTER	
1 INTRODUCTION	1
Signaling Cascades Involved in Tooth Formation	2
TGF- β /BMP superfamily signaling pathway.....	2
FGF signaling pathway	3
WNT signaling pathway	4
SHH signaling pathway	5
Tooth Biology	5
Dental anatomy and histology	5
Dental pulp.....	10
Odontoblasts	11
Dentinogenesis.....	13
Dentin extracellular matrix (DECM)	14
Types of dentin	15
Ameloblasts and amelogenesis	17
Root formation.....	19
Cementum	20
Periodontal ligament and alveolar bone.....	21
DECM Proteins	21

SIBLINGs	21
MEPE	22
ASARM peptide.....	24
TGF- β 1.....	24
Diseases of Bone and Dentin	26
Camurati-Engelmann disease.....	26
X-linked hypophosphatemic rickets	28
Dentinogenesis imperfecta and dentin dysplasia type II.....	29
Radicular dentin dysplasia	30
Current dentin disease therapies	32
Murine Models for Studying Tooth Formation	33
Summary and Dissertation Objective	34
2 REDUCED DENTIN MATRIX PROTEIN EXPRESSION IN CAMURATI-ENGELMANN DISEASE MOUSE MODEL	36
Abstract	37
Introduction.....	38
Materials and methods	39
Results.....	44
Discussion	48
References.....	53
3 MEPE LOCALIZATION IN THE CRANIOFACIAL COMPLEX AND FUNCTION IN TOOTH DENTIN FORMATION	64
Abstract	65
Introduction.....	66
Materials and methods	68
Results.....	73
Discussion	79
References.....	83
4 GENERAL DISCUSSION AND FUTURE DIRECTIONS	101
GENERAL LIST OF REFERENCES	107
APPENDIX: INSTITUTIONAL ANIMAL CARE AND USE COMMITTEE APPROVAL FORMS	120

LIST OF FIGURES

<i>Figure</i>	<i>Page</i>
1 - INTRODUCTION	
1 Anatomy of the tooth and its supporting structures	6
2 Morphogenetic events of molar tooth development	9
2 - REDUCED DENTIN MATRIX PROTEIN EXPRESSION IN CAMURATI- ENGELMANN DISEASE MOUSE MODEL	
1 Gross view and radiography of 28-day-old male littermates.....	56
2 Micro-computed tomographic (μ CT) 3D reconstructions of 28-day-old WT and CED littermate specimens.....	57
3 μ -CT 2D sagittal micrographs of WT and CED mandibular first molars harvested from 105-day-old male littermates	58
4 Primary cell culture morphology and growth kinetics.....	59
5 Quantitative reverse transcriptase PCR microarray performed using cDNA of incisor pulp cells harvested from 105-day-old WT and CED male littermates.	60
6 Quantitative reverse transcriptase PCR performed using cDNA derived from 105-day-old WT and CED male littermates.....	61
7 Immunohistochemistry of 3dPN and 9dPN WT and CED mouse incisors	62
8 Western blot analysis of activation of TGF- β signaling in mouse dental pulp (MD10 -A11) and mouse odontoblast-like (MD10-A2 and MO6-G3) cell lines	63

3 - MEPE LOCALIZATION IN THE CRANIOFACIAL COMPLEX AND FUNCTION IN TOOTH DENTIN FORMATION

1	<i>In situ</i> hybridization of <i>Mepe</i> expression in molar crown and root development	90
2	Immunohistochemical analyses of MEPE in 3PN mouse dental tissues and alveolar bone of undecalcified mandibular sections.....	91
3	Immunolabeled bone cells and matrix in undecalcified sections of mouse calvarial bone	93
4	Radiographic analysis of day 3PN WT and <i>Mepe</i> ^{-/-} cranial halves; representative of 3 sets of specimens	95
5	Histological analysis of day 3PN <i>Mepe</i> ^{-/-} first molars	97
6	qRT-PCR analysis of gene expression fold change in <i>Mepe</i> ^{-/-} mouse whole tooth cDNA as compared to WT.....	99

4 – GENERAL DISCUSSION AND FUTURE DIRECTIONS

1	Potential roles for TGF- β 1 and MEPE in the dentin-pulp complex	106
---	--	-----

LIST OF ABBREVIATIONS

ASARM	acidic, serine- and aspartic acid-rich motif
BMP	bone morphogenetic protein
CED	Camurati-Engelmann disease
DECM	dentin extracellular matrix
DGI	dentinogenesis imperfecta
DMP-1	dentin matrix protein-1
DSPP	dentin sialophosphoprotein
HERS	Hertwig epithelial root sheath
IBSP	bone sialoprotein
MEPE	matrix extracellular phosphoglycoprotein
NCP	non-collagenous protein
NFI-C	nuclear factor I-C
PHEX	phosphate-regulating gene with homologies to endopeptidases on the X-chromosome
RDD	radicular dentin dysplasia
SIBLING	small integrin-binding ligand, N-linked glycoprotein
SMAD	Sma and Mad Related Family
SPP1	secreted phosphoprotein 1 (also known as osteopontin, OPN)
TGF- β	transforming growth factor beta
UTR	untranslated region

1 - INTRODUCTION

A window to overall well-being, oral health is an intertwined relationship among the condition of the teeth, alveolar bone, and gingival connective tissue (1-4). The tooth is unique, in that it is the sole organ that protrudes from the body, yet is not covered with a layer of epithelium. *Homo sapiens* are diphyodont, meaning that during their lifetime, they function with two sets of teeth: 20 deciduous (or primary) teeth and then up to 32 permanent (or secondary) teeth (5). Obviously important in speech, mastication, and esthetics, teeth are often underestimated as stationary, mineralized structures, yet are metabolically active within their core. The pulp is the living central component of the tooth that has inductive, formative, sensory, nutritive, and protective functions and responds to bacterial, mechanical, thermal, and chemical insults (6). The vitality of the dental pulp is paramount in the lasting prognosis of a tooth.

Teeth also provide mechanical stimulation for surrounding alveolar bone homeostasis. When teeth are either lost due to events such as facial trauma or periodontal disease, or are congenitally absent, the surrounding alveolar bone atrophies (7). Over time, resorption of the jaw bone, particularly the mandible, may become so severe that pathologic fracture is a concern. Therefore, the presence and health of the dentition extends to the fitness of the entire oral cavity (including the gingival connective tissue, the periodontal ligament, the alveolar bone), and even to systemic well-being.

Signaling Cascades Involved in Tooth Formation

Teeth are individual epithelial-mesenchymal-derived organs that are guided by the orchestration of molecular messages from evolutionarily-conserved signaling cascades. Indeed, four principal signaling pathways have major roles in the odontogenesis, or tooth formation: transforming growth factor- β (TGF- β) superfamily, fibroblast growth factor (FGF), wingless integrated (WNT), and sonic hedgehog (SHH) pathways (8-10). In fact, signaling components of each pathway are required at each major stage of tooth development, which will be discussed in detail below.

TGF- β /BMP superfamily signaling pathway

The transforming growth factor-beta (TGF- β) superfamily consists of the TGF- β proteins, bone morphogenetic proteins (BMPs), growth differentiation factors (GDFs), glial-derived neurotrophic factors (GDNFs), activins, inhibins, Nodal, Lefty, and Müllerian inhibiting substance (MIS). Ligands of the TGF- β superfamily form dimers which bind to heterodimeric receptor complexes consisting of type I and type II receptor subunits possessing serine/threonine kinase domains. Following ligand binding, the type II receptor phosphorylates and activates the type I receptor, which in turn phosphorylates the receptor-regulated SMAD, or R-SMAD, which can bind SMAD4, the coSMAD. The R-SMADs SMAD 2 and 3 are activated by TGF- β type I receptor ligands, while BMP type I receptor ligands activate SMAD 1, 5, and 8. The R-SMAD/coSMAD complexes induce or repress transcriptional activity, regulating gene expression. Inhibitory SMAD6 and 7, which may be induced by both TGF- β and BMP signaling, antagonize activation

of R-SMADs. TGF- β and BMP pathways are modulated by MAPK signaling at multiple levels (11).

In keeping with the idea of TGF- β being a “master morphogen” (12), members of the TGF- β family are required during development for dorso-ventral patterning, mesoderm induction and patterning, limb bud formation, bone and cartilage formation, neuron differentiation, and the development of a variety of additional tissues and organs, including teeth (13). During odontogenesis, the TGF- β /BMP signaling pathway has been shown to play critical roles in regulating odontoblast cytodifferentiation and matrix formation and mineralization (14). Reciprocal BMP signaling in particular plays a key role in the differentiation of the ectomesenchymal cells of the forming pulp cavity into a layer of functional odontoblasts, which secrete the dentin matrix. This matrix becomes mineralized in the process of dentinogenesis (15, 16). These same molecular mechanisms involved in tooth development also play a critical role in dentin repair.

FGF signaling pathway

The fibroblast growth factor (FGF) ligand family is very diverse, with genetic splicing in receptors alone contributing to over 50 isoforms (15). Receptors may be activated by multiple FGFs, and in many cases, the FGFs themselves can also activate more than one receptor. FGF signals mediate a variety of biological events, including initiating developmental processes, regulating tissue homeostasis, and overseeing metabolic processes. FGFs orchestrate their diverse functions via heparin sulfate-assisted FGF receptor dimerization, tyrosine kinase regulation, receptor cis-autoinhibition, and tyrosine trans-autophosphorylation (14). As one might imagine, these intricate molecular

mechanisms can be disrupted by structural anomalies, leading to an array of pathologies. A demonstrated necessity in skeletogenesis and Apert's syndrome (17, 18), FGF signaling is also critical in tooth development, aimed at regulating epithelial-mesenchymal interactions occurring in the dental epithelium (19).

WNT signaling pathway

The WNT family constitutes a group of signaling proteins that communicate via three pathways: the canonical WNT pathway, the noncanonical planar cell polarity pathway, and the noncanonical WNT/calcium pathway. All three pathways are activated by the binding of a WNT-protein ligand to a Frizzled family receptor, which conveys the biological signal to the protein Dishevelled inside the cell. The canonical WNT pathway leads to regulation of gene transcription, while the noncanonical planar cell polarity pathway regulates the cytoskeleton that is responsible for the shape of the cell. The noncanonical WNT/calcium pathway modulates intracellular calcium. WNT signaling pathways utilize either nearby paracrine or autocrine signaling and are highly evolutionarily conserved (20).

Given their strong degree of similarity amongst species, WNT signaling pathways are gatekeepers of embryonic processes, including body axis patterning, cell fate specification, cell proliferation, and cell migration. The clinical importance of this pathway has been validated time and again by studies of mutations that lead to a variety of diseases, including cancer, diabetes, and tooth agenesis (20). Animal studies have confirmed the effects of WNT regulation of developing mineralized tissue formation and adult homeostasis, documenting the molecular crosstalk between WNT and BMP

signaling in osteoblast differentiation. The WNT signaling pathway also plays an important role in tooth formation by managing the differentiation and proliferation of cementoblasts and odontoblasts, as well as tooth size. (21).

SHH signaling pathway

Sonic hedgehog (SHH), the best-studied ligand of the hedgehog signaling pathway, is critical in embryonic organogenesis. SHH signals through transmembrane receptors Patched (PTC) and Smoothened (SMO) to activate downstream signaling cascades. Without SHH present, SMO activity is repressed by PTC. Transcription factors GLI1, 2, and 3 regulate SHH signaling to affect expression of downstream targets. Negative regulators of hedgehog signaling include Hedgehog-interacting protein (Hip1) and growth arrest-specific gene (Gas1) (22, 23).

In the developing tooth germ, SHH, its receptors, and downstream targets have been shown to be expressed and play pivotal roles in every stage of tooth development. SHH expression in the dental epithelium helps determine crown width and cusp formation, as well as regulate amelogenesis (24). Indeed, inactivation of *Shh* leads to impaired growth and aberrant tooth formation, indicating an essential role for SHH in tooth morphogenesis (25).

Tooth Biology

Dental anatomy and histology

Evolutionary embryology associates the presence of teeth, a hallmark of vertebrate origin, with the appearance of the neural crest (26). Permanent human teeth are

categorized by morphology into four groups: incisors, canines, premolars, and molars (27). Teeth are divided anatomically into the crown, extending from the gingiva, or gums, into the oral cavity, and the root, firmly secured in the alveolar socket via a myriad of fibrous networks (6). Eruption of the developing tooth into the oral cavity typically occurs when the crown is mineralized and the root is two-thirds of the way formed (27). The crown is shielded by enamel, while the root is enclosed with cementum. Dentin, underlying both the enamel and cementum, surrounds the pulp which contains nerve fibers, blood vessels, lymphatics, immune cells, and multipotent stem cells (6).

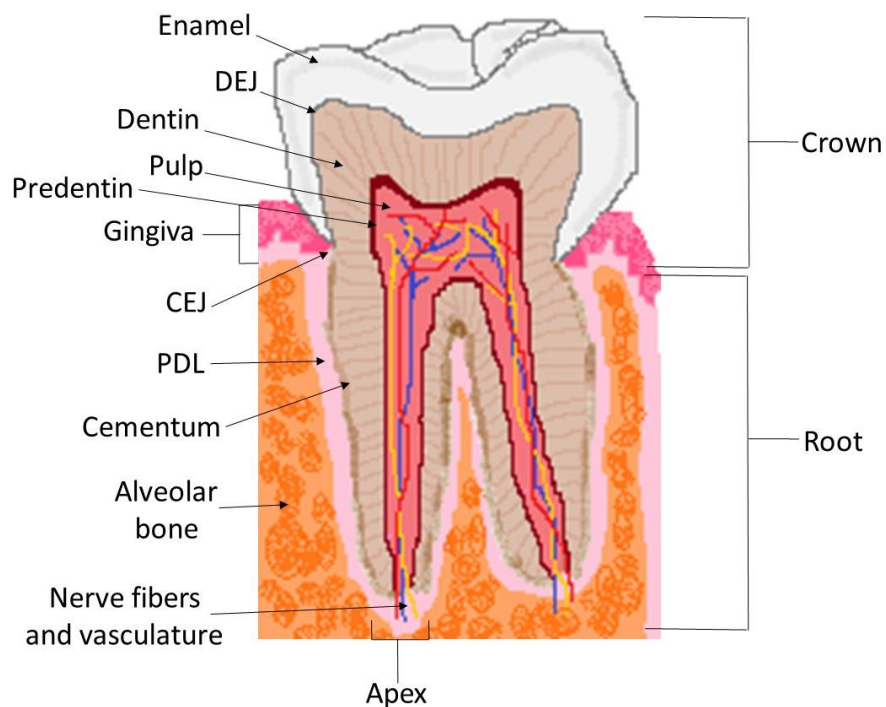


Figure 1. Anatomy of the tooth and its supporting structures

The tooth is formed via an orchestrated cascade of reciprocal interactions between epithelial and mesenchymal tissues. These events commence at the sixth week of human

embryonic development and lessen after about eight weeks (6, 27). In mice, tooth formation begins between embryonic days 9 and 11. The initial sign of tooth development is the presence of the dental lamina, a thickened layer of oral epithelial cells, which later invaginates into the mesenchyme to form a tooth bud (bud stage) in either the future maxilla or mandible (6, 27). Developing adjacent to the dental lamina are mesenchymal neural crest cells, which are under the influence of *Dlx1* and *2* and *Msx1* and *-2* (10, 27). Located apical to the developing dental lamina is a circular structure called Meckel's cartilage which acts as a support for the forming mandibular bone. The first stage of tooth formation after the dental lamina lengthening is the bud stage, which employs *Pax9*, along with growth factors from all four primary signaling pathways previously mentioned. *Pax9* is essential for tooth formation, as initiation cannot progress to the bud stage if this protein is absent (28). During the bud stage, ectomesenchymal cells of the neural crest condense around the invaginating epithelium. The oral epithelium continues to invaginate around the ectomesenchymal condensation to form a cap-like structure along the upper aspects, hence the beginning of the cap stage. WNT factors allow for the continuation of tooth development via interaction with β -catenin (10).

Many of the permanent distinguishing features of the developing tooth are hallmarks of the cap stage. At the late cap stage, the inner enamel epithelium (IEE) cells are present. It is not until the late bell stage that the odontoblasts differentiate from committed mesenchymal cells of the dental papilla. Clusters of specialized epithelial cells known as the enamel knot form at the most superior aspects of the inner enamel epithelium. The enamel knot is a transient structure which will not be present in the mature tooth, yet contributes to the signaling events that dictate tooth morphology,

particularly the formation of the cusps, as well as those processes necessary for induction of odontoblast differentiation (29).

The epithelial cells from the inner and outer enamel epithelium continue to differentiate into the bell shape. As the cap stage continues, cells of the dental follicle begin to form around the bottom of the dental pulp and eventually will surround the growing dental papilla. The inner region of the bell is known as the dental papilla, while the outer epithelial lining of the bell forms the bilayered enamel organ (6, 27). Between the inner and outer epithelial layer of the enamel organ resides the stellate reticulum, which serves as a space maintainer to separate the two epithelial layers. The dental papilla will become the dental pulp, and the inner enamel organ epithelium will undergo cytodifferentiation to become the ameloblasts. The layer of cells along the outermost edge of the dental papilla will differentiate to become odontoblasts. Meanwhile, the outer dental epithelium continues to collapse down towards the inner enamel epithelium, causing the stellate reticulum to reduce over the cusp. Angiogenesis gives rise to the vasculature in the forming pulp. At the inferior aspects of the enamel organ, the inner and outer enamel epithelia fuse to form a cervical loop. This cervical loop begins to grow apically, thereby defining the future tooth crown and forming the root sheath (6, 25).

Meanwhile, the odontoblasts which have been differentiating at the outer lining of the developing pulp begin secreting predentin. The secretion of predentin causes the inner dental epithelial cells to differentiate to ameloblasts. The predentin collagenous network becomes infiltrated with mineralization vesicles to gradually form a mineralized dentin layer adjacent to the predentin. The ameloblasts mature and begin secreting enamel

adjacent to the dentin, with initial enamel formation occurring at the cusps and progressing apically toward the direction of the cervical region of the crown (6, 25).

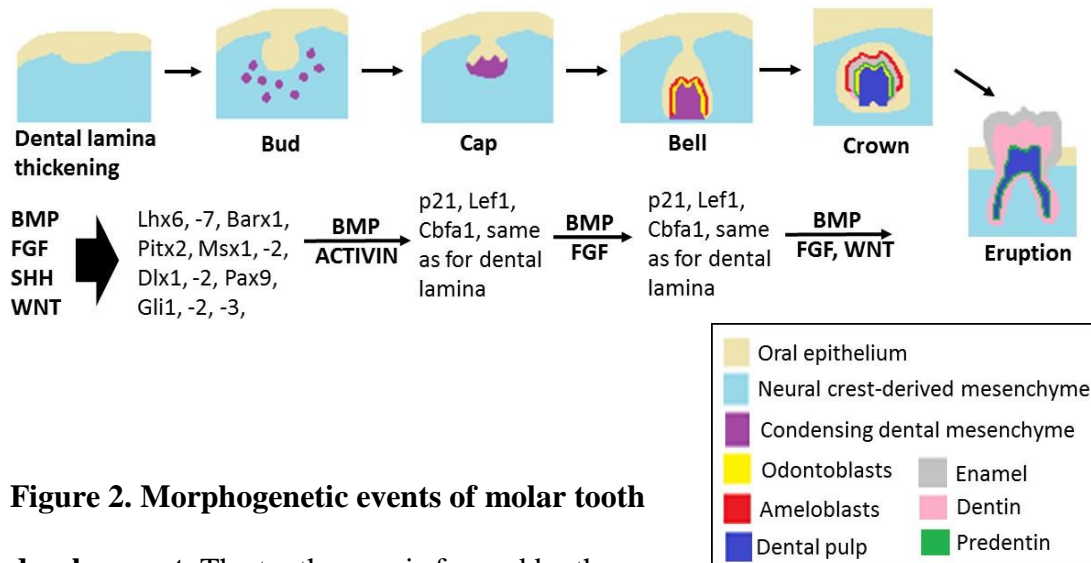


Figure 2. Morphogenetic events of molar tooth

development. The tooth germ is formed by the

interactions of the oral epithelium and the mesenchyme derived from the cranial neural crest. The dental lamina of the oral epithelium thickens and migrates apically to transition to the bud stage. At this stage, dental mesenchyme condenses around the epithelial bud. From the bud to cap stage transition, the oral epithelium continues to invaginate as the histodifferentiation process occurs at the bell stage. Single rows of developing ameloblasts and odontoblasts, respectively indicated as red and yellow lines, form at the epithelial-mesenchymal junction. Maturation of these two cell layers brings about the formation of the dentin and enamel layers of the tooth. During the late bell stage, the dental lamina is disintegrating, while dentin and enamel are produced simultaneously at the cusp tip. The tooth erupts into the oral cavity following completion of crown formation and approximately two-thirds of root formation. The BMP, FGF, SHH, and WNT signalling pathways are necessary for tooth formation. Specific genes essential for

each stage of development are indicated. Black arrows represent the continuum of growth factor signalling between epithelium and mesenchyme during advancing tooth development.

Dental pulp

The dental papilla is referred to as the pulp when its outermost layer of mesenchymal cells differentiates to odontoblasts and begins secreting the extracellular matrix that will eventually become the dentin (6). The dental papilla is the cellular origin of other mesenchymal dental tissues, including cementum, the periodontal ligament, and the alveolar bone. The remaining mesenchymal cells of the pulp contain a reservoir of stem cells that have the ability to migrate and become odontoblasts (29). Anatomically, dentinogenesis is initiated at the regions of the tooth that will become the cusp tips, a genetically predetermined site associated with special signaling centers. Formation of dentin progresses apically from the cusps towards the apical aspects of the forming crown and future root (8, 9).

Once dentin formation has begun, the ameloblasts undergo cytodifferentiation and commence enamel production (10). It is through reciprocal signaling crosstalk between the dental epithelial and mesenchymal tissues that dentin- and enamel-forming cells are formed and accomplish their destined function (10, 30). Dental pulp cells, which express receptors for TGF- β ligands (31), may self-regulate during differentiation via SMAD2/3 phosphorylation (32). Unlike odontoblasts, ameloblasts do not have the ability to regenerate in order to produce reparative enamel. Upon maturation of secreted enamel

matrix, ameloblasts undergo apoptosis and conclude production of the outer mineralized tissue layer (33-35).

Odontoblasts

Preodontoblasts differentiate to odontoblasts in part via temporal expression patterns of TGF- β superfamily members and their receptors, namely enhanced production of TGF- β 1, BMP-4, BMP-7, ALK-2/ACVR-1, ALK-3/BMPRI1A, and ALK-5/TGFBR1 (36). *In vitro*, osteogenic induction of dental pulp cells leads to an increase in the level and activity of alkaline phosphatase (ALP) (27), a marker for mineralization. Additional markers of odontoblastic differentiation have classically been proposed based on elevation of ALP activity and/or histological evidence of mineralization. These include DSPP, DMP-1 and MEPE, as their mRNA expression is elevated with osteogenic stimulation (37). Initially, TGF- β 1 was considered to be mitogen for dental pulp cells, reducing ALP expression with increasing TGF- β 1 concentrations (38). However, more recently, TGF- β 1 itself has also been shown to increase ALP activity in dental pulp cells, as well as the expression of DSP, OPN, and type I collagen (39).

Preodontoblasts are initially separated from preameloblasts, the cells derived from the inner dental epithelium, by a basal membrane. Differentiation of preodontoblasts to odontoblasts is a gradual process supported by interactions with the basal membrane and initiated by signaling molecules, such as Cpn1 which is expressed in preameloblasts and stimulates *Dspp* expression (27, 40, 41). These events require that preodontoblasts on the basal membrane side withdraw from the cell cycle (stop proliferating), while cells on the pulpal aspect become quiescent as undifferentiated Höhl cells. The cytoplasmic processes

of the preodontoblasts extend through the basement membrane as it degrades to come into close association with the preameloblast.

Preodontoblasts gradually develop into tall polarized odontoblasts, reflecting their secretory function associated with secretion of extracellular proteins and production of the extracellular matrix. The polarization of odontoblasts is characterized by three histological attributes: morphology of the cell, distribution of intracellular components, and secretion of matrix components. Presenting as elongated, columnar cells, odontoblasts extend long branched cellular processes named odontoblast cell processes into the dentin matrix that are subsequently incorporated into the forming dentinal tubules. The cell nucleus of the odontoblast is found on the pulpal associated end, opposite to the secretory apparatus and cell process located on the dentin matrix associated side. This provides for the unidirectional secretion of the cell. Mitochondria and vesicles, as well as endoplasmic reticulum and a well-developed Golgi apparatus, are located adjacent to the nucleus on the dentin matrix side of the odontoblast. The odontoblast process itself lacks major cellular organelles, but contains an abundance of longitudinally organized filaments and microtubules that facilitate the trafficking of secretory molecules. Located at the periphery of the dental pulp, odontoblasts are dense with approximately 45,000 odontoblasts per mm² in the coronal or crown dentin (27). The dentinal tubules flare out toward the dentino-enamel junction (DEJ), decreasing in density and size as they radiate from the pulp chamber (25).

Dentinogenesis

Mature, elongated odontoblasts begin the secretion of predentin. Predentin is an organic collagenous extracellular matrix adjacent to the odontoblast cell body and is gradually mineralized distally to form the dentin layer. However, a layer of unmineralized predentin always remains next to the odontoblast cell layer throughout the lifespan of the tooth. Distal to the predentin at the mineralization front, the calcification of the predentin collagen meshwork occurs and progresses toward the future dentin enamel junction. The maturation of predentin involves progressive thickening and compacting of collagen fibrils. Thick, large fibers of type III collagen, called von Korff's fibers, are found intercellularly in the odontoblast layer and are characteristic of newly-differentiated odontoblasts (25).

The mineralized matrix is located distal to the odontoblast and contacts the overlying enamel matrix. The predentin zone is proximal to the mineralization front interfacing the mature dentin layer and the odontoblast cell layer. These layers are formed by two active sites of secretion by odontoblasts: at the end of the cell body and distally within the odontoblast cell process at the mineralization front. Organic molecules are synthesized by the odontoblast and transported within the cellular process to the site of specific secretion. Collagen and noncollagenous proteins (NCPs) are organized in the extracellular space in a fashion that supports coordinated deposition of hydroxyapatite. Due to the presence of enamel and stationary ameloblasts surrounding the forming dentin, the odontoblast cell body retreats towards the pulp with continuing matrix deposition. As the initial site of organic matrix secretion becomes more distant from the odontoblast cell body. The odontoblastic processes secrete the building blocks of

hydroxyapatite, namely Ca^{+2} and PO_4^{-3} , which are incorporated into the collagen scaffold. This highly organized fashion of secretion of the various molecular components allows for formation of functional dentin (25).

As a consequence of dentin deposition, odontoblasts cell bodies move pulpally, leaving their cytoplasmic extensions within the forming matrix surrounded by peritubular dentin. In this way, the special tubular structure of dentin, or dentinal tubules containing the odontoblastic processes, is formed. Dentinal tubules service the tooth by forming a network for the diffusion of nutrients. The size of the pulp chamber decreases over time, as odontoblasts must occupy a smaller area and become increasingly crowded within the pulp. Thus, the single layer of odontoblasts present in early development maintains its viability throughout the lifespan of an erupted tooth.

Dentin extracellular matrix (DECM)

Calcification of the tooth, which starts during the fourth fetal month in humans, begins with the dentin. Dentin, the mineralized layer covering the coronal (crown) and radicular (root) pulp, makes up the majority of the connective tissue in a tooth. It is generated throughout the life of the tooth as long as the pulp is able to supply nutrients to the odontoblasts (27). The dentin extracellular matrix (DECM), a mineralized collagen matrix similar to bone, contains two distinct layers which are secreted by odontoblasts: predentin (unmineralized) and dentin (mineralized). Mature odontoblasts secrete collagen at the cell border, forming predentin and then release NCPs needed for the transformation of predentin to mineralized dentin distally at the mineralization front (42-45).

The organic portion of the tooth, about 30% by volume, is comprised primarily of collagen (90%), specifically type I collagen (27). Collagen type I fibers are the basic building blocks for both dentin and bone matrices. Structurally, mature collagen type I forms a triple-helix which serves as a scaffold to bind and orient hydroxyapatite. Making up approximately 50% volume of the DECM, hydroxyapatite crystals $[\text{Ca}_{10}(\text{OH})_2(\text{PO}_4)_6]$ maintain the rigidity and structural support for enamel and mastication (27). Carbonate, sodium, magnesium, as well as trace elements including fluoride, are also found in the dentin. Non-collagenous proteins (NCPs) and lipids make up the remaining 10% and may be found interspersed within the collagen scaffold (27). The NCPs, which assist in regulating mineralization of bone and dentin and mediating cell attachment, include ALP, osteocalcin, proteoglycans, and the SIBLING proteins. SIBLINGs, or small integrin-binding ligand, N-glycosylated proteins, represent the majority of NCPs in bone and dentin; these molecules will be discussed later. Finally, water comprises 20% of the dentin by volume and helps maintain the shape of the collagen dentin meshwork.

Types of dentin

As previously mentioned, the dentin extends within both the crown and root structures of the tooth. Pertaining to the crown, cuspal dentin is formed before cervical dentin, which is generated before apical dentin. The oldest dentin is that which is initially formed at the DEJ, while the newest dentin is always found on the pulpal side (27). The dentin found in the crown of a tooth is produced prior to and more rapidly than the dentin located in the tooth root (7). Histologically, coronal dentin appears to be S-shaped conforming to the contours of the crown, while root dentin appears to be straight (7).

Aside from these observations, pathologies of coronal and radicular dentin are most often differentiated when referring to dentin dysplasia, a tooth mineralization disorder which will be discussed at a later point.

Histologically, dentin is classified relative to juxtaposition to dentinal tubules. Loosely-packed intertubular dentin is located between the odontoblastic processes, providing the bulk structure. A second layer of denser and more mineralized dentin, called peritubular or intratubular dentin, is found surrounding the dentinal tubules (27). Additionally, two patterns of dentin mineralization can be identified histologically: linear and globular or calcospheric, patterns. Mineralization of dentin begins in small spherical areas, and can continue as either a straight line (linear) or globular/calcospheric, with semi-random arrangement of mineralization (27).

Dentin may be classified into three main categories based upon chronology and health of the tooth: primary, secondary, and tertiary dentin. Primary dentin is rapidly formed during initial tooth development; it includes an outer layer of mantle dentin, middle zone of globular dentin, and inner ring of circumpulpal dentin (27). Mantle dentin is uniquely different from other forms, as it is mineralized by matrix vesicles from immature odontoblasts and is devoid of dentin sialoprotein (DSP) and dentin phosphoprotein (DPP) (27). A layer of globular dentin separates the immature, initial layer of mantle dentin from the more mature circumpulpal dentin. Globular dentin has been found to be irregular in mineralization disorders such as vitamin D-resistant rickets (46, 47).

Secondary dentin is formed following root formation and continues after eruption of the tooth throughout the lifespan of the dental pulp. Produced at a reduced rate

compared to its predecessor primary dentin, secondary dentin formation is a physiologic process (7).

Due to various types of injuries (thermal, mechanical, bacterial, etc.), the tooth may respond to its loss of odontoblasts and insults to the pulp by recruiting pulpal stem cells to rapidly differentiate to odontoblasts (48). Reparative (also known as reactionary or tertiary) dentinogenesis is, therefore, a pathologic phenomenon, resulting in the formation of an irregular, mineralized layer of peritubular dentin by the odontoblast cells lining the pulpal chamber (29, 49). Tertiary dentinogenesis allows restorations to be placed more apically in older individuals with smaller pulp chambers as compared to adolescents, for example, with pulp chambers extending further coronally. Because the life span of odontoblasts is equal to that of a viable tooth, tertiary dentin can totally obliterate the pulp chamber due to aging, severe damage, or prolonged irritation to the tooth.

Bone and dentin share many structural components, as will be discussed later. However, unlike the constant remodeling that osseous tissue undergoes, once dentin is produced, it can only undergo moderated repair (tertiary dentin). Dentinogenesis, then, is a multi-tiered event that begins with the earliest stages of tooth formation and continues throughout an individual's lifetime. As long as the tooth is vital within the oral cavity and has not undergone endodontic therapy or necrosis, dentin will be formed.

Ameloblasts and amelogenesis

During the cap stage, the establishment of the inner and outer enamel epithelium is initiated as well as the enamel knot or signaling center. The pre-ameloblasts formed from

the inner enamel epithelium help drive odontoblast formation through BMP, FGF, SHH, and WNT signaling pathways (which will be addressed later) by way of a reciprocal relationship that is mediated by a number of transcription factors. Concurrently, cuboidal pre-ameloblasts differentiate to become columnar, polarized enamel-secreting ameloblasts. This occurs only through signaling from the ectomesenchymal cells of the dental papilla. Ameloblasts achieve full function after the predentin has been laid down by the odontoblasts.

Enamel, the hardest tissue in the body, is generated in three stages: presecretory, secretory, and maturation. During the presecretory phase, ameloblasts align, polarize, and mature. The nuclei are positioned nearer to the stratum intermedium, away from the secretory end. Ameloblasts produce matrix proteins, notably amelogenin, a major calcium-binding protein in enamel. The initial mineralized layer of enamel accumulates at the DEJ. The organic component of the enamel is a conglomerate of enamel matrix proteins, namely amelogenin (AMELX), ameloblastin (AMBN), enamelin (ENAM), amelotin (AMTN), and odontogenic ameloblast-associated protein (ODAM); dentin/bone matrix proteins, specifically dentin sialophosphoprotein (DSPP – DSP/DPP), dentin matrix protein-1 (DMP-1), and bone sialoprotein (BSP); and enamel proteinases matrix metalloproteinase 20 (MMP-20) and kallikrein 4 (KLK-4) (27).

During the final stage of enamel formation, ameloblasts employ enzymatic processing via KLK-4 and MMP-20 to degrade matrix proteins that are removed, and thereby allowing enamel maturation. A transition phase occurs at this time, during which ameloblast morphology deviates and 25% of these cells undergo apoptosis. Gradually over 90% of the protein and water components are removed, forming enamel that is 96%

mineral. Enamel rods are formed by the addition of densely-packed cylindrical hydroxyapatite crystals, beginning within the tooth at the DEJ, continuing toward the incisal edge, and progressing apically toward the cemento-enamel junction (CEJ). Enamel formation can take up to five years to complete. The remainder of the ameloblasts, an irreplaceable subset of cells, are lysed during tooth eruption. For this reason, when tooth enamel is lost due to erosion or masticatory/parafunctional wear, it is gone forever (20).

Root formation

A critical structure, the root is necessary to support the tooth within the jaw and to maintain the alveolar bone around the tooth via mechanical loading (50). Root development, which precedes eruption of the tooth into the oral cavity, is initiated by a cascade of morphogenetic events once crown formation has concluded. A progression of epithelial-mesenchymal interactions stimulate mesenchymal cells located at the inferior-most aspect of the tooth to proliferate and form the cervical loop (51, 52). The most apical portion of the cervical loop region forms a bilayered structure known as Hertwig's epithelial root sheath (HERS), which continues to migrate distally, dictating the root morphology. The epithelial cells of the lengthening root induce differentiation of adjacent dental papilla cells into odontoblasts. Thus, radicular dentinogenesis begins, signaling degradation of the HERS leaving remnant patches known as the epithelial rests of Malassez.

As will be discussed later, NFIC is deemed the master transcription factor regulating root formation. A transient period of secretion of BSP and OPN by the HERS stimulates progression of root formation. Another critical component of cellular signaling

during root development is the SHH pathway (53). NFIC, SHH, and SMAD4 constitute a triad that provides specific molecular instructions for root formation. Without SMAD4, the HERS proliferates but is not capable of elongating (53). Furthermore, TGF- β /BMP signaling is required for SHH induction in the HERS, and SMAD4 is necessary for NFIC expression in the cranial neural crest (CNC)-derived dental mesenchyme (52). Detailed temporal expression studies indicated NFIC-SHH signaling both prior to and following root development. Interestingly, SHH is increased and CNC-derived dental mesenchyme function is impaired when *Nfic* is deleted in the mouse (54). Research has also shown that growth and differentiation factors may play roles in the development of the periradicular attachment apparatus of periodontal tissues, as pluripotent dental follicle cells have been shown to differentiate into osteoblasts, cementoblasts, or periodontal fibroblasts (55).

Cementum

Cementogenesis occurs late in tooth development, supported by mesenchymal cells from the dental follicle. A relatively soft mineralized tissue, cementum thinly covers the root surface and serves as an attachment for the periodontal ligament. Cementum, which lacks blood vessels and nerves, has three primary roles: cover and protect the dentin, provide attachment to periodontal fibers, and protect the root from resorption. Thinnest towards the cervical region of the tooth, cementum is relatively non-resistant to wear but is resilient to resorption, owed to its avascular nature. The two useful marker molecules in cementum are cementum attachment protein and insulin growth factor (56). Interestingly, cementum regeneration has been achieved *in vitro* through induction of the canonical Wnt signaling pathway (57).

Periodontal ligament and alveolar bone

Both the periodontal ligament (PDL) and alveolar bone are derived from the mesenchymal cells of the dental follicle or sac. The PDL is composed of collagen, fibroblasts, blood vessels, and nerve fibers. The intricate architectural support of alveolodental and transseptal collagen fibers facilitates the PDL's primary function in stabilizing the tooth in its bony socket. Innervated by the trigeminal nerve, the PDL affords an individual exceptional mechanoreceptive and proprioceptive abilities. The PDL is a unique dental connective tissue in that it houses progenitor cells that can differentiate into osteoblasts to be employed for the remodeling of alveolar bone (27). Furthermore, the PDL itself may be regenerated by bFGF stimulation of FGFR1 and 2 (58).

The alveolar bone is attached to the radicular cementum by way of the periodontal ligament. A tooth-supporting tissue continuous with the basal bone of the jaws, the alveolar process develops geographically in coordination with the presence of teeth through TGF- β /BMP and WNT signaling (9). Alveolar bone gradually resorbs after tooth loss due to lack of mechanical loading. Together, the cementum, PDL, and alveolar bone form a specialized supporting apparatus that maintain teeth in function (27).

DECM Proteins

SIBLINGS

The DECM shares many properties with bone, including common NCPs that are thought to regulate mineralization. The major group of NCPs found in dentin and bone are the SIBLINGs, which include DMP-1, DSPP, BSP, SPP1, and MEPE (formerly

OF45), the most recently identified and least characterized member (44, 59). While DSPP is expressed in both bone and dentin, its level is relatively lower in bone compared to dentin and thus serves as a marker of dentin formation. The SIBLING gene cluster, on human chromosome 4q21, contains loci for several human genetic dentin diseases including dentinogenesis imperfecta types II and III and dentin dysplasia type II (60, 61). Interestingly, *in vivo* reactionary dentin was found to exhibit greater levels of BSP and OPN compared to primary dentin (29), and BSP is thought to behave as a nuclear of hydroxyapatite crystal formation (30). In addition to regulating mineralization, SIBLING proteins mediate cell attachment, which is necessary for cell signaling, and act as signaling molecules that affect transcription (44).

MEPE

Matrix extracellular phosphoglycoprotein (MEPE) has been classified as a hormone in the bone-renal vascular axis. MEPE plays an inhibitory role in mineralization and more importantly, is a potent anti-remodeling molecule actively involved in skeletogenesis (62). Studies have demonstrated that MEPE is important for normal phosphate regulation in the skeleton and dentition of mammals. Previous studies have shown MEPE expression in bone by fully differentiated rat bone marrow-derived osteoblasts and in human osteocytes embedded in bone matrix. MEPE has elevated expression during matrix mineralization (63, 64). Contrasting with these studies are reports demonstrating that MEPE expression is reduced during mineralization in human osteoblast culture systems (65). Nonetheless, MEPE acts as a potent anti-remodeling molecule and is currently associated with an inhibition of bone formation and mineralization (66). The

Mepe^{-/-} mouse has increased bone mass, due to an increased number of osteoblasts with enhanced mineralization activity, and increased dentin mineralization (64).

Produced by odontoblasts and pulp cells, MEPE has been proposed to be used as a marker for odontoblast differentiation, being down-regulated when dental pulp stem cells reach confluence and initiate mineralization *in vitro*. The exact role of MEPE in odontogenesis is unclear, though its C-terminal domain termed the ASARM peptide has been shown to be active in dentinogenesis (67). MEPE expression, induced by BMP-2, is thought to occur in part by SMAD protein interactions (68), and a peptide portion of MEPE known commercially as Dentonin stimulates dental pulp stem cell mitosis (69). A likely target of TGF- β 1 signaling, MEPE, like TGF- β 1, is expressed during tooth formation by odontoblasts and is incorporated into the DECM.

Mice heterozygous and homozygous for the *Mepe* mutations were normal, fertile, and healthy, with no obvious pathology. Serum chemical analysis showed no statistically significant alterations in blood phosphate or calcium content. Whole-body x-rays of *Mepe*^{-/-} mice at four months of age revealed normal skeletal patterning and structure, while high resolution x-rays of femurs showed a slight increase in trabecular bone volume. Femurs of both heterozygote and knockout animals at one year showed a pronounced increase in the amount of trabecular bone. Ablation of *Mepe* expression in the mouse also resulted in resistance to age-associated trabecular bone loss, increased mineral apposition rate, accelerated mineralization in *ex vivo* osteoblast cultures, and normophosphatemia (66). There are no published reports concerning the relative expression levels TGF- β signaling molecules in the *Mepe*^{-/-} animal.

ASARM peptide

The acidic serine-aspartate rich MEPE-associated motif (ASARM) peptide is an active component that can induce or repress mineralization of extracellular matrix proteins (70). The enzyme PHEX (phosphate regulating gene with homologies to endopeptidases on the X chromosome) binds and cleaves MEPE to regulate mineralization (71). ASARM is currently thought to inhibit mineralization by binding to hydroxyapatite. Studies suggest that MEPE inhibits mineralization and PHEX activity and leads to increased FGF23 production. The coordination of mineralization by ASARM peptides may serve a physiological role in regulating systemic phosphate homeostasis to meet the needs for bone mineralization (72).

TGF- β 1

TGF- β 1, a ubiquitous cytokine, is essential for embryonic development, cell proliferation, migration, and differentiation; and extracellular matrix (ECM) secretion. Of the three isoforms, TGF- β 1 is the most abundant form found in dentin. Odontoblasts, as well as their precursor cells, express *TGFB1* mRNA. Furthermore, the expression pattern of *Colla1*, from type I collagen, mRNA resembles that of TGF- β 1, which is now known to play a role in initiation of collagen synthesis and cytodifferentiation of odontoblasts (73). TGF- β 1 regulates a broad range of biological processes during primary tooth formation and secondary and tertiary dentin secretion.

There are two forms of TGF- β 1 found in the human body: latent TGF- β 1 (which accounts for 90% of the cytokine) and mature free TGF- β 1 (making up the remaining 10%). Latent TGF- β , a homodimer, is composed of mature TGF- β and a precursor,

latent-associated peptide or LAP. This latent complex is biologically inactive. TGF- β -LAP is covalently linked to latent TGF- β -binding protein (LTBP), which forms a biologically inactive complex attached to the ECM. This controls the level of TGF- β activity in the matrix. The release of LTBP depends on plasmin acting on the protease-sensitive hinge region, to release one portion and leave an amino terminal portion of LTBP attached to the matrix. The cleaved LTBP together with TGF- β -LAP then attaches to a binding site on the cell surface. The mature TGF- β homodimer must be dissociated from LAP to become biologically active (74).

TGF- β 1 is an active component of the DECM that is associated with the regulation of differentiation of odontoblasts-like cells, and especially of matrix biosynthesis, particularly when a tooth has been damaged. TGF- β 1 is expressed in developing tooth from the initiation stage through adulthood. During mouse tooth development, TGF- β 1 is expressed initially in the oral epithelium at embryonic day 13. As tooth morphogenesis continues, its expression extends into the mesenchymal compartment (precursor dental pulp cells) and becomes confined to the ectomesenchymal layer (odontoblasts). The odontoblast-restricted expression of TGF- β 1 persists throughout life in mice (75). The expression pattern of TGF- β 1 mRNA resembles that of type I collagen, which comprises the majority of the organic phase of dentin. Importantly, TGF- β 1 mediates odontoblast cytodifferentiation from immature dental papilla mesenchymal cells but appears to have spatial and temporal modes of action on dental tissues as it is up-regulated during odontoblast differentiation and down-regulated following dentin formation (75).

Tgfb1 deficiency in mice leads to early lethality (all animals die by 3-4 weeks of age) associated with multifocal inflammation (76, 77). Interestingly, *Tgfb1*^{-/-} neonates show no striking dentin abnormalities during the first two weeks of life, which is hypothesized to be due to the maternal transfer and compensation of TGF- β 1 (78). However, older *Tgfb1*^{-/-} mice demonstrate progressive loss of the dental hard tissues through a gradual destruction of both the enamel and the underlying dentin, with no evidence for compensation by *Tgfb2* or *Tgfb3* (79).

Studies of odontoblasts and other cells of the pulp of mature human molar teeth indicate the presence of both TGF β RI and II, with odontoblasts showing the strongest expression, particularly of TGF β RI (80). In embryonic WT mice, TGF β RII, SMAD2/3 and SMAD4 are co-expressed during early steps of tooth development indicating that TGF- β 1 signaling can occur beginning at embryonic day (E)11.5 (81). Furthermore, *in vitro* studies have confirmed that the SMAD pathway is functional in the mouse odontoblast MDPC-23 cell line. Smad3 appears to be involved in down-regulation of *Dspp* by exogenous TGF- β 1, suggesting that Smad signaling plays a role in dentinogenesis (82). DECM that is being replaced demonstrated increased activation of TGF- β pathway signaling, via higher expression of SMAD2/3 and BSP compared to normal dentin. *TGFB1* is also known to decrease DMP-1 and DSPP levels (73).

Diseases of Bone and Dentin

Camurati-Engelmann disease

Camurati-Engelmann disease (CED), also known as progressive diaphyseal dysplasia, is an autosomal dominant disorder characterized by progressive bilaterally

symmetrical sclerosis of the diaphysis of the long bones (83). Initially documented in the scientific literature in 1920 (84), CED has been linked to heterogeneous mutations of the *TGFBI* gene on chromosome 19q13.1-q13.3 (85-87). In fact, *TGFBI* is the only gene known to be associated with CED (74). CED is diagnosed based on the following clinical findings: thickening of the long bones and skull, bone marrow dysfunction, limb pain, muscular weakness, and delayed sexual development (74, 85, 88-91). At least ten different mutations in *TGFBI* have been identified in CED families (86, 87, 92, 93). The R218C mutation, found in 19 of 30 reported families, is the most prevalent worldwide (85, 91, 93). Data have shown that there is no correlation between the mutation type or location and the severity of the clinical manifestations. CED exhibits low penetrance, as not every individual possessing the mutation has visible traits of the disease. Furthermore, there is no documentation of a dental phenotype present in humans recorded to date.

A disease of disrupted bone formation and endocrine dysregulation, CED has been studied via a transgenic mouse model expressing mutated *TGFBI* (94). The transgenic model exhibits a CED-derived *TGFBI* point mutation (H222D) directed by the *Col1a1* promoter, leading to excess production of TGF- β 1 and uncoupled bone remodeling (94). Collagen I production has been shown to be prevalent during tooth formation, especially crown and root dentinogenesis (95). Of the many documented cases of CED in the literature, none describe the effects on the dentition. This may be due to other overarching facets of this lifelong painful, progressive disease. Current therapies for CED are palliative at best and include corticosteroids, bisphosphonates, anti-inflammatories, and pain relievers (96, 97).

X-linked hypophosphatemic rickets

A pathology of bones and teeth more recently being investigated is X-linked hypophosphatemic rickets, or XLH. A disorder caused by any of 200 mutations in *PHEX* (phosphate-regulating gene with homologies to endopeptidases on the X-chromosome), XLH is the most prevalent hereditary form of hypophosphatemia (98, 99). Other forms of hypophosphatemic rickets inherited via other modes of transmission have been linked to mutations in *PHEX*, *FGF23*, *DMPI*, *VDR*, and other genes. XLH is characterized by low blood phosphate levels, which leads to impaired skeletal and dentin mineralization (98, 99). While clinical symptoms vary even within families, children often present with abnormally short stature, bowing of the lower extremities, and bone pain. Adults with XLH often exhibit osteomalacia, abnormal vitamin D metabolism, elevated serum FGF23 levels, and spontaneous dental abscesses (99).

Presently, it is theorized that due to alterations in *PHEX* endopeptidase function, serum FGF23 and ASARM fragments are elevated. Increased FGF23 production dramatically inhibits renal reabsorption of phosphate, leading to hypophosphatemia and its associated pathological features. Additionally, accumulation of ASARM peptides, which are common to all SIBLINGs, is also thought to contribute to impaired mineralization activity (100). Evidence of increased degraded fragments of SPP1 and MEPE in dentinal tubules and DECM was reported in studies of extracted teeth from XLH patients (101). More specifically, aberrant organization of the pulp-dentin complex and faulty polarization of odontoblasts leads to unmerged mineralization units and enlarged pulp chambers (101).

Currently, treatment for XLH is limited to exogenous phosphate and 1,25-dihydroxyvitamin D₃. *In vitro* studies show some promise of strengthened dentin when recombinant ASARM (Dentonin) is introduced (100). With increased understanding of the molecular events occurring in XLH, therapies involving FGF23, PHEX, and ASARM peptides of SIBLINGs may be revealed and facilitate recovered mineralization of bones and teeth.

Dentinogenesis imperfecta and dentin dysplasia type II

Also known as hereditary opalescent dentin due to the characteristic brownish-bluish discoloration of teeth, dentinogenesis imperfecta (DGI) has classically been divided into three subtypes (102). DGI type I occurs as part of osteogenesis imperfecta (brittle bone disease), which is caused most often by mutations in *COL1A1* or *COL1A2*. Seven mutations in *DSPP* have been identified in patients with DGI type II and type III, as well as one *DSPP* mutation in dentin dysplasia (DD) type II (103, 104). Due to genetic analyses, the current classification system proposes that DGI type II and type III, along with DD type II, are to be considered allelic or variable forms of the same disorder (105). Therefore, the following descriptions of DGI are intended to represent DGI types II and III and DD type II.

Inherited in an autosomal dominant fashion, dentinogenesis imperfecta (DGI) occurs in 1:8,000 whites typically of English or French ancestry. Characterized by discolored, translucent teeth, individuals with DGI exhibit weaker dentin that have been observed to be nearly five times softer than normal (106). Consequently, the dentition is

at high risk of damage by attrition and trauma due to the separation of enamel from the defective dentin. Both sets of dentition can be affected.

Radiographic hallmarks of DGI include bulbous crowns, cervical constriction, thin roots, and early obliteration of the root canals and pulp chamber (102). Treatment for DGI is solely prosthetic in nature and entails either full-coverage restorations for teeth with nearly normal shape and size, or dentures when teeth succumb to inflammatory lesions of the root canals, cervical fracture, and significant attrition. Unfortunately, for many patients, this leads to full dentures and/or implants by the time they are 30 years old (102). While newer materials and interventions may expand options for patients, genetic testing and molecular interventions may someday provide preventative treatment for afflicted individuals.

Radicular dentin dysplasia

Radicular dentin dysplasia (RDD), also known as rootless teeth or dentin dysplasia (DD) type I, is a rare disorder affecting dentin and root development in both primary and permanent teeth (107, 108). While the enamel and coronal dentin clinically normal, the radicular dentin is loosely organized and subsequently shortened dramatically. Wide variation in root formation occurs due to dentinal disorganization taking place during different stages of tooth development. As one might imagine, if the dentin organization is affected early in dental development, severely deficient roots are the outcome. However, minimal root malformation occurs with later-stage disruption of dentinogenesis. Interestingly, the variability is most pronounced in permanent teeth and may vary from tooth to tooth within the same patient (102).

Hallmark features of RDD include restricted or absent root formation, premature exfoliation of teeth, extensive pulpal calcification, and periapical pathosis, including spontaneous abscesses (102, 107, 109). With a reported prevalence of 1 in 100,000 (110), RDD has been documented to occur in at least 111 persons since 1976 (109, 111-143). Many of these reports detail a single or a few unrelated individuals' experience often through clinical and radiographic findings. Remarkably, nearly half of all the cases reported involve entire families, indicating the heritable aspect of RDD. Thought to be due to a mesodermal defect, RDD has also been associated with atubular dentin formation, hypothesized to lead to abrogated root formation (124, 131, 133, 139). Dental findings have wide variation due to timing of developmental disruption, often affecting both primary and permanent dentitions, yet also reported to be limited to a single tooth or region of teeth (114-116, 122, 132). Additionally, reports of dental anomalies concomitant with skeletal dysplasias contribute to the variation in clinical presentation of RDD (141, 143).

A clear genetic explanation for RDD has yet to be discovered. While many studies recount autosomal dominant modes of inheritance, yet extreme variation in penetrance and expressivity, only two publications give evidence of autosomal recessive transmission of RDD (112, 144). The most recent report involves family members of a consanguineous marriage (112). Based on its critical role in root formation, *NFIC* is a strong candidate gene for this disorder.

Within the past three years, a new gene in the dental literature has surfaced in association with dental anomalies. Homozygous mutations in *SMOC2*, a family member of extracellular calcium-binding proteins expressed in early embryogenesis (145, 146),

were reported to be the cause of autosomal recessive dentin dysplasia, microdontia, oligodontia (missing teeth), and teeth with altered morphology (147, 148). Studies of *smoc2* knockdown in zebrafish have demonstrated not only a phenotype resembling that of dentin dysplasia, but also that expression of tooth-forming genes *dlx2*, *bmp2*, and *pitx2* was dysregulated (148). With our expanding knowledge of the spectrum of phenotypes, advances in diagnosis and genetic research for RDD are key to have the opportunity to provide more than full-mouth prosthodontic rehabilitation for patients.

Current dentin disease therapies

As one might imagine, losing teeth unexpectedly and due to unknown etiology (lack of trauma or minimal dental caries) is devastating. Unfortunately, a biologically regenerative option has not been yet possible for individuals afflicted with heritable dentin diseases such as RDD. Oral hygiene measures are most important to prevent further loss of connective tissue support around mobile teeth; this is often difficult to maintain due to tooth sensitivity and relentless periodontal attachment weakening (117, 149). Until more is known about the pathological etiology, we must focus on restoring dental function and esthetics. Presently, treatment of dentin mineralization disorders includes removal of painful, infected, hypermobile teeth; root canal therapy in teeth with long roots to replace pulp tissue with a rubber-like filler and hopefully resolve periapical radiolucencies. Bone grafts and sinus elevations to restore resorbed jaw bone due to absent tooth roots, and complex full-mouth rehabilitation procedures involving the fabrication of complete dentures and/or placement of dental implants and crowns (107, 113, 118, 119, 138, 149, 150). Treatment often begins in childhood and extends

throughout adulthood. As with any dental treatment, the best outcomes are most often due to the best planning. For proper planning to be in place, dentists, especially pediatric specialists, must be adept at recognizing the signs of dentin disorders in their patients and formulating treatment plans.

Murine Models for Tooth Formation Studies

The studies performed using mouse models over the past several decades have contributed largely to our current level of understanding of tooth formation. Murine specimens have been popular in dental research for a multitude of reasons. Though the *Drosophila* species (non-vertebrate) does not develop teeth, a high degree of evolutionarily conserved dental gene sequences are found in fruit flies, mice, non-human primates, and humans. Genetic similarities among mice and higher phylogenic groups of vertebrates have also facilitated a multitude of gene promoter and gene activation/silencing studies to be performed, with findings extrapolated to human conditions. Because mice may begin reproduction at eight weeks of age, and with the gestation period lasting between 19 to 21 days, a mouse population may expand relatively quickly. A female mouse may give birth to five litters per year, with an average of six to eight pups born in each litter, allowing for sample size to be achieved readily. Finally, compared to larger vertebrates such as dogs, mouse populations are more easily and economically maintained.

Considering the favorable aspects of using mouse models, one must also be aware of the differences in dental anatomy between mice and humans. The murine dentition, consisting of a single incisor and three molars in each quadrant, is reduced compared to

that of humans, which generally develop sequential sets of dentition (primary or deciduous and secondary or permanent). The adult human dentition includes two incisors, one canine, two bicuspid, and at least two molars per quadrant. The mouse incisor is distanced from the triad of molars via a diastema, or gap; additionally, the four murine incisors grow continually throughout life due to a pool of cervical stem cells instead of a conventional root structure (9). Stages of dental development begin in mice at embryonic day 10 (initiation), with predentin formation starting at embryonic day 19 and tooth eruption concluding at about postnatal day 30 (15). Despite these variations in morphology and tooth count between mice and man, similar molecular and cellular mechanisms have been shown to drive all mammalian tooth formation events.

Summary and Dissertation Objective

Odontoblasts are critical cellular members of the dental pulp, and when their function is disturbed, tooth formation and function are compromised. The past two decades of dental research have highlighted a multitude of signaling molecules with proven roles in odontoblast differentiation and dentinogenesis, though many dots remain unconnected and there remains much to be learned about how a tooth crown and root are formed. During the research conducted in part for this dissertation, two major goals were pursued: (1) explore the effect of hyperactive TGF- β 1 on tooth development and (2) investigate the significance of MEPE in dentinogenesis. Taken together, these studies will provide novel insight in understanding molecular regulation of odontoblast differentiation and mineralization by TGF- β and may lead to developing new strategies

for treating patients with pulpal calcification due to attrition, erosion, dental restorations, trauma, and various mineralization disorders of the bones and teeth.

CHAPTER 2
REDUCED DENTIN MATRIX PROTEIN EXPRESSION IN CAMURATI-
ENGELMANN DISEASE TRANSGENIC MOUSE MODEL

by

ANGELA GULLARD, CHRISTINA CRONEY, XIANGWEI WU, OLGA MAMAEVA,
PHILIP SOHN, XU CAO, MARY MACDOUGALL

Journal of Cellular Physiology

Copyright
2015
by
Wiley-Blackwell

Used by permission

Format adapted for dissertation

ABSTRACT

Overexpression of transforming growth factor-beta 1 (TGF- β 1) has been shown to lead to mineralization defects in both the enamel and dentin layers of teeth. A *TGFB1* point mutation (H222D), derived from published cases of Camurati-Engelmann disease (CED), has been shown to constitutively activate TGF- β 1, leading to excess bone matrix production. Although CED has been well documented in clinical case reports, there are no published studies on the effect of CED on the dentition. The objective of this study was to determine the dental manifestations of hyperactivated TGF- β 1 signaling using an established mouse model of CED-derived TGF- β 1 mutation. Murine dental tissues were studied via radiography, micro-CT, immunohistochemistry, and qRT-PCR. Results showed that initial decreased dental mineralized tissue density is resolved. Proliferation assays of incisor pulp and alveolar bone cell cultures revealed that cells from transgenic animals displayed a reduced rate of growth compared to alveolar bone cultures from wild-type mice. TGF- β family gene expression analysis indicated significant fold changes in the expression of *Alpl*, *Bmp2-5*, *Col-1*, -2, -4 and -6, *Fgf*, *Mmp*, *Runx2*, *Tgfb3*, *Tfibr3*, and *Vdr* genes. Assessment of SIBLINGs reveals downregulation of *Ibsp*, *Dmpl*, *Dspp*, *Mepe*, and *Spp1*, as well as reduced staining for BMP-2 and VDR in mesenchymal-derived pulp tissue in CED animals. Treatment of dental pulp cells with recombinant human TGF- β 1 resulted in increased SIBLING gene expression. Conclusions: Our results provide *in vivo* evidence suggesting that TFG- β 1 mediates

expression of important dentin extracellular matrix components secreted by dental pulp, and when unbalanced, may contribute to abnormal dentin disorders.

INTRODUCTION

Mineralized tissue development occurs through a series of molecule-driven tissue changes. A progressive disease involving expansion and sclerosis of the diaphyses and cranial hyperostosis, Camurati-Engelmann disease (CED, MIM#131300) was first described in 1920 (Cockayne, 1920; Sparkes and Graham, 1972). Camurati (1922) and Engelmann (1929) described similar case reports and suggested a genetic predisposition due to multiple cases in families. Also known as progressive diaphyseal dysplasia, CED causes severe limb pain, muscle weakness, a characteristic waddling gait, headaches, fatigue, blindness, and deafness (Sparkes and Graham, 1972; Neuhauser *et al.*, 1948). Thought to be transmitted in an autosomal dominant fashion, it was shown by Janssens and colleagues (2000) that CED occurs due to heterozygous mutations in the transforming growth factor-beta 1 gene (*TGFB1*), found on human chromosome 19q13. TGF- β 1, a ubiquitous component of extracellular matrix (ECM) throughout the body (Saharinen *et al.*, 1999; Hyytiäinen *et al.*, 2004), was initially identified in neoplastic tissues (Derynck *et al.*, 1985). *Tgfb1* has been shown to be expressed as early as embryonic day 13 in the oral epithelium of murine molars and becomes confined to ectomesenchymal tissue, namely the odontoblasts, during tooth formation (Vaahtokari *et al.*, 1991; D'Souza *et al.*, 1998). When *Tgfb1* is knocked out, mice only live to approximately one month of age and suffer from systemic inflammatory cell infiltration, altered cartilage growth plates, and reduced mineralization of long bones (Kulkarni and

Karlsson, 1993). Interestingly, dental abnormalities in *Tgfb1* ^{-/-} mice are not apparent histologically, and *Tgfb1* deficiency is speculated to be compensated for by TGF- β 2 and - β 3, as well as maternal TGF- β 1 (D'Souza and Litz, 1995). On the contrary, excess TGF- β 1 in dental pulp leads to increased collagen and dentin extracellular matrix (DECM) production yet reduced dentin sialophosphoprotein (DSPP) production, while enamel is lost due to defective ameloblast function (Thyagarajan *et al.*, 2001; Haruyama *et al.*, 2006).

To gain more insight into the specific effects of excess TGF- β 1 on DECM production and tooth formation, experiments focused on dental pulp and molars, starting from newborn to three and a half months postnatal using an established mouse model of CED (Tang *et al.*, 2009). This CED mouse model develops a novel phenotype mimicking progressive diaphyseal dysplasia. We present here a detailed analysis of this phenotype and discuss the role of TGF- β 1, as well as potential downstream molecular targets, in dentinogenesis. Overall, results of the present study identified that although *in vivo* dental matrix formation is disrupted, resolution of the phenotype occurred even with dysregulation of TGF- β /BMP family members.

MATERIALS AND METHODS

Transgenic TGFB1 mice with CED-derived mutation

The animal study was approved by the Institutional Animal Care and Use Committee at the University of Alabama at Birmingham (internal animal project number: 131009954), and was conducted in compliance with IACUC guidelines. For all studies, only male

C57B/L6 wild-type (WT) and CED-transgenic *TGFB1* mice were studied to limit possible effects of estrogen on bone remodeling.

The transgenic CED mouse model was generated with a CED-derived TGF- β 1 point mutation (H222D) driven by the *Colla1* promoter (Tang *et al.*, 2009). Genotyping was performed as previously described (Tang *et al.*, 2009). WT and CED (transgenic *TGFB1*) mouse specimens were collected and studied at the following ages: newborn (NB), and postnatal days (PN) 3, 9 (data not shown), 28, and 105.

Murine primary cell cultures

WT and CED incisor pulp and alveolar bone samples were harvested from male littermates 105 days of age (3.5 months old). Primary explant cultures were cultivated using α -MEM media containing 10% FBS and 50 μ M ascorbic acid, supplemented with 10 μ M beta-glycerophosphate in 6-well plates until reaching approximately 70% confluence. Cultures were then expanded and maintained for the studies described below.

Immortalized murine dental cell lines

Mouse dental pulp mesenchymal (MD10-A11) and odontoblast-like (MD10-A2 and M06-G3) cells were plated and cultured to 80% confluence under culture conditions as previously described (MacDougall *et al.*, 2008).

Cell proliferation

The CellTiter 96® AQueous One Solution Cell Proliferation Assay (Promega, Madison, WI) was used according to manufacturer's instructions to determine proliferation rates of incisor pulp cells. Cells were seeded to 96-well plate at a concentration of 10⁴ cells/ml

and cell turnover was assayed every other day from day 1 to day 9. Error bars indicate standard deviation; n=8 for each group at each time point.

Alkaline phosphatase cytochemistry

Primary cultures (passage 5) from incisor pulp of 3.5-month-old WT C57BL/6 male mice were cultivated for 3 days and then assayed for presence of alkaline phosphatase using a cytochemical staining kit (Sigma-Aldrich, St. Louis, MO; catalog #85L-2) following manufacturer's instructions.

Radiographic and micro-computed tomographic analysis

Formalin-fixed sagittal cranial halves of WT and CED mice were examined. Radiography of specimens was performed using the MX-20 Cabinet X-ray System for 10 s at 18 kV (Faxitron X-Ray Corporation, Lincolnshire, IL). To examine three-dimensional (3D) tooth structure, the specimens were scanned by a Scanco μ CT40 desktop cone-beam scanner (Scanco Medical AG, Brüttisellen, Switzerland) using 20 mm specimen tubes. Scans were performed at the following settings: 10 μ m resolution, 70kVp, 114 μ A with an integration time of 200ms. Scans were automatically reconstructed into 2D slices, and the regions of interest were outlined in each slice using μ CT Evaluation Program (v5.0A, Scanco Medical). 3D reconstructions were generated and assessed for relative mineralized tissue content. Six male, 28-day-old, C57BL/6 littermates, three WT and three transgenic mutant TGF- β 1 (CED) mice, were analyzed initially. Teeth from 105-day-old littermates (n=3 each group) were also analyzed. Nikon imaging software (NIS-Elements, Melville, NY) was used to perform measurements of tooth parameters.

Quantitative reverse-transcription PCR (qRT-PCR)

Mandibular incisors of 105-day-old male WT and CED mice were dissected and used for qRT-PCR analysis of tooth matrix gene expression. Total mRNA was isolated using RNA STAT-60 (Tel-Test, Inc., Friendswood, TX), converted to cDNA with TaqMan Reverse Transcriptase Reagents (Applied Biosystems, Carlsbad, CA), and used for real time PCR amplification of tooth transcripts using an ABI PRISM 7000 Sequence Detection System (Applied Biosystems). Reaction wells for each gene assessed were performed in triplicate. Each reaction well contained 12.5ul of 2X SYBR Green mix (Applied Biosystems), 10.5ul of primer mix (5 pmoles of each primer), and 2ul of template (cDNA or control) for a total volume of 25ul. Thermal cycler parameters were 50°C for 1 s, 95°C for 10 min, and 40 cycles of 95°C for 15 s and 60°C for 1 min. Raw data were normalized against *Gapdh* mRNA levels in each corresponding sample, and results are shown as relative quantities of cycle changes in steady-state transcription of a gene. Commercial primer sets (SABiosciences/Qiagen, Germantown, MD) for the following genes were utilized according to manufacturer's instructions: *Gapdh*, *Acvr1*, *Bmpr1a*, *Bmpr1b*, *Colla1*, *Dmpl*, *Dspp*, *Ibsp*, *Mepe*, *Nfic*, *Spp1*, *Tgfb1*, and the mouse osteogenesis pathway PCR array (cat no. PAMM-026Z). Data were analyzed and reported using the RT² Profiler PCR Array Data Analysis version 3.5 (SABiosciences).

Immunohistochemistry

Histological sections of 3dPN and 9dPN WT and CED mouse incisors were prepared from paraffin-embedded tissue blocks, deparaffinized and rehydrated. Sodium citrate

antigen retrieval was then performed and the sections were subsequently blocked in 3% goat serum and 1% bovine serum albumin (BSA) in PBST for 20 min at room temperature before incubation with primary antibodies. Sections were then incubated with rabbit polyclonal antibodies anti-BMP-2 (1:200; NBP1-19751, Novus Biologicals, Littleton, CO) and anti-VDR (1:7,000; ab3508, Abcam, Cambridge, MA) overnight at 4°C. The following day, the sections were incubated with a broad spectrum HRP Polymer conjugate (SuperPicture™ 3rd Gen IHC Detection Kit, Invitrogen, Waltham, MA), visualized with DAB, washed, counterstained with hematoxylin (Sigma-Aldrich, St. Louis, MO), and mounted. All images were made with an inverted microscope (Nikon Instruments, Tokyo, Japan) at 4x, 10x, and 40x magnification.

TGF- β 1 treatment experiments

Reconstitution of recombinant human TGF- β 1 (cat no. 240-B-010, R&D Systems, Minneapolis, MN) was performed according to manufacturer's instructions. Aliquots at 5ng/ml and 10ng/ml concentrations were stored at -80°C and thawed just prior to *in vitro* treatments. Cell culture wells were incubated with TGF- β 1 treatments for 48 hours prior to harvesting whole cell protein lysate using RIPA lysis buffer system (Santa Cruz Biotechnology, Inc.) according to manufacturer's instructions. Expression of Smad2/3 and pSmad2 was achieved using anti-Smad2/3 (1:1500, BD Biosciences, Franklin Lakes, NJ) and anti-pSmad2 (1:500, Cell Signaling, Beverly, MA) antibodies. Beta-actin was used as a loading control (1:10,000, Sigma-Aldrich). Protein expression analysis was carried out and visualized according to the LI-COR Biosciences (Lincoln, NE) Western blot protocol using the Odyssey Classic (LI-COR) imaging equipment.

RESULTS

Decreased Density and Volume in CED Mouse Molars

Initially, 1-month-old male CED mice were identified as having tooth morphology differences compared to WT littermates (Fig. 1A, F). The mandibular incisors of the transgenic mice grew much longer and a diastema developed between these teeth. Animals with moderate-severe difficulty in jaw closure were euthanized due to inadequate feeding ability. Fracturing of lower incisors was not noted. Radiology revealed thinning of mandibular incisors, radiographic absence of maxillary incisors, and a lesser mineralized cranium (Fig. 1G, H) in CED mice versus controls (Fig. 1B, C). Upon further investigation of a separate set of male 1-month-old littermates, radiography revealed no discernible differences in cranial mineralization (Fig. 1D, I). Similarly, a third set of male littermates followed to 3.5 months of age also demonstrated comparable mineralization patterns (Fig. 1E, J).

Micro-computed tomography (μ CT) of the initial 1-month-old littermates confirmed the differences in tooth structure and density. While the mineralized tissue density (dentin and enamel assessed) of the WT mouse incisors was 15% less than that of CED mouse littermates, the total tooth volume of WT incisors was comparable (5% greater) compared to CED animals (Fig. 2A, D, numerical data not shown). Interestingly, the mineralized tissue density of the WT mouse molar was 30% greater than the CED mouse counterpart, and the total tooth volume of the WT molar was 20% greater than the CED mouse molars (Fig. 2B, E, numerical data not shown). The 3D reconstructions of the mandible (Fig. 2C, F) allowed for visualization of the mal-positioning of incisors in the CED mouse.

Upon assessment of first mandibular molars from 3.5-month-old mice, μ CT studies indicated that density and volume (Fig. 3C, E) area shown as parameter on graph, multiplied by factor of 1 as calculated by μ CT imaging software) of enamel and dentin were comparable in WT and CED mouse specimens (Fig. 3A, B). Furthermore, determination of crown and root molar measurements (Fig. 3D) also demonstrated similar values between WT and CED samples. Analysis revealed that crown height measured from most coronal portion of cuspal region to CEJ was comparable among WT and CED specimens. Furthermore, molar crown height and width and root length measurements varied between groups, mostly within 50 μ m differences. In contrast to the 1-month-old mice studied, 3.5-month-old animals showed no significant radiographic or densitometry variances among littermates, regardless of the genotype.

Reduced Cell Proliferation and Mineralization Potential of CED Dental Cells

To assess whether cellular turnover and mineralization potential may be at least partially responsible for the tooth phenotype seen in 1-month-old animals, primary cell cultures obtained from 3.5-month-old WT and CED mouse incisors were utilized. After seeding pulp cells to 6-well culture dishes and allowing cultures to reach approximately 70% confluence over the course of 72 hours, images of cell cultures were made (Fig. 4A) and dental pulp cells were stained for alkaline phosphatase activity (Fig. 4B). WT pulp cells demonstrated much more robust staining as compared to CED cells, indicating reduced potential for CED pulp cells to secrete mineralization proteins. Cell proliferation was evaluated over the course of 9 days, and CED dental pulp and alveolar bone cell cultures failed to demonstrate increasing replication over time. Contrarily, WT pulp and alveolar

bone cell cultures expanded with each time point assessed, with the exception of day 9 for the WT alveolar bone cells (Fig. 4C, D).

Altered Gene Expression of TGF- β /BMP Signaling Pathway Molecules

In order to determine how members of the TGF- β /BMP superfamily of signaling molecules may be affected by hyperactivated TGF- β 1 levels, quantitative real-time PCR studies were carried out utilizing a commercial PCR array providing data on 84 members of the signaling family. Primary cell cultures of incisor pulp from 3.5-month-old WT and CED mice were harvested for this study. The fold change data collected revealed significant overexpression of *Bmp2*, *Bmp3*, *Col1a1*, *Col2a1*, and *Tgfb3*, and significant underexpression of *Alpl*, *Bmp4*, *Bmp5*, *Col12a1*, *Col14a1*, *Col6a1*, *Col6a2*, *Fgf1*, *Fgfr2*, *Gdf10*, *Icam1*, *Igf1r*, *Mmp10*, *Mmp8*, *Runx2*, *Tgfb3*, *Tnf*, and *Vdr* (Fig. 5).

We assessed levels of downstream molecules of TGF- β /BMP signaling which are also known to be involved in mineralized tissue and tooth formation: *Acvr1*, *Bmpr1a*, *Bmpr1b*, and *Nfic*. The fold change of these genes in CED alveolar bone cells alone revealed substantial downregulation of *Acvr1*, *Bmpr1a*, and *Nfic* and upregulation of *Bmpr1b*, with relatively no difference in fold change for CED dental pulp cells (Fig. 6A).

Decreased Levels of SIBLINGs in CED Pulp Cells

To confirm whether the observed phenotype was due to lower SIBLING protein levels in teeth of the CED mice, we performed quantitative real-time PCR using primary cell cultures from 3.5-month-old mice. Fold change expression levels on a logarithmic scale were calculated from relative expression of the five SIBLING genes: *Ibsp*, *Dmp1*, *Dspp*,

Mepe, and *Spp1* (Fig. 6B). Levels of *Colla1* were examined as a positive control, and as expected, *Colla1* levels were 3-fold greater in CED dental pulp cells as compared to WT. Levels of all five SIBLING genes as well as that of *Tgfb1*, were underexpressed in CED pulp cells as compared to control; the greatest decline in fold change was seen for *Ibsp* in both CED pulp and alveolar bone cell samples.

Decreased Levels of TGF- β /BMP Pathway Molecules in CED Dental Pulp Tissue

In order to assess expression of TGF- β /BMP pathway molecules *in vivo*, we also performed immunohistochemical analysis on the cross-sections of the mandibular incisors from 3-day-old mice, the age at which dentin matrix protein secretion is underway and mineralization events begin. BMP-2 and VDR levels were previously shown to exhibit 4-fold upregulation and downregulation, respectively, in CED incisor pulp cells from 3.5-month-old animals. Anti- Using anti-BMP-2 and anti-VDR antibodies were used to evaluate BMP-2 and VDR protein expression in incisor dental pulp (Fig. 7A, C), as well as surrounding oral epithelium (Fig. 7B, D) of WT and CED specimens. Similarly, VDR expression was assessed in dental pulp (Fig. 7G, I) and oral epithelium (Fig. 7H, J). Interestingly, BMP-2 and VDR expression was observed to be stronger in the dental pulp and odontoblast layer of WT tissue compared to that of CED specimens. Oral epithelial tissue also exhibited decreased expression in both WT and CED tissue. Negative controls (Fig. 7E, F) demonstrated no staining, as expected.

Activation of TGF- β Pathway in Mouse Dental Pulp Cells

As a comparison with primary cell cultures obtained from dental pulps of WT and transgenic *TGFB1* (CED) mice, we performed an *in vitro* study treating immortalized mouse dental pulp cells with 5ng/ml and 10ng/ml recombinant human TGF- β 1 (rhTGF- β 1). Activation of TGF- β pathway signaling was demonstrated by robust expression of downstream intracellular indicator pSmad2 in MD10-A11 mouse dental pulp cells (Fig. 8A). Levels of *Colla1* increased 1-2-fold compared to treatment groups receiving no rhTGF- β 1. Levels of *Dmp1*, *Dspp*, and *Mepe* increased to up to 3-fold overexpression with 48-hour exposure to 10ng/ml rhTGF- β 1 (Fig. 8B). Contrarily, the mouse odontoblast-like cell treatment groups (MD10-A2, MO6-G3) displayed faint bands for pSmad2 (Fig. 8A). While the fold change for *Colla1* in the MD10-A2 10ng/ml rhTGF- β 1 treatment group was nearly 6-fold greater than that of the group receiving no treatment (Fig. 8C), the fold change for *Colla1* in MO6-G3 cells was relatively unchanged compared to that of no treatment (Fig. 8D). Nevertheless, with the exception of *Dmp1* in MO6-G3 cells, a general trend of decreased fold-change of *Dmp1*, *Dspp*, and *Mepe* was observed in both sets of mouse odontoblast-like cells, with fold change that presented inversely proportional to the concentration of rhTGF- β 1 treatment.

DISCUSSION

The present study investigated the dental phenotype of a transgenic mouse bearing a mutated form of *TGFB1*, characterized by overexpression of TGF- β 1 in dental pulp cells. We first analyzed a pair of 1-month-old WT and CED mouse littermates, and identified the transgenic mouse displaying a severe tooth phenotype with volumetric and calcific

inadequacies (Fig. 1, 2). The fact that an analysis of animals from birth to 3.5 months of age did not reveal consistent findings, even at 1 month of age, suggests that, as in cases of humans with CED, the phenotype has variable penetrance and severity (Janssens *et al.*, 2006). Approximately 30% of littermates carried the CED transgene, and among these mice, not all of them exhibited the dental and cranial defects as seen in the first study of the 1-month-old CED mouse. The CED animals studied at 1 month and 3.5 months of age did not have overall dentin mineralization deficits, most likely due to the known variability and extent of CED (Fig. 3).

Interestingly, though radiographic differences in tooth formation were not visible at 3 days postnatal period (PN) (data not shown), immunohistochemical analysis revealed that several key regulators of dentin mineralization, including BMP-2 and VDR, were underexpressed in CED tissue (Fig. 7). BMP-2 is thought to enhance mineralization by stimulating pre-odontoblasts to differentiate to odontoblasts (Chen *et al.*, 2008), while a deficiency of VDR has been shown to lead to dentin hypomineralization (Zhang *et al.*, 2009). While dental tissues of 1-month-old WT and CED mice were not available for assessing BMP-2 and VDR protein expression, the decreased protein levels of these proteins may account for the reduced mineralized tissue density observed via radiography and μ -CT analysis in the initial pair of 1-month-old littermates. The negative fold change of SIBLING genes exhibited by CED dental pulp cells suggests that dentin matrix formation may be deficient at early stages of tooth formation (Fig. 6), and when this continues throughout tooth maturation, it may explain the volume and density differences in mandibular molars observed in the initial 1-month-old animals.

Despite a lack of morphological differences in mature teeth of 3.5-month-old mice, cellular dysregulation was still present, as evidenced by the diminished ability for cellular replication, lowered mineralization potential via reduced alkaline phosphatase gene expression and cellular staining, and decreased expression of SIBLING genes (Fig. 4, 6). Considering that tertiary dentin is secreted by odontoblasts after a tooth has erupted into the oral cavity, these differences in cellular activity and molecular expression likely do not result in a noticeable gross phenotype. However, with the CED-derived mutation expressed in the transgenic mice, it is known that excess TGF- β 1 is present (Tang *et al.*, 2009; Janssens *et al.*, 2003), and that enhanced TGF- β pathway signaling affects expression of DECM molecules, including BSP, DSPP, TGF- β receptors and SMAD proteins (D'Souza *et al.*, 1997; Hwang *et al.*, 2008; Salmon *et al.*, 2013). This effect was confirmed by the dysregulation of the TGF- β /BMP pathway signaling genes in CED pulp (Fig. 5).

Additionally, when dental pulp and odontoblast-like cell lines were treated with exogenous rhTGF- β 1, induction of downstream p-Smad2 signaling was demonstrated to be strongest in dental pulp cells alone (Fig. 8). These results suggest that undifferentiated dental pulp cells may have more receptors and other key molecules to orchestrate the cellular events of DECM secretion and mineralization. Furthermore, with rhTGF- β 1 treatment, the mouse dental pulp cells displayed underexpression in SIBLING gene levels at 5ng/ml rhTGF- β 1, but reverted to overexpression in *Dmp1*, *Dspp*, and *Mepe* levels with 10ng/ml rhTGF- β 1, suggesting a dose-dependent relationship of TGF- β 1 exposure and effects on expression of DECM mineralization genes. Similarly, mouse odontoblast-like cells displayed underexpression in SIBLING gene levels at both concentrations of

rhTGF- β 1, suggesting that an excess of TGF- β 1 may result in subdued mineralization events. These data suggest that in CED mice, at a threshold of excess TGF- β 1, dental tissues may receive signals to turn down secretion and maturation of dentin matrix molecules, leading to reduced structural volume and integrity of teeth. The fact that not all CED mice displayed the same dental phenotype indicates that compensatory mechanisms for managing excess TGF- β 1 may be in place so as not to disrupt the intricate processes of tooth formation.

The hyperactivated level of TGF- β 1 in CED mouse teeth may either be attenuated by compensatory signaling events or disrupt the downstream signaling cascade, which may result in problems with tooth development, namely dentin formation. While the precise molecular interactions among TGF- β 1 signaling pathway members and SIBLING proteins remain to be explored, it is known that decreased VDR and SIBLING protein levels are associated with deficient bone mineralization, impaired odontoblast function, and altered dentin mineralization (Zhang *et al.*, 2009; Salmon *et al.*, 2013; Thyagarajan *et al.*, 2001). More specifically, hypophosphatemia, dentinogenesis imperfecta, and dentin dysplasia are linked to reduced MEPE and DSPP levels (Maciejewska and Chomik, 2012; von Marschall *et al.*, 2012). In-depth investigation of the downstream TGF- β 1 signaling pathway will be necessary in order to target the specific molecular events that bring about these dentin/bone formation and mineralization disorders.

ACKNOWLEDGEMENTS

The authors received no financial support and declare no potential conflicts of interest with respect to the authorship and/or publication of this article. We thank the UAB Small

Animal Bone Phenotyping Core facility, with special recognition to Dr. Xingsheng Li, for assistance with the radiography and micro-computed tomography studies.

REFERENCES

- Camurati M. 1922. Di Uno raro caso di osteite simmetrica ereditaria degli arti inferiori. *Chir Organi Mov* 6:662-665.
- Chen S, Gluhak-Heinrich J, Martinez M, Li T, Wu Y, Chuang HH, Chen L, Dong J, Gay I, MacDougall M. 2008. Bone morphogenetic protein 2 mediates dentin sialophosphoprotein expression and odontoblast differentiation via NF- κ B signaling. *J Biol Chem* 283(28):19359-19370.
- Cockayne EA. 1920. Case for diagnosis. *Proc R Soc Med* 13(Sect Study Dis Child):132-136.
- Derynck R, Jarrett JA, Chen EY, Eaton DH, Bell JR, Assoian RK, Roberts AB, Sporn MB, Goeddel DV. 1985. Human transforming growth factor-beta complementary DNA sequence and expression in normal and transformed cells. *Nature* 316(6030):701-705.
- D'Souza RN, Litz M. 1995. Analysis of tooth development in mice bearing a TGF-beta 1 null mutation. *Connect Tissue Res* 32:41-46.
- D'Souza RN, Cavender A, Sunavala G, Alvarez J, Ohshima T, Kulkarni AB, MacDougall M. 1997. Gene expression patterns of murine dentin matrix protein 1 (Dmp1) and dentin sialophosphoprotein (DSPP) suggest distinct developmental functions in vivo. *J Bone Miner Res* 12(12):2040-2049.
- D'Souza RN, Cavender A, Dickinson D, Roberts A, Letterio J. 1998. TGF-beta1 is essential for the homeostasis of the dentin-pulp complex. *Eur J Oral Sci* 106(Suppl 1):185-91.
- Engelmann G. 1929. Ein fall von osteopathia hyperostotica (sclerotisans) multiplex infantilis. *Fortschr Geb Roentgenstr Nukl* 39:1101-1106.
- Haruyama N, Thyagarajan T, Skobe Z, Wright JT, Septier D, Sreenath TL, Goldberg M, Kulkarni AB. 2006. Overexpression of transforming growth factor-beta1 in teeth results in detachment of ameloblasts and enamel defects. *Eur J Oral Sci* 114(Suppl 1):30-4; discussion 39-41, 379.
- Hwang YC, Hwang IN, Oh WM, Park JC, Lee DS, Son HH. 2008. Influence of TGF-beta1 on the expression of BSP, DSP, TGF-beta1 receptor I and Smad proteins during reparative dentinogenesis. *J Mol Histol* 39(2):153-160.
- Hyttiäinen M, Penttinen C, Keski-Oja J. 2004. Latent TGF-beta binding proteins: extracellular matrix association and roles in TGF-beta activation. *Crit Rev Clin Lab Sci* 41(3):233-264.

Janssens K, Gershoni-Baruch R, Van Hul E, Brik R, Guañabens N, Migone N, Verbruggen LA, Ralston SH, Bonduelle M, Van Maldergem L, Vanhoenacker F, Van Hul W. 2000. Localisation of the gene causing diaphyseal dysplasia Camurati-Engelmann to chromosome 19q13. *J Med Genet* 37:245-249.

Janssens K, ten Dijke P, Ralston SH, Bergmann C, Van Hul W. 2003. Transforming growth factor-beta 1 mutations in Camurati-Engelmann disease lead to increased signaling by altering either activation or secretion of the mutant protein. *J Biol Chem* 278(9):7718-7724.

Janssens K, Vanhoenacker F, Bonduelle M, Verbruggen L, Van Maldergem L, Ralston S, Guañabens N, Migone N, Wientroub S, Divizia MT, Bergmann C, Bennett C, Simsek S, Melançon S, Cundy T, Van Hul W. 2006. Camurati-Engelmann disease: Review of the clinical, radiological, and molecular data of 24 families and implications for diagnosis and treatment. *J Med Genet* 43(1):1-11.

Kulkarni AB, Karlsson S. 1993. Transforming growth factor-beta 1 knockout mice. A mutation in one cytokine gene causes a dramatic inflammatory disease. *Am J Pathol* 143(1):3-9.

MacDougall M, Selden JK, Nydegger JR, Carnes DL. 2008. Immortalized mouse odontoblast cell line M06-G3 application for in vitro biocompatibility testing. *Am J Dent* 11(Spec No):S11-S16.

Maciejewska I, Chomik E. 2012. Hereditary dentine diseases resulting from mutations in DSPP gene. *J Dent* 40(7):542-548.

Neuhauser EB, Shwachman H, Wittenborg M, Cohen J. 1948. Progressive diaphyseal dysplasia. *Radiology* 51(1):11-22.

Saharinen J, Hyytiäinen M, Taipale J, Keski-Oja J. 1999. Latent transforming growth factor-beta binding proteins (LTBPs)--structural extracellular matrix proteins for targeting TGF-beta action. *Cytokine Growth Factor Rev* 10(2): 99-117.

Salmon B, Bardet C, Khaddam M, Naji J, Coyac BR, Baroukh B, Letourneur F, Lesieur J, Decup F, Le Denmat D, Nicoletti A, Poliard A, Rowe PS, Huet E, Vital SO, Linglart A, McKee MD, Chaussain C. 2013. MEPE-derived ASARM peptide inhibits odontogenic differentiation of dental pulp stem cells and impairs mineralization in tooth models of X-linked hypophosphatemia. *PLoS One* 8(2):e56749.

Sparkes RS, Graham CB. 1972. Camurati-Engelmann disease. Genetics and clinical manifestations with a review of the literature. *J Med Genet* 9:73-85.

Tang Y, Wu X, Lei W, Pang L, Wan C, Shi Z, Zhao L, Nagy TR, Peng X, Hu J, Feng X, Van Hul W, Wan M, Cao X. 2009. TGF-beta1-induced migration of bone

mesenchymal stem cells couples bone resorption with formation. *Nat Med* 15(7):757-765.

Thyagarajan T, Sreenath T, Cho A, Wright JT, Kulkarni AB. 2001. Reduced expression of dentin sialophospho-protein is associated with dysplastic dentin in mice overexpressing transforming growth factor-beta 1 in teeth. *J Biol Chem* 276(14):11016-11020.

Vaahrokari A, Vainio S, Thesleff I. 1991. Associations between transforming growth factor beta 1 RNA expression and epithelial-mesenchymal interactions during tooth morphogenesis. *Development* 113(3):985-994.

von Marschall Z, Mok S, Phillips MD, McKnight DA, Fisher LW. 2012. Rough endoplasmic reticulum trafficking errors by different classes of mutant dentin sialophosphoprotein (DSPP) cause dominant negative effects in both dentinogenesis imperfecta and dentin dysplasia by entrapping normal DSPP. *J Bone Miner Res* 27(6):1309-1321.

Zhang X, Beck P, Rahemtulla F, Thomas HF. 2009. Regulation of enamel and dentin mineralization by vitamin D receptor. *Front Oral Biol* 13:102-109.

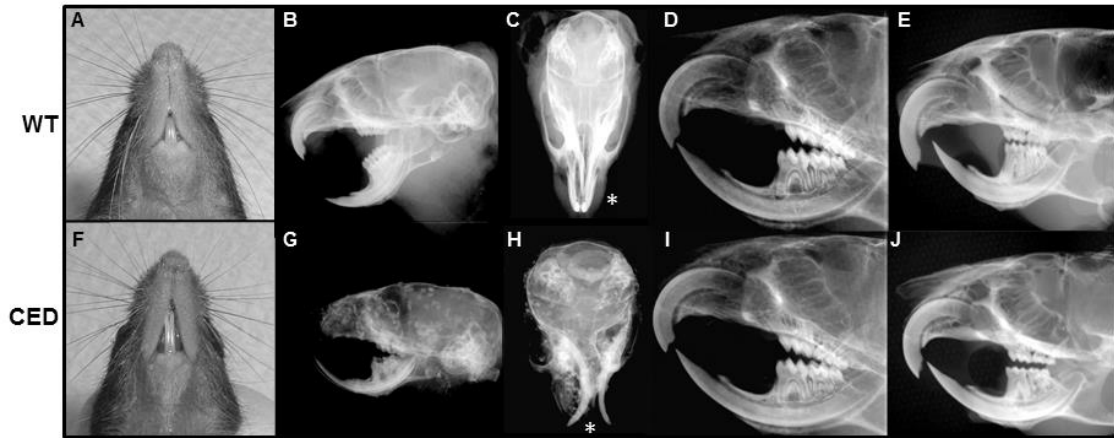


Figure 1 – 28-day-old male littermates: Gross view of (A) WT dentition and (F) CED dentition. Sagittal radiographs of (B) WT hemi-cranium and (G) CED hemi-cranium. Transverse radiographs of (C) WT cranium and (H) CED cranium; asterisks (*) indicate mandibular incisors. Separate set of 28-day-old male littermates: (D) WT hemi-cranium and (I) CED hemi-cranium. Separate set of 105-day-old male littermates: Sagittal radiographs of (E) WT hemi-cranium and (J) CED hemi-cranium.

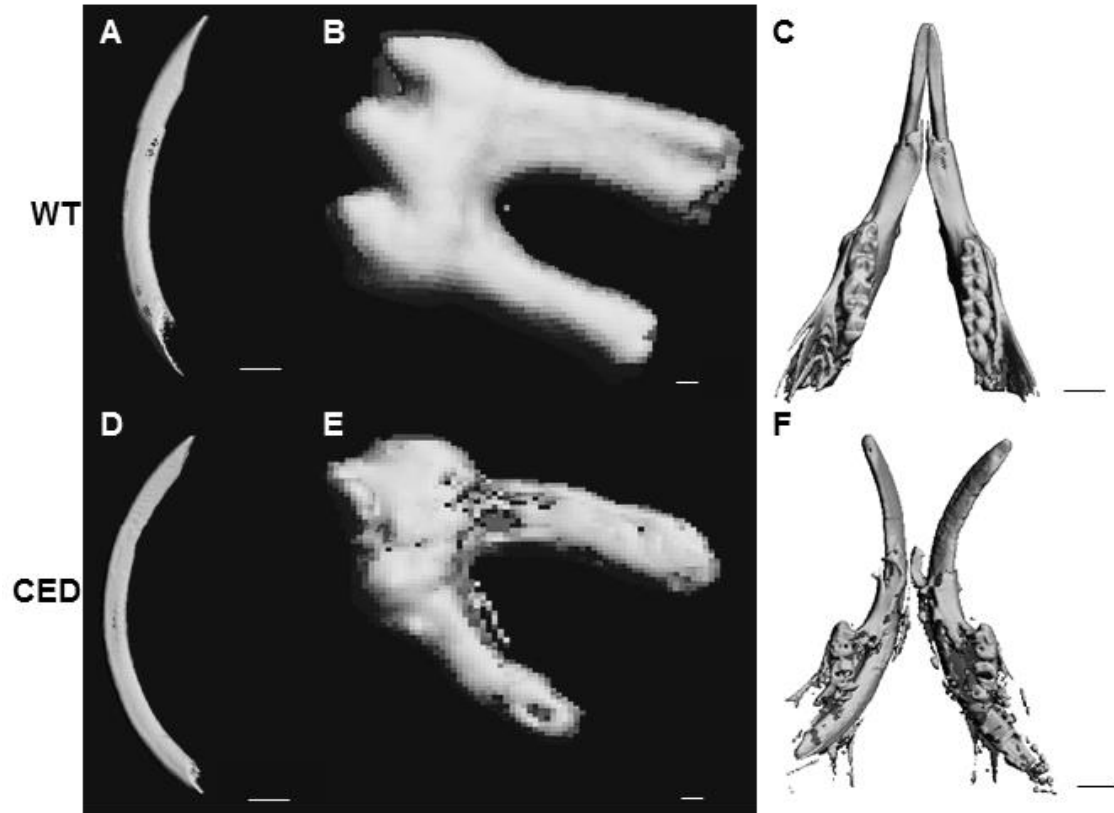


Figure 2 – Micro-computed tomographic (μ CT) 3D reconstructions of 28-day-old male WT and CED littermate specimens. WT mouse mandibular incisor (A), mandibular first molar (B), and (C) mandible. CED mouse mandibular incisor (D), mandibular first molar (E), and mandible (F). Scale bar = 1.0mm (A, C, D, F); = 100 μ m (B, E).

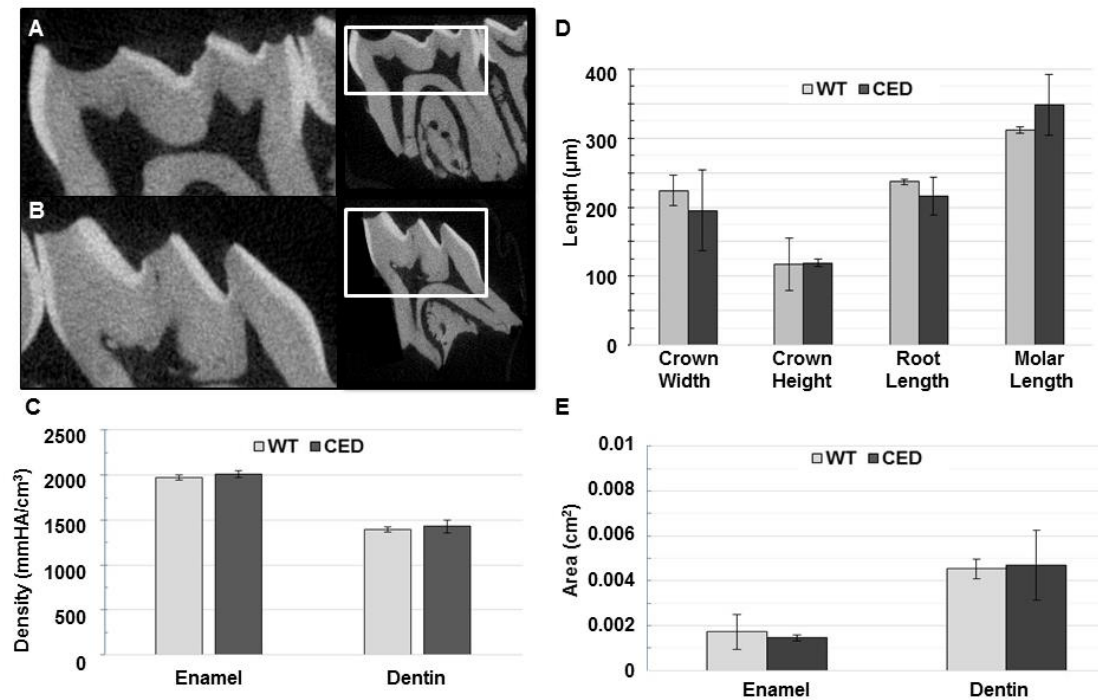


Figure 3 – μ -CT 2D sagittal micrographs of WT (A) and CED (B) mandibular first molars harvested from 105-day-old male littermates; inset to right identifying magnified coronal portion of tooth. Radiodensity measurements obtained from entire range of 500+ 2D tomographs: enamel and dentin relative density (C), crown and root components (D), and enamel and dentin relative area (E) of WT and CED specimens; n=3.

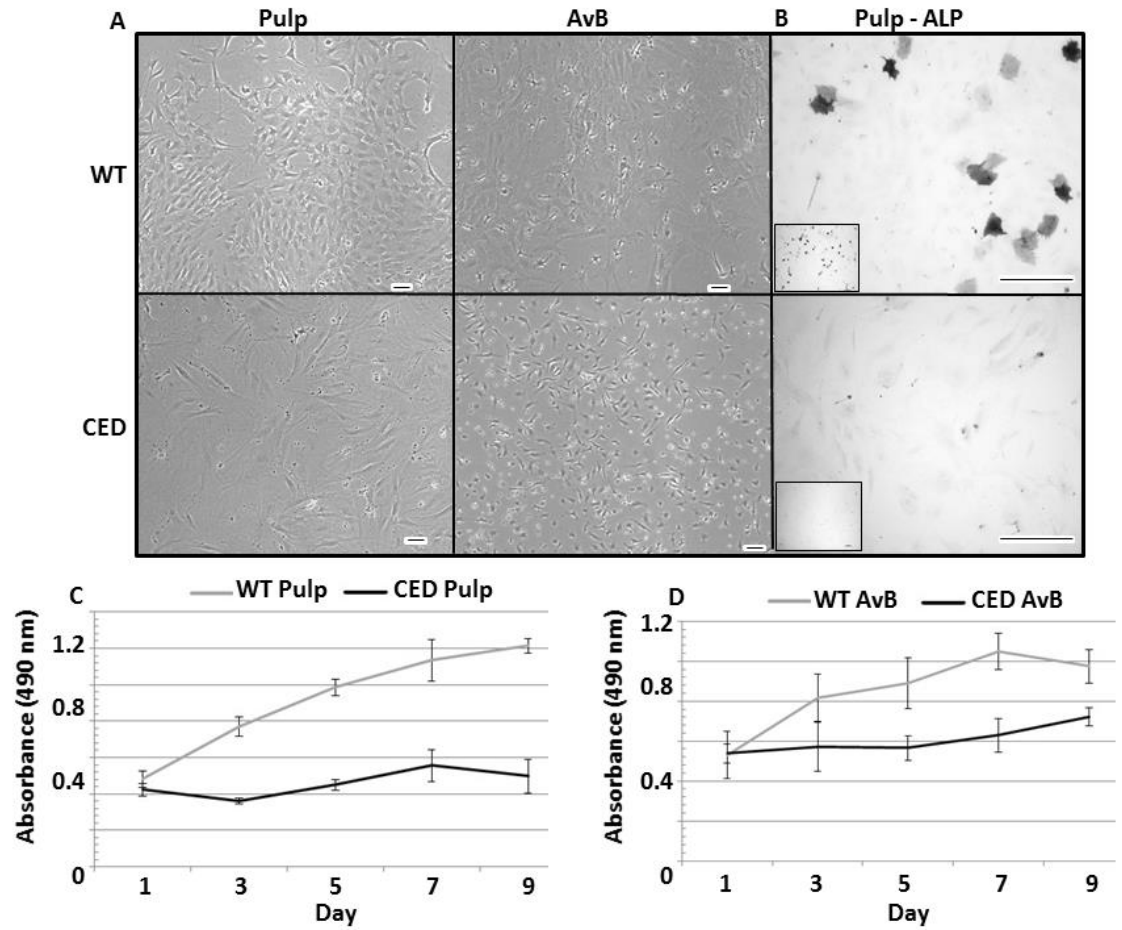


Figure 4 – Primary cell culture morphology and growth kinetics. Light micrographs of primary cultures of incisor pulp and alveolar bone of 105-day-old WT and CED littermates; scale bar = 50 μ m and magnification 10x (A). Pulp cells were cultured for 72 hours after seeding to culture well and then stained for alkaline phosphatase positivity; scale bar = 250 μ m and magnification 40x (B). Cell proliferation assay of primary cultures of WT and CED pulp (C) and alveolar bone (D) harvested from 105-day-old littermates; n = 3.

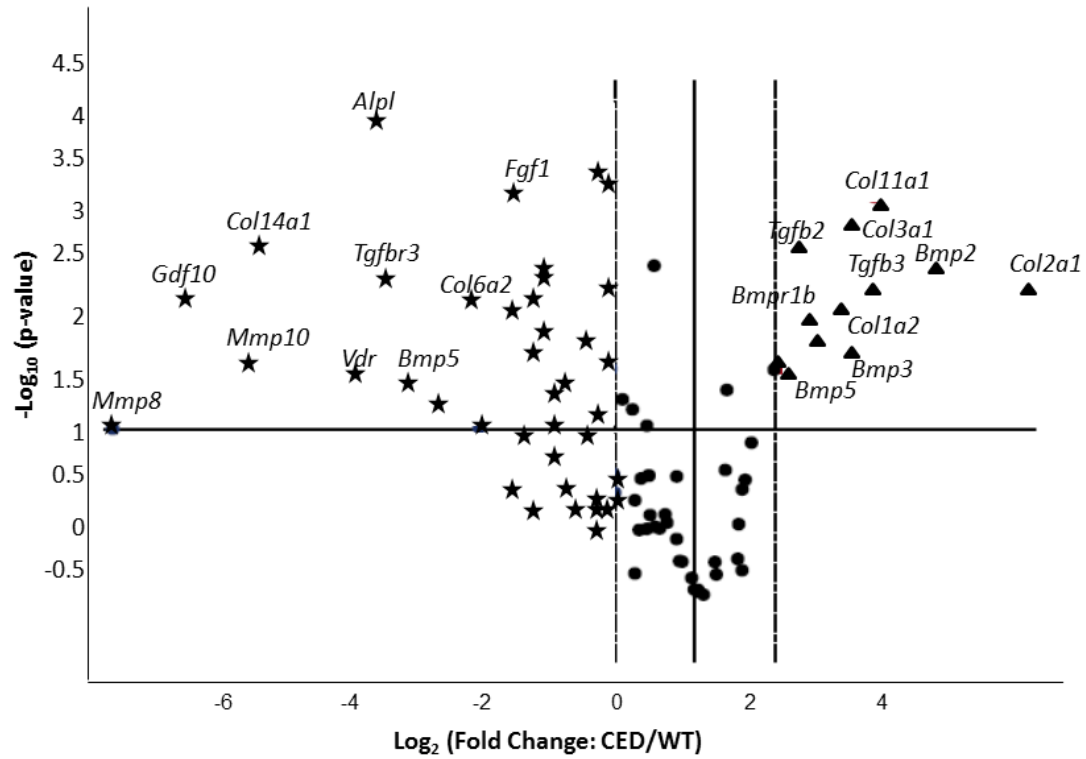


Figure 5 – Quantitative reverse transcriptase PCR microarray performed using cDNA of incisor pulp cells harvested from 105-day-old WT and CED male littermates. Volcano plot demonstrating relative downregulation (stars) and upregulation (triangles) of TGF- β /BMP family gene expression in CED pulp vs. WT pulp; $n = 3$, $p < 0.05$.

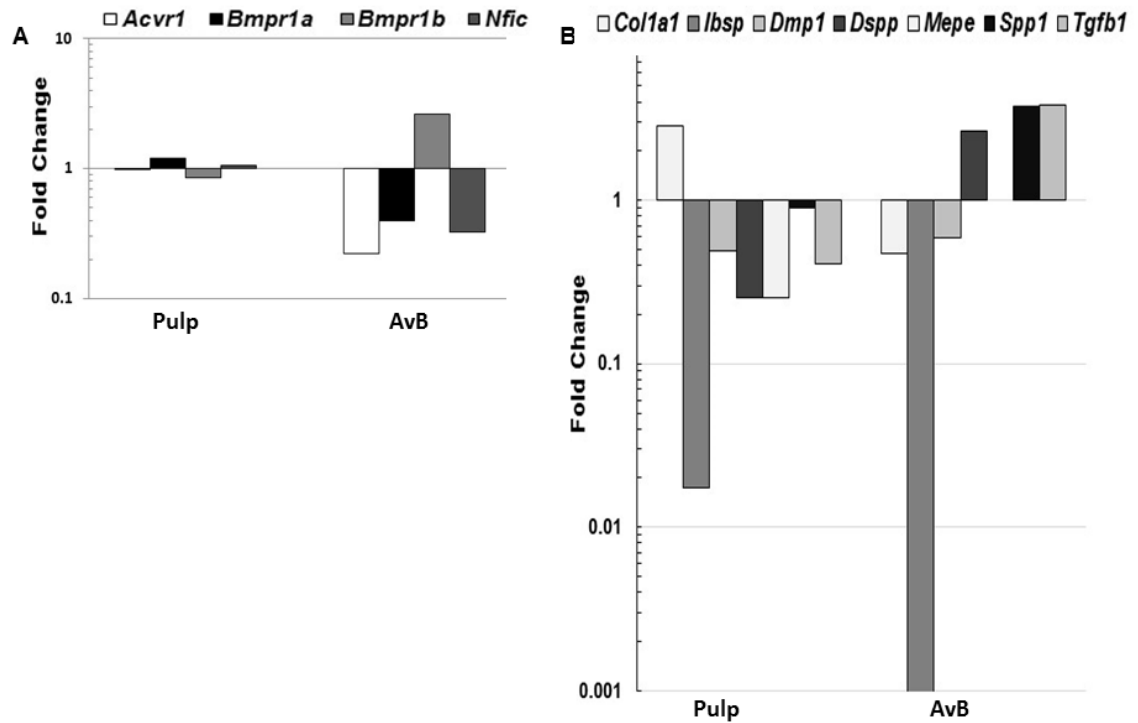


Figure 6 - Quantitative reverse transcriptase PCR performed using cDNA derived from 105-day-old WT and CED male littermates. Fold change of *Acvr1*, *Bmpr1a/b*, and *Nfic* in CED pulp and alveolar bone cells compared to WT (A). Fold change of *Col1a1*, SIBLING genes (*Ibsp*, *Dmp1*, *Dspp*, *Mepe*, *Spp1*), and *Tgfb1* in CED pulp and alveolar bone cells as compared to WT (B); n = 3.

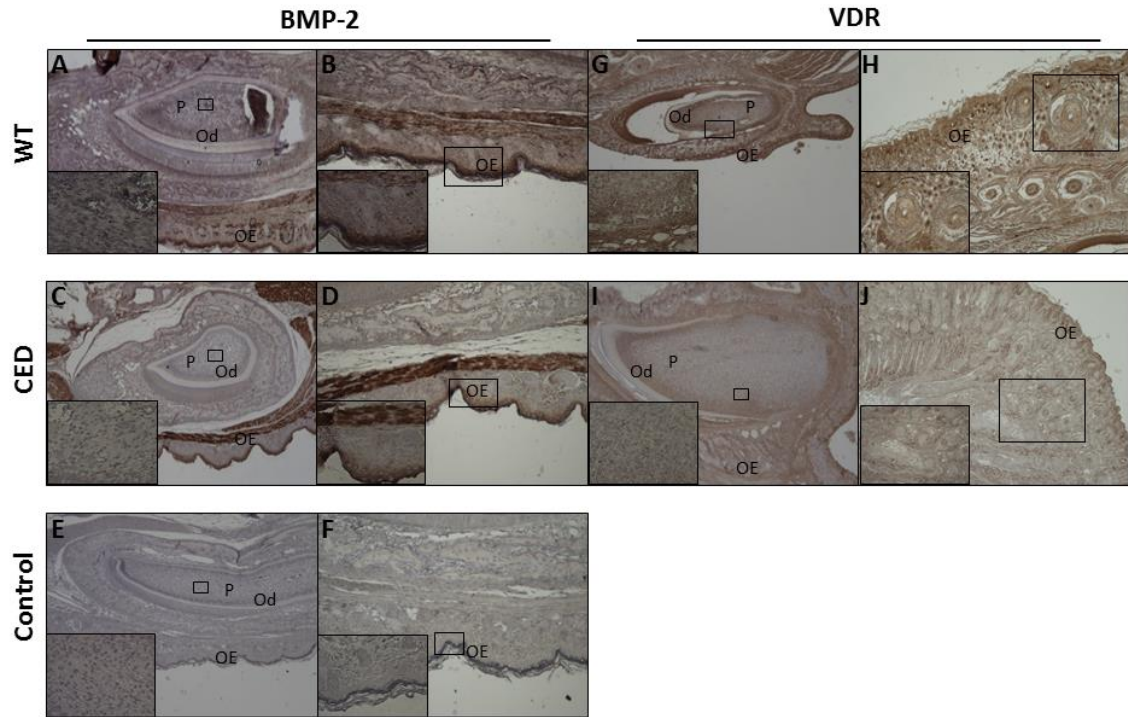


Figure 7 - Immunohistochemistry of 3dPN and 9dPN WT and CED mouse incisors. WT and CED incisors were stained for BMP-2 (3dPN, A-D) or VDR (9dPN, G-J), counterstained with hematoxylin, and visualized at 4x, 10x, and 40x (inserts) magnification. Control indicates no primary antibody control (E-F). Images depicted show the incisor and pulp (inserts) (A, C, E, G, I), epithelial layer (B, D, F), and hair follicles (H, J). P – dental pulp; Od – odontoblasts; OE – oral epithelium.

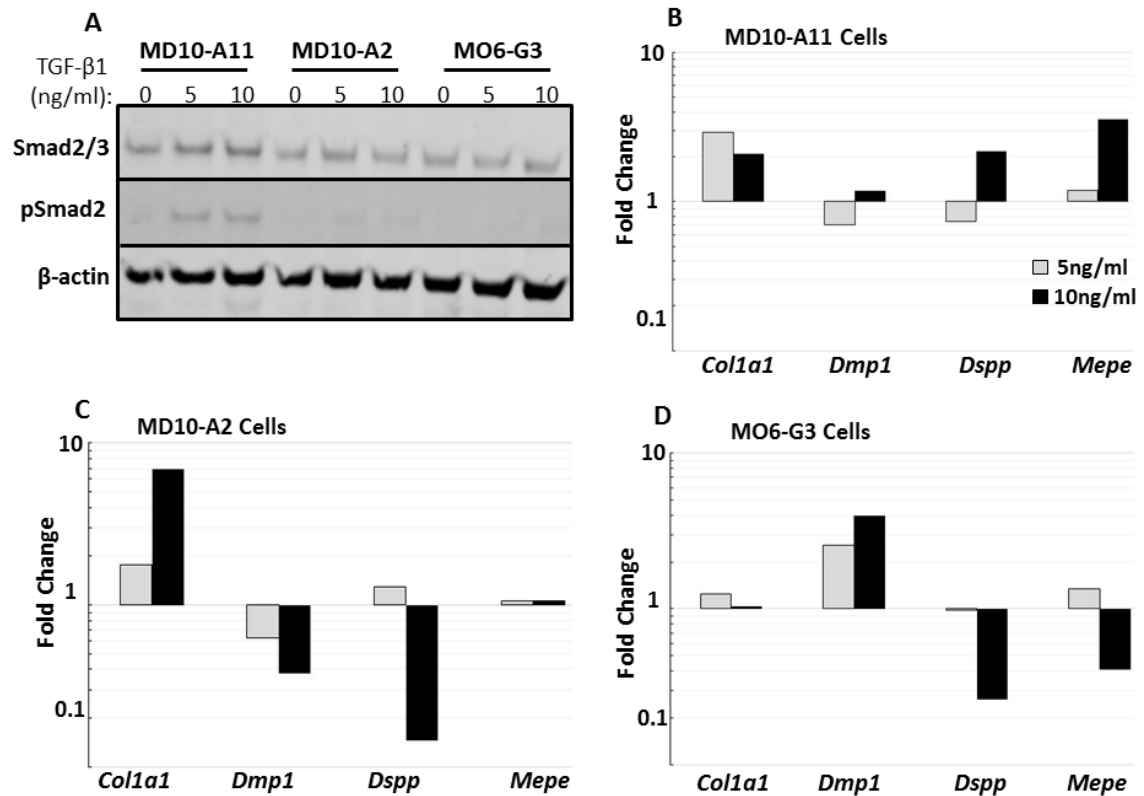


Figure 8 - Western blot analysis of activation of TGF- β signaling in mouse dental pulp (MD10 -A11) and mouse odontoblast-like (MD10-A2 and MO6-G3) cell lines. Cell cultures were treated with 5 and 10 ng/ml of rhTGF- β 1 and analyzed in triplicate for protein expression. Smad2/3 and p-Smad2 proteins were analyzed for each treatment group (A). Quantitative reverse transcriptase PCR performed using cDNA derived from MD10-A11 (B), MD10-A2 (C), and MO6-G3 (D) cell cultures treated with 5ng/ml and 10ng/ml rhTGF- β 1. Graphs depict fold change of *Col1a1*, *Dmp1*, *Dspp*, and *Mepe* in 5ng/ml rhTGF- β 1 and 10ng/ml rhTGF- β 1 treatment groups as compared to 0ng/ml rhTGF- β 1; n = 3.

CHAPTER 3

MEPE LOCALIZATION IN THE CRANIOFACIAL COMPLEX AND FUNCTION IN
TOOTH DENTIN FORMATION

by

ANGELA GULLARD, JELICA GLUHAK-HEINRICH, SILVANA PAPAGERAKIS,
PHILIP SOHN, AARON UNTERBRINK, SHUO CHEN, MARY MACDOUGALL

Submitted to *Journal of Histochemistry and Cytochemistry*

Format adapted for dissertation

ABSTRACT

Matrix extracellular phosphoglycoprotein is an extracellular matrix protein found in dental and skeletal tissues. Although information regarding the role of MEPE in bone and disorders of phosphate metabolism is emerging, the role of MEPE in dental tissues remains unclear. We performed RNA *in situ* hybridization and immunohistochemistry analyses to delineate expression pattern of MEPE during embryonic and postnatal development in craniofacial mineralizing tissues. *Mepe* RNA expression was seen within teeth from cap through root formation associated with the odontoblasts and cellular cementoblasts. More intense expression was seen in the alveolar bone within the osteoblasts and osteocytes. MEPE immunohistochemistry showed biphasic dentin staining in incisors and more intense staining in the alveolar bone matrix and forming cartilage. Analysis of *Mepe* null mouse molars showed overall mineralized tooth volume and density of enamel and dentin comparable to wild-type samples. However, *Mepe* ^{-/-} molars exhibited increased thickness of predentin, dentin, and enamel over controls and decreased gene expression of *Enam*, *Bsp*, *Dmp1*, *Dspp*, and *Opn* by RT-PCR. In vitro *Mepe* overexpression in odontoblasts led to significant reductions of *Dspp* reporter activity. These data suggest MEPE may be instrumental in craniofacial and dental matrix maturation potentially functioning in the maintenance of non-mineralized matrix.

INTRODUCTION

The craniofacial complex contains numerous mineralized tissues, including bone, cartilage, cementum, dentin, and enamel. Bone and dentin in particular are extremely similar in composition and mechanism of formation, consisting of a predominantly collagenous matrix containing mostly type I collagen and a number of non-collagenous proteins (NCPs) involved in mineralization (Butler, 1998; Bleicher et al., 1999). The majority of these dentin/bone NCPs share common structural and molecular features and have been classified as members of the small integrin-binding ligand, N-linked glycoprotein (SIBLING) family of proteins (Fisher and Fedarko, 2003) located in a cluster on human chromosome 4q21 (MacDougall et al., 2002). The SIBLING family contains five members: dentin sialophosphoprotein (DSPP), dentin matrix protein 1 (DMP-1), bone sialoprotein (IBSP), osteopontin (SPP1), and matrix extracellular phosphoglycoprotein (MEPE). Three SIBLINGs have been associated with the pathogenesis of human genetic disease altering mineralization: 1) DSPP with autosomal dominant dentin structural diseases (dentinogenesis imperfecta types II and III, and dentin dysplasia type II), 2) DMP-1 with autosomal recessive form of hypophosphatemic rickets (ARHR1 OMIM #24152, Lorenz-Depiereux et al., 2006) and chronic kidney disease (Pereira et al., 2009); and 3) MEPE with oncogenic hypophosphatemic osteomalacia (OHO) (Rowe et al., 2000; Imanishi et al., 2012). SIBLING proteins were initially described associated with the formation and mineralization of bone and dentin but their synthesis and secretion has also been found in other tissues such as cartilage and enamel. MEPE was the last SIBLING protein identified and is the least well-characterized, especially related to tooth formation and mineralization.

MEPE (also known as osteocyte/osteoblast factor 45, OF45), initially cloned as a secreted protein from a OHO tumor (Rowe et al., 2000), is highly expressed in bone (Petersen *et al.*, 2000). MEPE exhibits high homology among species (mouse, rat, monkey, and human) and major structural features similar to SIBLING proteins (Rowe et al., 2000; Argiro et al., 2001; MacDougall et al., 2002). These features include: a putative signal peptide, an RGD cell attachment motif, a glycosaminoglycan attachment site (SGDG), and several phosphorylation motifs. A specific feature of MEPE protein is the occurrence near the C-terminus of a serine-rich sequence, which displays homology with DSPP and to a lesser extent DMP-1 and OPN (Rowe et al., 2000). The cleaved C-terminal serine-rich peptide fragment of MEPE, known as ASARM-peptide or Dentonin, has been shown to down-regulate odontoblast differentiation in vitro (Liu *et al.*, 2004), while MEPE's RGD motif appears to enhance proliferation of dental pulp stem cells (Wang *et al.*, 2010). These studies corroborate previous observations in bone showing MEPE suppresses mineralization. MEPE has been shown to be expressed by osteoblasts and osteocytes within trabecular and cortical bone, and its expression is increased during in vitro osteoblast-mediated matrix mineralization (Petersen et al., 2000; Argiro et al., 2001). Studies have demonstrated that MEPE behaves as an inhibitor of mineralization, being down-regulated during osteoblast differentiation (Siggelkow *et al.*, 2004). Analysis of the long bones of *Mepe* *-/-* mice reveals increased density, indicating that MEPE is critical in inhibiting bone formation (Gowen *et al.*, 2003). As a regulator of phosphate metabolism, MEPE has a role in renal physiology (Kiela and Ghishan, 2009) and has been implicated in disrupted systemic phosphate levels (White *et al.*, 2006).

While a substantial body of literature has investigated the role of MEPE in bone, knowledge of its expression pattern and activity in dental tissues remains limited. We demonstrated the expression pattern of MEPE in the craniofacial complex and teeth at the RNA and protein level. We investigated the interactions and potential effect of MEPE on other SIBLING dentin matrix proteins. Our data showed that MEPE is present during development of mineralized tissues of the craniofacial complex: teeth, bone, and cartilage. Ablation of *Mepe* results in increased collagen matrix volume, though overall tooth mineral density remains unchanged compared to control. *Mepe* overexpression causes a decrease in expression of *Dspp*, a critical component of matrix mineralization and marker of odontoblast cytodifferentiation. Based on its developmental expression by cells involved in the synthesis of mineralized matrices of teeth, bone, and cartilage, MEPE may not only have similar roles with other bone/dentin matrix proteins, but could also function as a specific early matrix-forming marker related to the non-mineralized phase dentinogenesis, osteogenesis, and chondrogenesis.

MATERIALS AND METHODS

Animals and procedures

This study was approved by the Committee on Animal Care at the University of Texas Health Science Center at San Antonio. Pregnant ICR Swiss mice were purchased (Harlan Laboratories, Indianapolis, IN) or *Mepe*-null animals were bred and allowed to give birth. Pups were sacrificed at postnatal day (PN) 1, 2, and 3 for immunohistochemistry in wild type (WT) mice and at embryonic day (E) 20, PN1, -2, and -3 for *Mepe*^{-/-} mice. For in situ hybridization and tooth measurement studies,

C57/BL6 mice (The Jackson Laboratory, Bar Harbor, ME) were purchased and bred.

Animals were housed in a temperature- and humidity-controlled room with a 12-hr light, 12-hr dark cycle and were provided with food and water ad libitum.

In situ hybridization

Histological sections for *in situ* hybridization and antisense and sense RNA probes for *Mepe* were prepared as previously described (Gluhak-Heinrich *et al.* 2007). Mouse mandibular tissues sectioned at 6-8 μ m thickness were prepared from animals at E16 and PN-3, -5, and - 9.

Sections were deparaffinized with xylene and 100% ethanol, treated with proteinase K solution (Proteinase K, 5 mg/ml in 50mM Tris, 5mM EDTA pH 7.6) for 10 minutes at 37°C, re-fixed in 4% formaldehyde in PBS (0.2M phosphate buffer, 3M NaCl), acetylated (100mM triethanolamine, 0.25% acetic anhydride), and dehydrated through ethanol. Hybridization was carried out at 55°C overnight, in a humid chamber with 50 μ L of hybridization mixture. The hybridization mixture contained 50% formaldehyde, 20mM Tris-HCl (pH 8.0), 1mM EDTA, 0.3M NaCl, 10% dextran sulfate, 1X Denhardt's solution, 100 μ g/ml denatured SS-DNA, 500 μ g/ml tRNA and 2x10⁷/ml 32P rUTP labeled RNA probe. After hybridization, slides were rinsed in 2X SSC at room temperature, then incubated with RNase solution (40mg/ml RNase A1, 10U/ml RNase T1, 0.3M NaCl, 10mM Tris, 5mM EDTA) at 37°C for one hour. Consecutive 5-minute washes at 57°C were done twice with 2X SSC, 4 times in 0.5X SSC, and 3 times in 0.1X SSC. A final dehydration in ethanol containing 0.3M ammonium acetate was performed before autoradiography. Air-dried slides were dipped in emulsion (Kodak NTB 3) diluted

1:1 with 0.6M ammonium acetate at 42°C. After exposure (1-3 weeks), the emulsion was developed in a Kodak D-19 developer. The slides were counterstained with hematoxylin, dehydrated, and mounted with Permount (Fisher scientific SO-P-1.5).

Immunohistochemistry

Histological sections (5µm) of PN3 mice were prepared for immunohistochemistry as previously described (MacDougall et al. 1998). MEPE immunostaining was performed using a MEPE polyclonal COOH-peptide antibody (Rowe et al., 2004). All rinsing and incubations were performed using 0.05 M Tris NaCl (pH 7.6) at room temperature. After dehydration, sections were pretreated with 0.3% H₂O₂ for 10 min to inhibit endogenous peroxidase activity. After rinsing, the sections were incubated for 30 min with a 1:10 dilution of pre-immune goat serum (Dako Corporation, Carpinteria, CA). Sections were then incubated for 1 hr with the MEPE antibody diluted 1:100 in 0.05 M Tris NaCl (pH 7.6), containing 1% bovine serum albumin and 1% normal goat serum, followed by washing. Next, a 1:100 dilution of anti-rabbit goat IgG conjugated to peroxidase was incubated for 40 min and detected using rabbit anti-peroxidase IgG conjugated to peroxidase, diluted 1:100 (PAP system, Dako) and incubated for 30 min. Immunoreactive sites were visualized with 3-3' tetrachloride diaminobenzidine oxidization in 0.1 M Tris NaCl (pH 7.6) with 0.03% H₂O₂. Sections were rinsed in Tris NaCl, dehydrated, and mounted in Cytoseal XYL (Stephens Scientific, Kalamazoo, MI). Sections were counterstained with Harris hematoxylin solution (Sigma) and photographed using an Axioplan photomicroscope (Zeiss, Jena, Germany). Normal mouse serum (Sigma; 1:200) and non-specific IgGs (Sigma, 1:100)

served as negative controls, replacing the primary antibody. DMP-1 and DSP immunostaining was performed using the same method as for MEPE with polyclonal antibodies directed specifically against these proteins at 1:100 and 1:200 dilutions, respectively (MacDougall et al., 1985; MacDougall et al., 1998).

Radiographic analysis and micro-computed tomography

Radiography of wild-type (WT) and *Mepe*^{-/-} PN3 mouse heads was performed using the MX-20 Cabinet X-ray System for 10 s at 18 kV (Faxitron X-Ray Corporation, Lincolnshire, IL). To examine three-dimensional tooth structure, the specimens were scanned by a Scanco μ CT40 desktop cone-beam scanner (Scanco Medical AG, Brüttisellen, Switzerland) using 20 mm specimen tubes. Scans were performed at the following settings: 10 μ m resolution, 70kVp, 114 μ A with an integration time of 200ms. Scans were automatically reconstructed into 2-D slices, and the region of interest was outlined in each slice using the μ CT Evaluation Program (v5.0A, Scanco Medical).

Molar tooth matrix analysis

The thickness of predentin, dentin, and enamel layers were determined using H&E stained histological sections of PN3 WT and *Mepe*^{-/-} mouse mandibles. NIS-Elements microscope imaging software (Nikon, Melville, NY) was used to perform measurements of dentin and enamel layers in triplicate at the mesial and distal cervical aspects, as well as lengths of each layer at the peak of the mesial and distal cusps of first molars.

Quantitative reverse transcription PCR (qRT-PCR)

Mepe^{-/-} and WT mice (PN3) mandibular first molars were dissected and used for qRT-PCR analysis of tooth matrix gene expression profiles. Total mRNA was isolated using RNA STAT-60 (TEL-TEST, Inc.), converted to cDNA with TaqMan Reverse Transcriptase Reagents (Applied Biosystems), and used for real time PCR amplification of tooth transcripts using an ABI PRISM 7000 Sequence Detection System (Applied Biosystems). Each reaction well contained 12.5µl of 2X SYBR Green mix (Applied Biosystems), 10.5µl of primer mix (5 pmoles of each primer), and 2µl of template (cDNA or control) for a total volume of 25µl. Thermal cycle parameters were 50°C for 1 s, 95°C for 10 min, 40 cycles of 95°C for 15 s, and 60°C for 1 min. Raw data were normalized against cyclophilin-A mRNA levels in each corresponding sample, and results are shown as relative quantities of cycle changes in steady-state transcription of a gene.

Dspp promoter-reporter and Mepe cDNA expression constructs

A mouse 2.6 kb (Xba/HindIII) *Dspp* promoter segment in the pGL-3 luciferase (LUC) basic expression vector was used for this study (Feng et al., 1998). Mouse *Mepe* primers (S-5'CACCATGAAGATGCAGGCTGTGT and AS-5'CTAGTCACCATGACTCTCACT) were used to amplify the full-length mouse *Mepe* cDNA, which was subcloned into the pcDNA 3.1/V5-His TOPO vector (Invitrogen) according to manufacturer instructions and confirmed by DNA sequence analysis.

Co-transfection and luciferase assay

Both vectors, with the control Renilla TK, were transiently co-transfected into the mouse odontoblast cell line MD10-A2 (MacDougall et al., 1995; Gonzales et al, 2010). One day prior to transfection, mouse odontoblast MD10-A2 cells were seeded in 12-well plates and grown to 70% confluence. The *Mepe* cDNA construct or empty construct, *Dspp*-Luc promoter, and Renilla luciferase vector (Promega) were complexed with the PLUS reagent (BRL) in a serum free media (Opti-MEM, BRL) and incubated. Lipofectamine (Life Technologies, Inc.) reagent was then added and incubated. While the DNA/PLUS complexes were forming, the media on cells was replaced with serum free Opti-MEM media (Life Technologies, Inc.). The DNA-PLUS-Lipofectamine mixture was added to each culture, incubated at 37°C at 5% CO₂ for 3 hours, and then α -MEM media with 20% fetal bovine serum (FBS) was added. Cells were harvested after 48 hours. Cells were extracted in passive lysis buffer (Promega), centrifuged, and the supernatant was transferred to a new tube. Firefly reagent (Promega) was added and the pGL3 activity was measured with a luminometer, directly followed by addition of Stop and Glow, to measure Renilla activity. Luciferase activity was normalized using the Renilla luciferase values. Statistical analysis was performed using one-way ANOVA.

RESULTS

Localization of Mepe RNA in the Developing Molar

RNA *in situ* hybridization with *Mepe* anti-sense probes revealed that *Mepe* is expressed throughout tooth formation from cap through root formation in mouse mandibular molar development. Initially, *Mepe* was uniformly expressed in both epithelial

and mesenchymal components of the tooth organ (Fig.1B) at E16. Then, *Mepe* signal intensity decreased and became more restricted to the alveolar bone at PN3 (Fig.1D). The odontoblasts were less intensely labeled than the osteoblasts in the surrounding bone. At PN5, increased intensity of *Mepe* signal was evident in odontoblasts and within the dental pulp, with further expansion of signal within the bone cells surrounding the tooth (Fig.1F). At PN8, there was increased signal in the bone around the tooth (Fig.1H). At PN10, signal was detected within the forming roots with major signal found in the bone (Fig.1J). The same pattern was also seen at PN14. However at the bifurcation of the roots, signal was seen in the odontoblasts and the late maturation stage ameloblasts in the crown region (Fig.1L). Within the root apex region at PN70, strong signal was seen in the osteoblasts and osteocytes. Within the tooth root, strong signal was seen in the cementoblasts of the cellular cementum. No signal was evident in the acellular cementum lining the coronal two-thirds of the root (Fig.1O-P).

Immunohistochemistry in developing mouse craniofacial tissues

Immunohistochemistry was performed to characterize the spatial expression pattern of MEPE during the development of the craniofacial mineralized tissues, including: tooth, bone, and cartilage. The expression pattern of MEPE was investigated during early post-natal mouse development, allowing investigation of cell differentiation, extracellular matrix (ECM) deposition and biomineralization during odontogenesis, osteogenesis, and chondrogenesis. Alveolar bone surrounding forming teeth and craniofacial bones served as positive controls for IHC studies, as bone is known to express MEPE. The expression of

MEPE by cells involved in the synthesis of mineralized matrices of tooth, bone, and cartilage was shown to differ in both developmental and spatial patterns.

In tooth, the expression of MEPE was continuously observed from day one through three of postnatal development within the predentin layer, whereas enamel was only slightly stained above background (Fig.2A-B; E-J). Similar MEPE cellular and ECM distribution patterns were seen in both molar (Fig.2A) and incisor (Fig.2E). MEPE localization in incisor showed an inverse gradient, with increasing MEPE protein towards the mineralization front within the dentin. MEPE protein was generally concentrated within the predentin layer, becoming biphasic with stronger signals detected adjacent to the odontoblasts and distally at the dentin mineralization front (Fig. 2F-G). Furthermore, while polarized odontoblasts were positive, the enamel-free area at the cusp tips of the molar was not immunopositive for MEPE (Fig.2B). MEPE labeling appears in differentiated osteoblasts (Fig.2A; inset B). IHC for MEPE results in an intense reaction within the dentin (Fig.2A) and the surrounding alveolar bone. Similar to its expression pattern in molars, MEPE was detected in incisor (Fig.2E), in both mesenchymal and epithelial cells. Within the dentin, labeling became biphasic with strong staining close to the odontoblasts cell body and also located distally at the dentin mineralization front (Fig. 2F). The immunoreaction was generally concentrated within the predentin layer (Fig.2G). Young odontoblasts, as well as the later mature odontoblast facing dentin, strongly expressed MEPE (Fig.2F inset; G: arrowhead). Heavy staining was also detected in the alveolar bone, formerly the dental follicle (Fig.2H). Contrary to odontoblasts, young presecretory ameloblasts were immunopositive (Fig.2I) while mature ameloblasts failed to show staining (Fig.2J).

MEPE was detected in the mandibular alveolar bone surrounding forming teeth in early postnatal development (PN3, Fig. 2A). MEPE was present in early committed bone cells lining the bone surface (Fig. 2A-C, 3A). Similarly, differentiated osteoblasts (Fig. 3A,C) and osteocytes (Fig. 3D), as well as the surrounding mineralized bone matrix (Fig. 3B), contained significant amounts of MEPE. Similar to MEPE expression in bone, the cartilage matrix appeared heavily stained in early cartilage formation versus mature matrix. (Fig. 3E-I). In contrast, at the same stage the hypertrophic chondrocytes were only sporadically immunopositive for MEPE (Fig. 3E-F). During further development of facial cartilage, the highest level of MEPE expression remained localized in the matrix, whereas chondrocytes became completely immunonegative. Immunohistochemistry controls using preimmune or non-specific IgGs appeared negative in all the tissues investigated including tooth (Fig. 2D, 4C), mesenchymal undifferentiated osteoprogenitor cells, osteoblasts, osteocytes and forming bone ECM (Fig. 2D). Negative controls on serial samples, in regions where the MEPE immunolabeling in cartilage was significant (matrix and cells), were devoid of any detectable labeling (Fig. 3I).

Radiographic and micro-CT analysis of Mepe^{-/-} mouse cranium and molars

Radiographic analysis of PN3 WT and *Mepe*^{-/-} craniums revealed that the *Mepe*^{-/-} heads are smaller in size and less mineralized (Fig.4A-B). Furthermore, while incisors of *Mepe*^{-/-} are grossly visible, they appeared truncated on radiographs, possibly due to tooth density not detected at the radiographic parameters utilized. The absence of the protein in *Mepe*^{-/-} teeth was tested by immunohistochemistry using the polyclonal peptide MEPE antibody. No detectable staining for MEPE was detected in any of the

tissue including those of the developing tooth in null mice (Fig. 6C). Upon micro-CT analysis of molars from PN3 WT and *Mepe*^{-/-} mice, sagittal cross-sections through the middle of the tooth display greater thickness of dentin and enamel in *Mepe*^{-/-} specimens (Fig. 4C-D). Three-dimensional (3D) reconstructions of first molars were generated using the entire sequence of 2D cross-sections of *Mepe*^{-/-} mouse molars (Fig. 4E-F).

Interestingly, densitometric analysis of 3D reconstructions demonstrates that *Mepe*^{-/-} mouse molars have not only very similar mean density of dentin and enamel as compared to WT, but also comparable ratios of dentin and enamel volume compared to total volume, which consists of the predentin, dentin, and enamel layers.

Histological analysis of Mepe^{-/-} mouse molars

Histological analysis of 3PN *Mepe*^{-/-} first molars was performed in order to measure thickness of the enamel, dentin (black layer), and predentin (black arrowhead) layers (Fig.5A). These measurements were performed at the mesial and distal cusps (red arrows) to represent greatest extent of tooth mineralization, as well as at the mesial and distal cervical regions (red arrowheads) of the crown to represent the least extent of tooth mineralization. Low and high magnification (Fig.5B and C, respectively) of 3PN *Mepe*^{-/-} first molar shows hypermineralization of the enamel, as suggested by shearing of enamel due to sectioning. The predentin, dentin, and enamel all demonstrated increased thickness at cervical (Fig.5D) and cuspal (Fig.5E) aspects of molars in *Mepe*^{-/-} specimens. The greatest percent increase in thickness (>600%) occurred in enamel of both cervical (Fig.5F) and cuspal (Fig.5G) aspects of *Mepe*^{-/-} specimens. Conversely, the percent increase in

thickness was the least for the predentin at the cuspal aspect of the *Mepe*^{-/-} mouse molar (Fig.5G).

Expression of odontoblast and ameloblast markers in Mepe^{-/-} mice

Quantitative reverse-transcription PCR analysis (qRT-PCR) using cDNA obtained from 3PN WT and *Mepe*^{-/-} mouse molars was performed to compare expression of odontoblast and ameloblast marker genes (Fig. 6A). Ameloblast markers *Ambn* and *Enam*, major structural proteins of enamel matrix, exhibited no change and 30% decrease, respectively. Levels of SIBLING genes *Ibsp* and *Dmp1* were approximately 50% of WT levels, while *Dspp* and *Spp1* levels were decreased by 20% in *Mepe*^{-/-} specimens as compared to control. In general, this suggests a general down-regulation of mineralization associated transcripts correlating with the increased hypermineralization for the extracellular matrix. At the protein level, both DMP-1 and DSPP had a more diffuse staining pattern than previously documented in the literature with prolonged staining seen in the ameloblast layer (Fig 6. D,E).

In vitro regulation of MEPE on Dspp expression

Promoter studies were performed to analyze the/ effect of *Mepe* over-expression on *Dspp* in MD10-A2 mouse odontoblast-like cells and in MD10-H1 mouse dental pulp cells. Significant reduction of *Dspp* level resulted from 48-hour transient transfection of *Mepe* in both MD10-A2 and MD10-H1 cells.

DISCUSSION

The data presented here are the first to show the broader expression pattern of MEPE in craniofacial tissues and the dental phenotype of *Mepe*^{-/-} mice. We have revealed for the first time that *Mepe* mRNA is expressed in the developing tooth germ and that its expression is primarily localized in the differentiated odontoblasts with only transient expression in the incisor preameloblasts. The most intense expression of *Mepe* mRNA was seen in the alveolar bone forming around the tooth organs. Our studies confirmed the presence of MEPE in the alveolar bone and the presence of MEPE in mature odontoblasts, predentin, and pre-secretory ameloblasts (Hou et al., 2012). A restricted expression pattern of MEPE, with reduction of staining as ameloblasts undergo cytodifferentiation, suggests that the ASARM (acidic serine-aspartate rich motif) peptide of MEPE may function to prevent enamel mineralization until establishment of the initial enamel extracellular matrix (Rowe et al., 2004; Addison et al., 2008; Atkins et al., 2011). Our results indicate that the COOH-terminal region encompassing the MEPE ASARM motif (Rowe et al., 2000) is an early marker related to the non-mineralized phase of matrix formation. The differences in *Mepe* mRNA and MEPE protein expression patterns in tooth are probably due to proteolytic processing and accumulation of the protein and likely indicate a distinct functional role for MEPE and/or processed peptides including the COOH-terminal ASARM-motif/epitope in mineralized tissue homeostasis.

MEPE has been extensively studied in the context of endochondral ossification. Conversely, cortical bone repair has been the sole setting of the documented role of MEPE in intramembranous ossification (Lu et al., 2004). The majority of craniofacial bones develop without a cartilage intermediate via intramembranous ossification. Here

we show that MEPE was expressed in calvarial tissue, both by bone-lining osteoblasts and embedded osteocytes. The most intense staining occurred in the region of osteoblast-secreted matrix, indicating that MEPE has a supporting role during the mineralization of calvarial osteoid.

MEPE expression in the hypertrophic zone of craniofacial cartilage was in concordance with recent studies that have shown *Mepe* mRNA and MEPE protein localization in the growth plates of proximal tibiae in three to four-week old mice (Staines et al., 2012). Here we studied the cartilage in PN3 mouse tissue. As the transition is made from the hypertrophic region to the calcifying cartilage zone, MEPE expression was reduced, implying the importance of post-translational modifications, specifically the cleavage of MEPE to the ASARM peptide and subsequent phosphorylation of ASARM, for its mineralization inhibiting function (Addison et al., 2008; Boskey et al., 2010).

Because bone and tooth share molecular components and developmental aspects, altering the transcript numbers of *Mepe* in a mouse model will likely affect both bone and tooth. Indeed, ablation of *Mepe* in the mouse genome has been reported to be associated with increased bone formation due to increased osteoblast activity (Gowen et al., 2003), while overexpression of MEPE led to decreased bone density, reduced calvarial mineralization, and a lower number of osteoclasts compared to control mice (David et al., 2009). Here we demonstrated that in the developing mouse molar, deletion of *Mepe* was associated with seemingly unchanged density or total tissue volume of dentin and enamel. However, upon measuring widths of predentin, dentin, and enamel from histological sections of PN3 *Mepe*^{-/-} molars, it was evident that all three layers are thicker by at least 100% compared to WT sections. Because the densitometry of whole

Mepe^{-/-} molar crowns was performed using three-dimensional reconstructions of micro-computed tomography scans, it was likely that the increased tissue thickness and density was cancelled out and any differences minimized because the entire crown was proportionally greater in volume and density as compared to the WT samples. The enlarged crown may be due to larger pulp chambers in *Mepe*^{-/-} molars compared to control. Via histological analysis, the individual matrix layers were distinguishable and quantified. Increased thickness of mineralized tissue in the *Mepe*^{-/-} molar implied that augmented odontoblast activity, with subsequent biomineralization of predentin to dentin, may also be regulating the greatly increased enamel thickness. Furthermore, these data revealed that compensatory mechanisms to limit excess predentin and immature enamel secretion were not in place.

Closer examination of skull radiographs from PN3 *Mepe*^{-/-} mice revealed that cranial bones were less mineralized than the WT counterparts. While this observation may seem contradictory to previous studies which demonstrated substantially increased bone density in 4-month- and 1-year-old *Mepe*^{-/-} mouse femurs (Gowen et al., 2003), it should be noted that the femur ossifies endochondrally while calvaria undergo intramembranous ossification. Perhaps the lacking cartilaginous template, particularly hypertrophic chondrocytes that normally express MEPE, confers a contrasting biochemical environment in intramembranous bone formation in the *Mepe*^{-/-} cranium. Additionally, investigation of osteoclast activity in *Mepe*^{-/-} mice might offer greater insight of these events.

Mepe shares homology with its SIBLINGs bone sialoprotein, DMP-1, DSPP, and osteopontin, and it is possible that compensatory mechanisms are in place during tooth

development to ensure appropriate mineralized tissue formation. However, with ablation of *Mepe* expression, mouse molar crowns also exhibited reduced levels of all other SIBLING genes and decreased enamelin level, suggesting that a dysregulation of dentin and enamel mineralizing proteins occurred. These findings confirmed previous studies of the counter situation, in which MEPE overexpression in dental pulp cells led to increased levels of odontoblast markers (namely bone sialoprotein, dentin sialoprotein, and collagen type I) and enamelin (Wei et al., 2012). Enamelin and ameloblastin, two molecules involved in enamel maturation, are also found on human chromosome 4q21, the same locus as the SIBLINGs (MacDougall, 2003). Level of ameloblastin, which has recently been associated with tooth root formation (Hirose et al., 2013), were unchanged in the *Mepe*^{-/-} tooth crown. MEPE, therefore, is thought to play a key role in mediating tooth matrix formation and mineralization.

In vitro assays aimed at determining direct effects of *Mepe* revealed that *Dspp* levels were significantly down-regulated with *Mepe* over-expression. Expression of *Dspp*, a marker for odontoblasts (Wei et al., 2007), may be dependent upon a threshold of *Mepe* expression. When *Mepe* is completely eliminated, *Dspp* is slightly reduced by 20%. However, in the presence of excess *Mepe*, a critical threshold is reached and *Dspp* expression is dampened.

In conclusion, the present study illustrated MEPE distribution during the development of the mineralized tissues of the craniofacial complex, namely bone, cartilage, and teeth. These expression profiles will serve as a reference for future studies that assess the individual functions of MEPE peptide sequences in the ECM. Additionally, we also presented the dental findings of the *Mepe*^{-/-} mouse, which exhibited increased thickness of

matrix layers and down-regulated expression of SIBLING genes. While we have demonstrated regulation by *Mepe* of tooth formation and mineralization, it still remains unclear whether this is via direct or indirect signaling events. Importantly, the data we have shown provide novel insight into the types of molecular associations that MEPE may be regulating in pathological mineralization states of excess MEPE (as in X-linked hypophosphatemia; Salmon et al., 2013) and deficient MEPE (as found in hypophosphatasia; Rodrigues et al., 2012).

ACKNOWLEDGEMENTS

The authors declare no potential conflicts of interest with respect to the authorship and/or publication of this article. The authors of this project received the following funding for their training: F30 DE021945 to AG.

REFERENCES

- Addison WN, Nakano Y, Loisel T, Crine P, McKee MD (2008). MEPE-ASARM peptides control extracellular matrix mineralization by binding to hydroxyapatite: an inhibition regulated by PHEX cleavage of ASARM. *J Bone Miner Res* 23:1638-49.
- Argiro L, Desbarats M, Glorieux FH, Ecarot B (2001). Mepe, the gene encoding a tumor-secreted protein in oncogenic hypophosphatemic osteomalacia, is expressed in bone. *Genomics* 74:342-51.
- Atkins GJ, Rowe PS, Lim HP, Welldon KJ, Ormsby R, Wijenayaka AR (2011).

- Sclerostin is a locally acting regulator of late-osteoblast/preosteocyte differentiation and regulates mineralization through a MEPE-ASARM-dependent mechanism. *J Bone Miner Res* 26:1425–36.
- Bleicher F, Couble ML, Farges JC, Couble P, Magloire H (1999). Sequential expression of matrix protein genes in developing rat teeth. *Matrix Biol* 18:133-43.
- Boskey AL, Chiang P, Fermanis A, Brown J, Taleb H, David V, Rowe PS (2010). MEPE's diverse effects on mineralization. *Calcif Tissue Int* 86:42-6.
- Butler WT (1998). Dentin matrix proteins. *Eur J Oral Sci* 106 Suppl 1:204-10.
- Chen S, Chen L, Jahangiri A, Chen B, Wu Y, Chuang HH, Qin C, MacDougall M (2008). Expression and processing of small integrin-binding ligand N-linked glycoproteins in mouse odontoblastic cells. *Arch Oral Biol* 53:879-80.
- David V, Martin A, Hedge AM, Rowe PS (2009). Matrix extracellular phosphoglycoprotein (MEPE) is a new bone renal hormone and vascularization modulator. *Endocrinology* 150:4012-23.
- Feng JQ, Luan X, Wallace J, Jing D, Ohshima T, Kulkarni AB, D'Souza RN, Kozak CA, MacDougall M (1998). Genomic organization, chromosomal mapping, and promoter analysis of the mouse dentin sialophosphoprotein (Dspp) gene, which codes for both dentin sialoprotein and dentin phosphoprotein. *J Biol Chem* 273:9457-64.
- Fisher LW, Fedarko NS (2003). Six genes expressed in bones and teeth encode the current members of the SIBLING family of proteins. *Connect Tissue Res* 44 Suppl 1:33-40.
- Gonzales CB, Simmons D, MacDougall M (2010). Competing Roles of TGF β and

- Nma/BAMBI in Odontoblasts. *J Dent Res* 89:597-602.
- Gowen LC, Petersen DN, Mansolf AL, Qi H, Stock JL, Tkalcevic GT, Simmons HA, Crawford DT, Chidsey-Frink KL, Ke HZ, McNeish JD, Brown TA (2003). Targeted disruption of the osteoblast/osteocyte factor 45 gene (OF45) results in increased bone formation and bone mass. *J Biol Chem* 278:1998-2007.
- Gluhak-Heinrich J, Pavlin D, Yang W, MacDougall M, Harris SE (2007). MEPE expression in osteocytes during orthodontic tooth movement. *Arch Oral Biol* 52:684-90.
- Hirose N, Shimazu A, Watanabe M, Tanimoto K, Koyota S, Sugiyama T, Uchida T, Tanne K (2013). Ameloblastin in Hertwig's epithelial root sheath regulates tooth root formation and development. *PLoS One* 8:e54449.
- Hou C, Liu ZX, Tang KL, Wang MG, Sun J, Wang J, Li S (2012). Developmental changes and regional localization of Dspp, Mepe, Mimecan and Versican in postnatal developing mouse teeth. *J Mol Histol* 43:9-16.
- Imanishi Y, Hashimoto J, Ando W, Kobayashi K, Ueda T, Nagata Y, Miyauchi A, Koyano HM, Kaji H, Saito T, Oba K, Komatsu Y, Morioka T, Mori K, Miki T, Inaba M (2012). Matrix extracellular phosphoglycoprotein is expressed in causative tumors of oncogenic osteomalacia. *J Bone Miner Metab* 30:93-9.
- Kiela PR, Ghishan FK (2009). Recent advances in the renal-skeletal-gut axis that controls phosphate homeostasis. *Lab Invest* 89:7-14.
- Lu C, Huang S, Miclau T, Helms JA, Colnot C (2004). Mepe is expressed during skeletal development and regeneration. *Histochem Cell Biol* 121:493-9.
- Liu H, Li W, Gao C, Kumagai Y, Blacher RW, DenBesten PK (2004). Dentonin, a

- fragment of MEPE, enhanced dental pulp stem cell proliferation. *J Dent Res* 83:496-9.
- Lorenz-Depiereux B, Bastepe M, Benet-Pages A, Amyere M, Wagenstaller J, Muller-Barth U, Badenhop K, Kaiser SM, Rittmaster RS, Shlossberg AH, Olivares JL, Loris C, Ramos FJ, Glorieux F, Vikkula M, Juppner H, Strom TM (2006). DMP1 mutations in autosomal recessive hypophosphatemia implicate a bone matrix protein in the regulation of phosphate homeostasis. *Nature Genet* 38:1248-50.
- MacDougall M (2003). Dental structural diseases mapping to human chromosome 4q21. *Connect Tissue Res* 44 Suppl 1:285-91.
- MacDougall M, Gu TT, Luan X, Simmons D, Chen J (1998). Identification of a novel isoform of mouse dentin matrix protein 1, spatial expression in mineralized tissues. *J Bone Min Res* 13:422-31.
- MacDougall M, Nydegger J, Gu TT, Simmons D, Luan X, Cavender A, D'Souza RN (1998). Developmental regulation of dentin sialophosphoprotein during ameloblast differentiation: a potential enamel matrix nucleator. *Connect Tissue Res* 39:25-37.
- MacDougall M, Simmons D, Gu TT, Dong J (2002). MEPE/OF45, a new dentin/bone matrix protein and candidate gene for dentin diseases mapping to chromosome 4q21. *Connect Tissue Res* 43:320-30.
- MacDougall M, Thiemann F, Ta H, Hsu P, Chen LS, Snead ML (1995). Temperature sensitive simian virus 40 large T antigen immortalization of murine odontoblast cell cultures: Establishment of clonal odontoblast cell line. *Connect Tissue Res* 33:97-103.

- MacDougall M, Zeichner-David M, Slavkin HC (1985). Production and characterization of antibodies against murine dentine phosphoprotein. *Biochem J* 232:493-500.
- Pereira RC, Juppner H, Azucena-Serrano CE, Yadin O, Salusky IB, Wesseling-Perry K (2009). Patterns of FGF-23, DMP1, and MEPE expression in patients with chronic kidney disease. *Bone* 45:1161-8.
- Petersen DN, Tkalcevic GT, Mansolf AL, Rivera-Gonzalez R, Brown TA (2000). Identification of osteoblast/osteocyte factor 45 (OF45), a bone-specific cDNA encoding an RGD-containing protein that is highly expressed in osteoblasts and osteocytes. *J Biol Chem* 275:36172-80.
- Qin C, Baba O, Butler WT (2004). Post-translational modifications of sibling proteins and their roles in osteogenesis and dentinogenesis. *Crit Rev Oral Biol Med* 15:126-36.
- Rajpar MH, Koch MJ, Davies RM, Mellody KT, Kielty CM, Dixon MJ (2002). Mutation of the signal peptide region of the bicistronic gene DSPP affects translocation to the endoplasmic reticulum and results in defective dentine biomineralization. *Hum Molec Genet* 11:2559-65.
- Rodrigues TL, Foster BL, Silverio KG, Martins L, Casati MZ, Sallum EA, Somerman MJ, Nociti FH Jr (2012). Hypophosphatasia-associated deficiencies in mineralization and gene expression in cultured dental pulp cells obtained from human teeth. *J Endod* 38:907-12.
- Rowe PS, de Zoysa PA, Dong R, Wang HR, White KE, Econs MJ, Oudet CL (2000). MEPE, a new gene expressed in bone marrow and tumors causing osteomalacia. *Genomics* 67:54-68.

- Rowe PSN, Kumagai Y, Gutierrez G, Garrett IR, Blacher R, Rosen D, Cundy J, Navvab S, Chen D, Drezner MK, Quarles LD, Mundy GR (2004). MEPE has the properties of an osteoblastic phosphatonin and minhibin. *Bone* 34:303–19.
- Salmon B, Bardet C, Khaddam M, Naji J, Coyac BR, Baroukh B, Letourneur F, Lesieur J, Decup F, Le Denmat D, Nicoletti A, Poliard A, Rowe PS, Huet E, Vital SO, Linglart A, McKee MD, Chaussain C (2013). MEPE-derived ASARM peptide inhibits odontogenic differentiation of dental pulp stem cells and impairs mineralization in tooth models of X-linked hypophosphatemia. *PLoS One* 8:e56749.
- Siggelkow H, Schmidt E, Hennies B, Hübner M (2004). Evidence of downregulation of matrix extracellular phosphoglycoprotein during terminal differentiation in human osteoblasts. *Bone* 35:570-6.
- Staines KA, Mackenzie NC, Clarkin CE, Zelenchuk L, Rowe PS, MacRae VE, Farguharson C (2012). MEPE is a novel regulator of growth plate cartilage mineralization. *Bone* 51:418-30.
- Wang H, Kawashima N, Iwata T, Xu J, Takahashi S, Sugiyama T, Suda H (2010). Differentiation of odontoblasts is negatively regulated by MEPE via its C-terminal fragment. *Biochem Biophys Res Commun* 398:406-12.
- Wei X, Ling J, Wu L, Liu L, Xiao Y (2007). Expression of mineralization markers in dental pulp cells. *J Endod* 33:703-8.
- Wei X, Liu L, Zhou X, Zhang F, Ling J (2012). The effect of matrix extracellular phosphoglycoprotein and its downstream osteogenesis-related gene expression on the proliferation and differentiation of human dental pulp cells. *J Endod* 38:330-8.

White KE, Larsson TE, Econs MJ (2006). The roles of specific genes implicated as circulating factors involved in normal and disordered phosphate homeostasis: frizzled related protein-4, matrix extracellular phosphoglycoprotein, and fibroblast growth factor 23. *Endocr Rev* 27:221-41.

Zhang X, Zhao J, Li C, Gao S, Qiu C, Liu P, Wu G, Qiang B, Lo WHY, Shen Y (2001). DSPP mutation in dentinogenesis imperfecta Shields type II. *Nature Genet* 27:151-2.

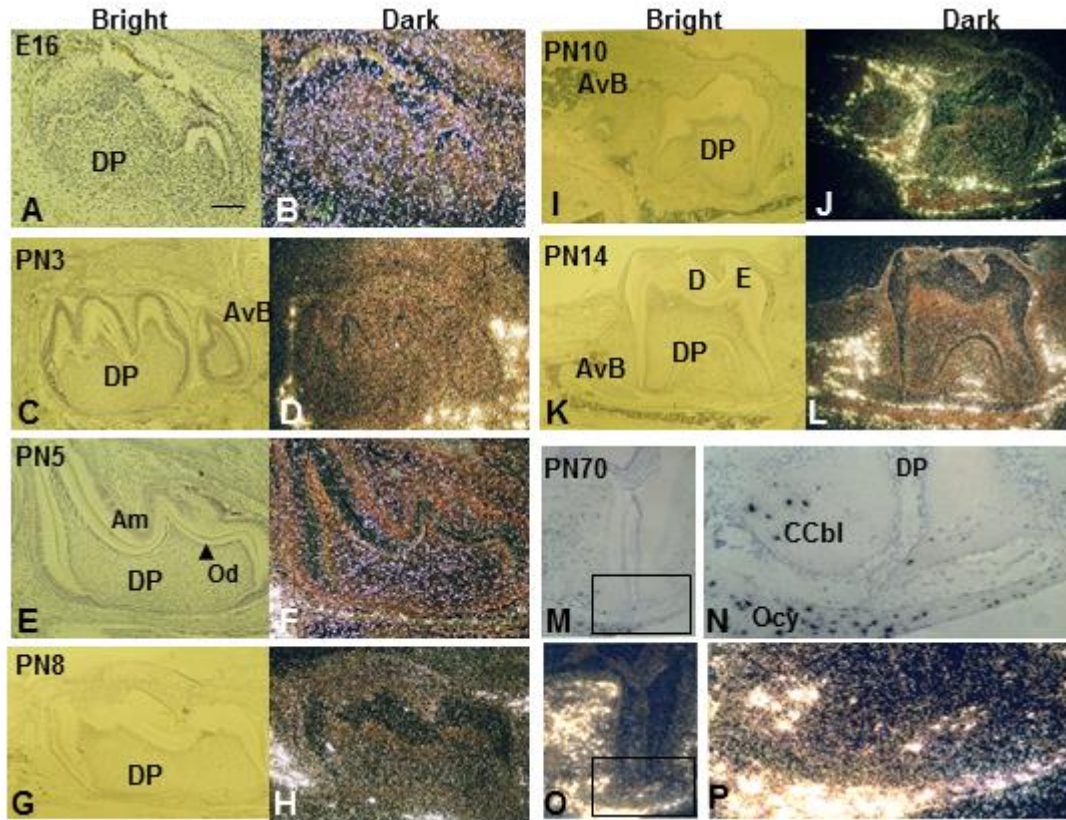


Figure 1. *In situ* hybridization of *Mepe* expression in molar crown and root development. Panels A, C, E, G, I, K, M, and N seen in bright field and panels B, D, F, H, J, L, O, and P shown in dark field. (B) Late cap/early bell stage showing general expression of *Mepe* within the tooth; (D) Intense *Mepe* expression in forming alveolar bone surrounding the molar; (F) Generalized *Mepe* expression at 5PN in the dental pulp with more intense signal in the odontoblast layer (E, arrowhead). The generalized tooth expression pattern continues through root formation (G-L) with intense foci of *Mepe* expression in the alveolar bone. At the root apex (M-P) strong *Mepe* expression is seen in the cellular cementoblasts on the dentin matrix surface and osteocytes also embedded in the bone (O-P). CCbl: cellular cementoblasts; Am: ameloblast layer, AvB: alveolar bone, D: dentin; DP: dental pulp mesenchyme; E: enamel, Od: odontoblast layer; and Ocy: osteocytes. Scale bar (A) = 200 μ m.

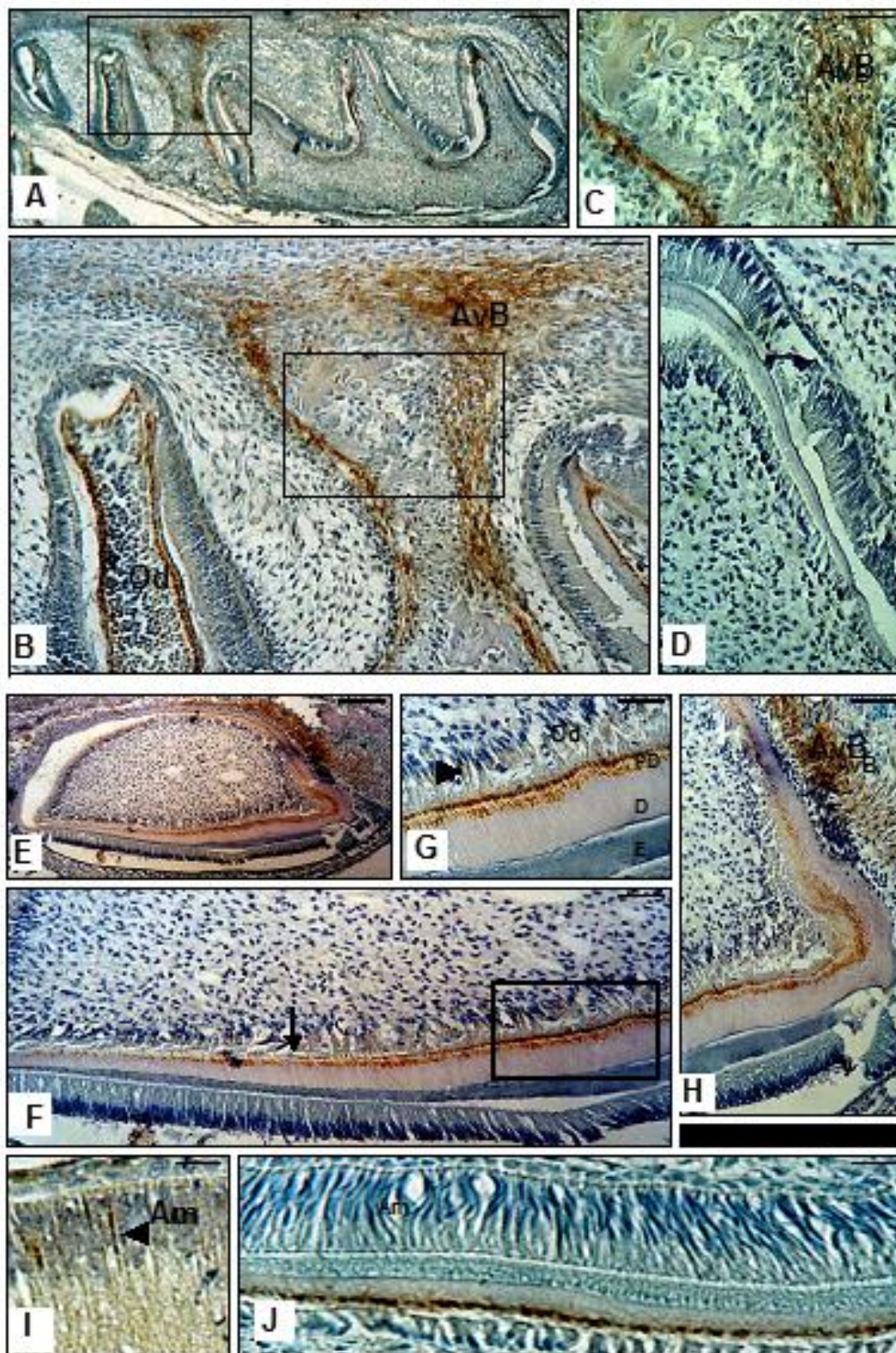


Figure 2. Immunohistochemical analyses of MEPE in 3PN mouse dental tissues and alveolar bone of undecalcified mandibular sections. MEPE labeling appears in bone-forming cells which are morphologically undifferentiated, as well as in differentiated osteoblasts (A-C). Labeling for MEPE is also seen in the dentin (A-B) and the polarized odontoblast cells (B). A lack of immunolabeling for MEPE was observed in the enamel-free area of the molar (B). Immunocontrol on a serial section (D). MEPE immunostaining in mouse mandibular incisor. Similar to its expression pattern in molars, MEPE protein was detected in incisor (E), in both mesenchymal and epithelial cells. The immunoreaction was generally concentrated within the predentin layer, whereas mineralized dentin stained only slightly. Panel F shows within the forming dentin matrix, labeling becoming biphasic (arrow) with a strong staining seen close to the odontoblast cell body and distally closer to the dentin mineralization front. Young odontoblasts as well as later stages of the odontoblast lineage were positive for staining (G, arrowhead). A most intense staining was again detected in the alveolar bone (H). Within the incisor, presecretory ameloblasts were immunopositive (I) whereas in the mature ameloblasts, no signal was detected (J). Abbreviations: AvB: alveolar bone; Am: ameloblasts; D: dentin; E: enamel; Od: odontoblasts; and PD: predentin. Scale bars = 200 μ m.

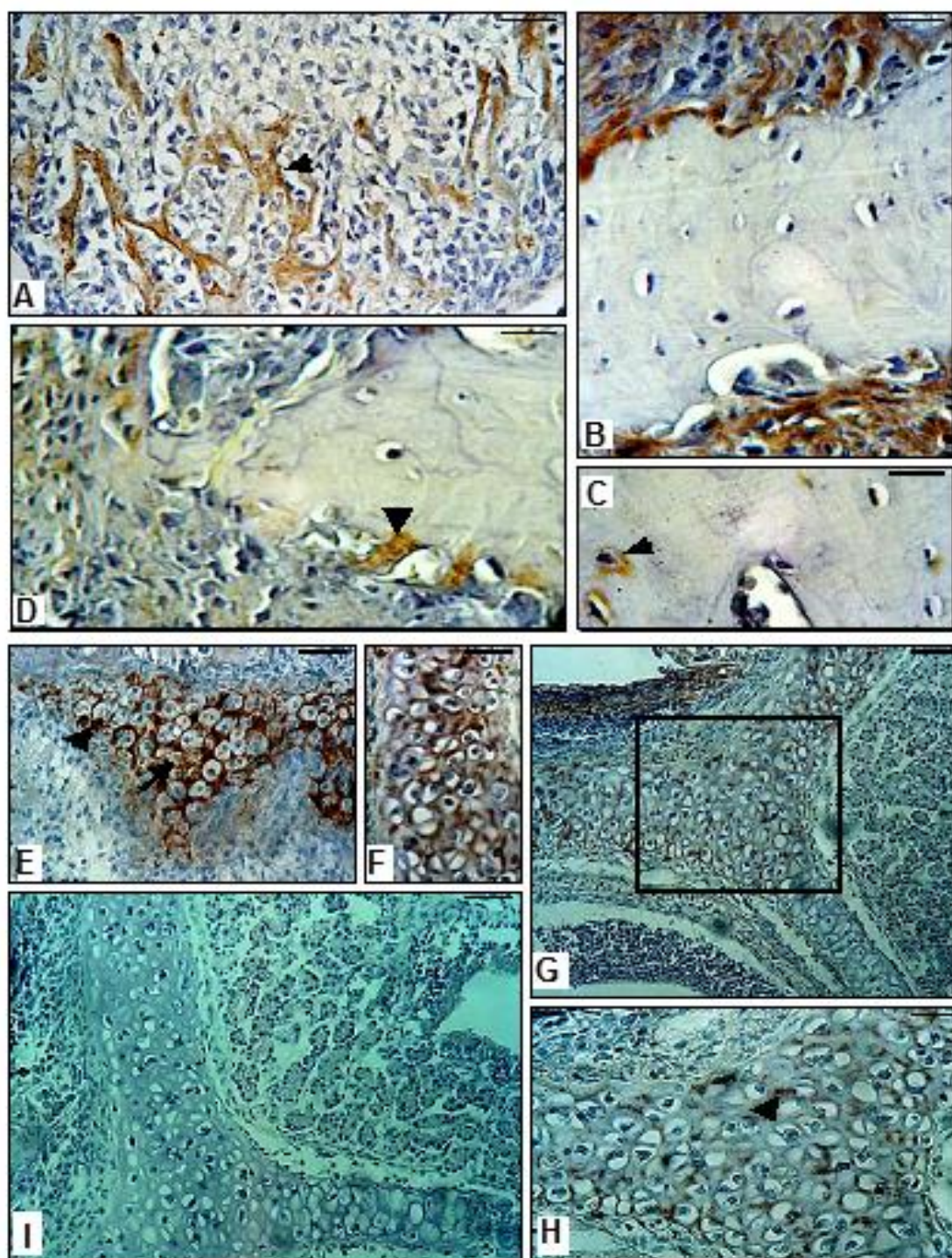


Figure 3. Immunolabeled bone cells and matrix in undecalcified sections of mouse calvarial bone (A-D). Bone matrix appeared to contain a high level of MEPE (arrowhead, pointing to matrix spiculi) with staining in the osteoblast cytoplasm as well (A). Inside the osteon (B) immunopositive signals were detected. Intense labeling was observed in osteoblasts lining the bone (C) as well as in some osteocytes (D). Immunohistochemistry with the MEPE antibody in mouse craniofacial cartilage (E-I). In early cartilage formation, the matrix is heavily stained (E, arrowhead), whereas hypertrophic chondrocytes have modest levels of MEPE (arrow). During further development of facial cartilage (G-H), the highest level of MEPE remains localized in the matrix (arrowhead), whereas chondrocytes became completely immunonegative (H). Negative control of cartilage on a serial section showed no detectable staining (I). Scale bars = 200 μ m.

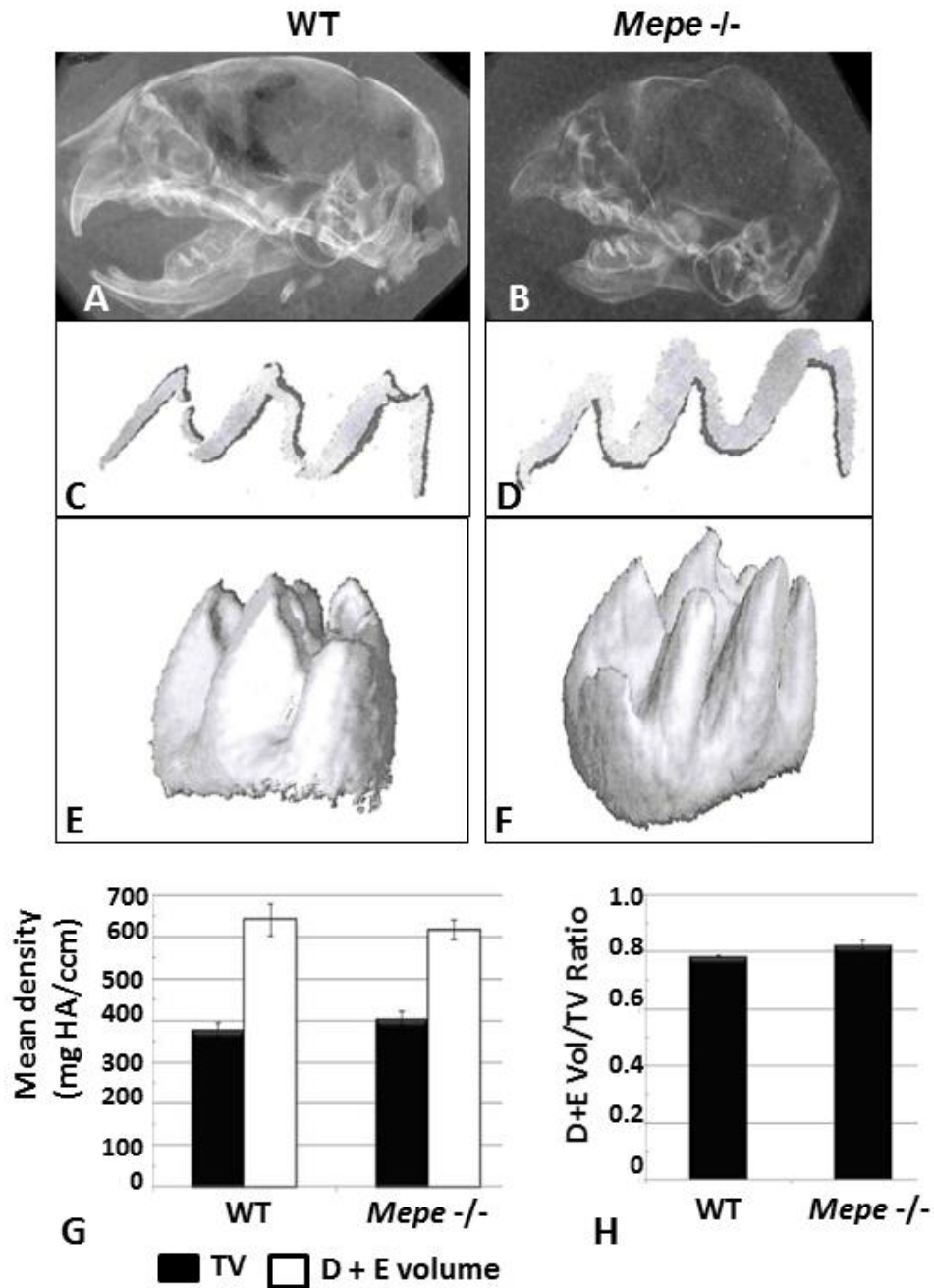


Figure 4. Radiographic analysis of day 3PN WT and *Mepe*^{-/-} cranial halves; representative of 3 sets of specimens (A-B). The *Mepe*^{-/-} specimen bone appears to be overall less mineralized compared to WT as compared to the forming teeth (B). Cross-sectional micro-CT analysis of day 3PN WT and *Mepe*^{-/-} first molars showing predentin, dentin, and enamel layers (C-D). Three-dimensional reconstructions of two-dimensional

micro-CT images of day 3PN WT and *Mepe*^{-/-} first molars (E-F). Mean density of dentin and enamel (D+E) volume and total volume (TV)* of day 3PN *Mepe*^{-/-} first molars as compared to WT (G; n=3). Comparable ratios of dentin and enamel volume/total volume in *Mepe*^{-/-} and WT specimens (H). *Total volume (TV) refers to the predentin, dentin, and enamel layers depicted as seen in panels C and D.

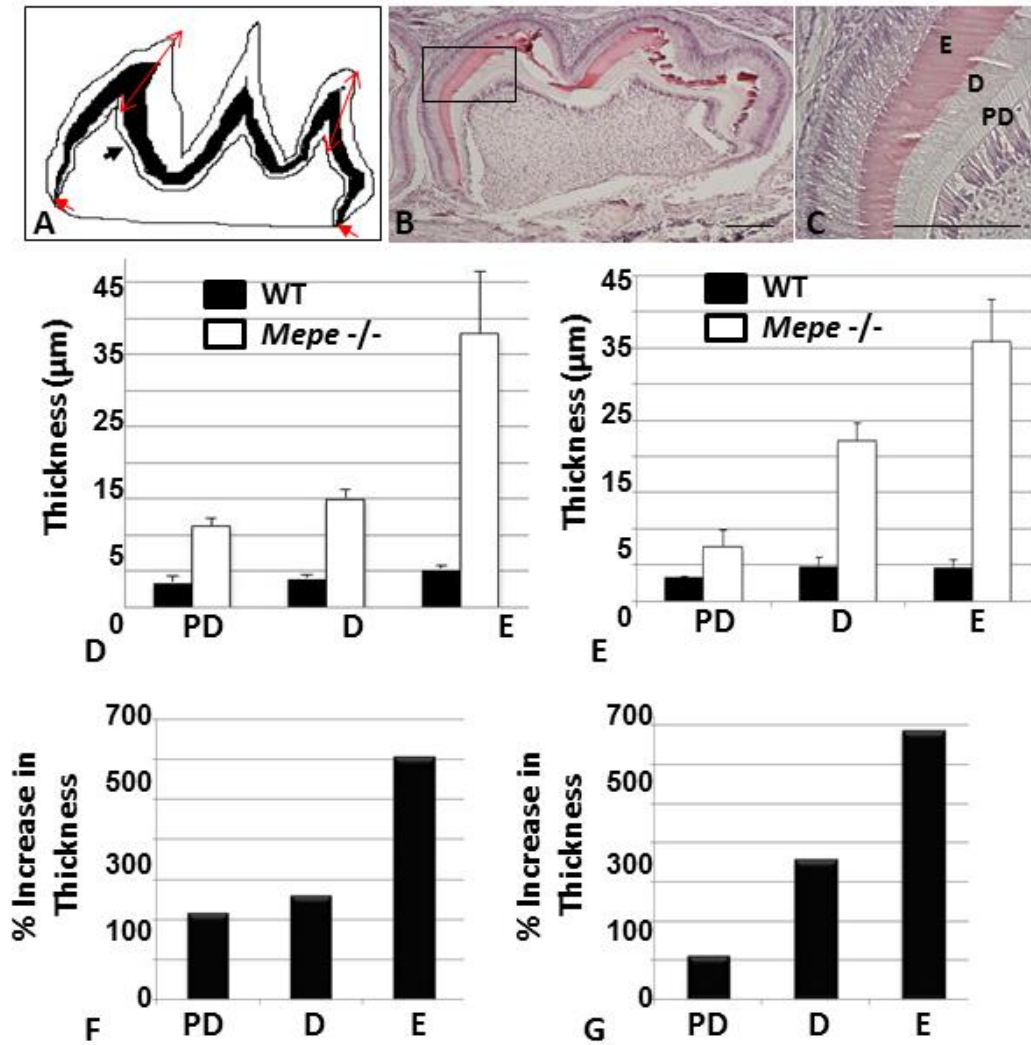


Figure 5. Histological analysis of day 3PN *Mepe*^{-/-} first molars. (A) Diagram showing regions where the measurements were obtained for enamel, dentin (black layer), and predentin (black arrowhead) at two cusps (red arrows) and mesial and distal cervical regions (red arrowheads) of mineralized tooth structure. Low (B) and high (C) magnification of 3PN *Mepe*^{-/-} first molar showing hypermineralization with expansion of dentin layer concurrent with increased predentin thickness. Increased thickness of predentin, dentin, and enamel at cervical (D) and cuspal (E) aspects of molars in *Mepe*^{-/-}

specimens. Percent increase in thickness at cervical (F) and cuspal (G) aspects of *Mepe* -
/- specimens as compared to WT. Abbreviations: D: dentin; E: enamel; and PD:
predentin. Scale bars = 200 μ m.

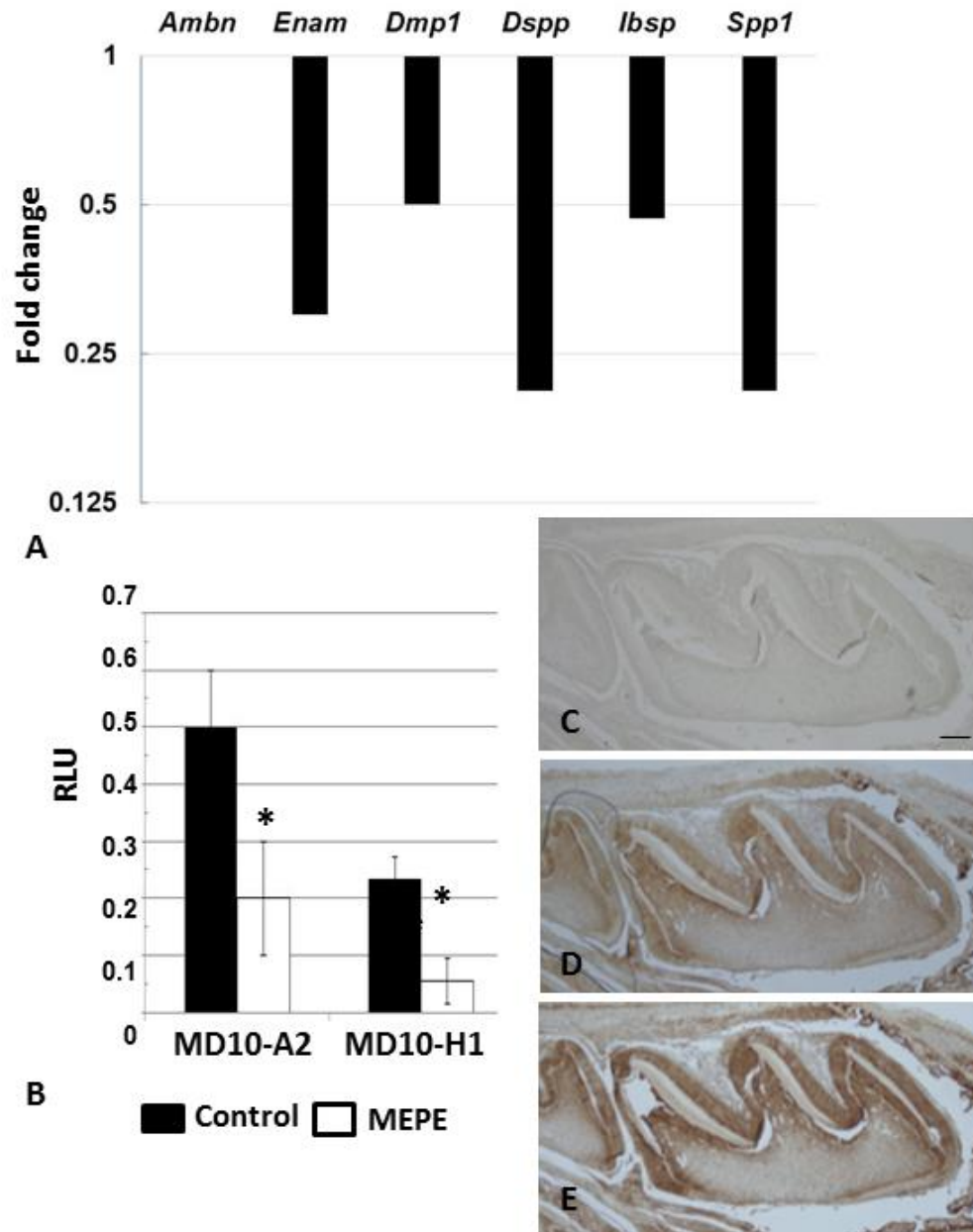


Figure 6. qRT-PCR analysis of gene expression fold change in *Mepe*^{-/-} mouse whole tooth cDNA as compared to WT; mandibular first molars were obtained from 3PN mice (A). Ameloblast marker genes *Ambn* and *Enam* showed no change and 30% decrease, respectively. Levels of SIBLING genes *Ibsp* and *Dmp1* were approximately 50% of WT levels; while *Dspp* and *Spp1* levels were decreased by 20% in *Mepe*^{-/-} specimens as

compared to control. Influence of *Mepe* over-expression on *Dspp* gene expression in MD10-A2 mouse odontoblast-like cells and MD10-H1 mouse dental pulp cells (B). Cells were transiently transfected for 48 hours, after which Luc/Renilla activity was quantified. Luciferase activity of *Dspp* 2.6 kb promoter construct co-transfected with an empty vector or *Mepe* expression construct. Activity was normalized using Renilla luciferase values. RLU = relative luciferase units; * = $p \leq 0.005$. Immunohistochemistry for DMP-1 (D) and DSPP (E) on PN3 *Mepe*^{-/-} molar tooth sections; control negative staining (C). Scale bar (C) = 200 μm .

4 – GENERAL DISCUSSION AND FUTURE DIRECTIONS

In this dissertation, two major research objectives were discussed in chapters 2 and 3: (1) explore the effect of hyperactive TGF- β 1 on tooth development and (2) investigate the significance of MEPE in dentinogenesis and the consequences of its genetic ablation on tooth formation.

To address the first aim, we used a transgenic Camurati-Engelmann disease mouse model to simulate constitutive activation of TGF- β 1. The mutation selected for the *TGFB1* transgene was based on published cases of human diagnosed with CED. Hyperactive TGF- β 1 signaling was driven by a *Colla1* promoter, and therefore, targeted in osteoblasts and odontoblasts. While this study was performed with focus on the dental mineralized tissues, the TGF- β superfamily of signaling molecules is present ubiquitously in vertebrates, with a great deal of molecular functional overlap within groups of TGF- β receptor ligands. Contrary to the osseous phenotype of excess bone formation in CED patients and the transgenic mouse model, the dental phenotype revealed a reduction in dentin matrix of CED. There is great variability of clinical systemic signs of CED in humans, and this presentation occurs in a spectrum. These seeming inconsistencies in gradation of altered mineralization in bone versus dentin events may be due to differential expression of downstream components, quenching mechanisms downstream of SMAD2/3/4 complex transcriptional regulation, or potential epigenetic events that are still unidentified.

Considering the genetic reproducibility of CED with a mutated transgene, the pathological mechanism at work in humans may be deduced by replicating the pathology in a mouse model. Researchers have recapitulated mineralization disorders, such as CED, osteoporosis, dentinogenesis imperfecta, in animal models. It is very likely that dental mineralization defects occur in individuals afflicted with CED. Dental anomalies occurring in the CED patient population have not been reported, possibly due to the fact that CED is rare, with approximately 200 published cases; that the patients are seen by multiple individual clinicians without interdisciplinary communication; and that there may be reduced overall oral health morbidity compared to the commonly-reported symptoms of severe bone pain, hearing loss, headaches, and blurred/lost vision loss. Compounded by the fact that CED is a rare disease, symptoms can range from mild to severe. However, with international online patient support organizations becoming more common place, collective investigation of the dental aspects of CED may yield more information about enamel or dentin defects associated with the disease.

The animal study discussed offers a snapshot view of two critical time points for evaluation of the dental mineralized tissues. In the future, we plan to further investigate the protein expression of SIBLINGs and downstream TGF- β pathway proteins in tooth formation. This would allow for a more detailed analysis of defects throughout the stages of tooth formation to try to identify key molecules that may be affecting DECM protein secretion. Experiments that define the direct or indirect molecules involved may be performed after generating immortalized cells lines derived from the dental pulp of the transgenic CED mouse. Chromatin immunoprecipitation studies may be performed to determine which SMADs are involved in the transcriptional regulation of altered

mineralization events. Additionally, delivery of TGF- β 1 inhibitors to immortalized cell lines from transgenic CED mouse dental pulp can aid in evaluating whether a molecule profile may be recovered as comparable to wild-type mouse dental pulp.

In addition to mechanistic studies, the effects of transgenic CED-derived *TGFB1* mutation on all mouse body systems should be further explored. In this dissertation, the baseline dental phenotype of mice overexpressing a CED-derived *TGFB1* mutation was described. One ultimate goal of our study of TGF- β family molecules and SIBLINGs is to determine their further potential as therapeutic targets for bone and dentin disorders. Future studies of these animals should focus on experimental models of abnormal dentinogenesis.

The second aim addressed in this dissertation revealed that MEPE is indeed present in all the mineralizing tissues of the craniofacial complex, including alveolar bone, cartilage, dentin, and enamel. MEPE has been documented to inhibit odontoblast differentiation through the release of its ASARM peptide “minhibin.” Upon deletion of *Mepe* in the mouse, DECM production is uncontrolled and elevated as indicated by the histological measurements of increased thickness in predentin, dentin, and enamel layers. Unregulated proliferation of odontoblasts from the dental pulp may be leading to the additional coronal tissue formation. Furthermore, due to MEPE’s role in phosphate metabolism, it was anticipated that with excess volume of predentin, dentin, and enamel, that the mineral density of the dentin and enamel would be augmented as well. Perplexingly, the densities and volume of mineralized tooth content, as determined in this study, was comparable in both control and *Mepe* knockout specimens. It is possible that

other transducers or repressors of mineralization at the post-translational modification level are leading to normalized measurements of dentinogenesis.

A detailed investigation of the ASARM peptide function in the *Mepe* knockout mouse model will be key to dissect out how genetically turning off a “mineralization switch” globally can preserve dentin structure. Additionally, scanning electron micrographs of the dentin and enamel layers from the *Mepe* knockout mouse may provide important clues of how these tissues are structured and allow for developing the next set of experiments in answering how the dental phenotype in the knockout can exist and then become camouflaged.

While much has been revealed over the past several decades in the field of the pulp-dentin complex, many mysteries still remain regarding how this unique tissue interface forms and functions. The mouse models discussed here have both been previously shown to display increased bone formation yet decreased SIBLING gene expression in dental pulp cells. Bone and dentin share expression of several common NCPs, though the mechanisms of mineralized tissue formation are not identical. As more mechanistic studies are performed on SIBLINGs, their ASARM peptides will likely become an important factor. The discovery of the SIBLINGs, particularly MEPE and its bone/renal/tooth axis, was an important breakthrough, and has been instrumental to many odontoblast studies performed since, including the experiments described in this dissertation. However, the mechanism of action of SIBLINGs within the DECM is not yet fully understood. Coupled with regulation by the TGF- β /BMP superfamily, questions regarding the post-transcriptional and epigenetic events occurring due to MEPE form a foundation for dentinogenesis. It is tempting to speculate that due to the shared presence

of SIBLINGs and other NCPs in bone and dentin that the signaling pathways responsible for alternative osseous mineralization events are the same pathways that drive dentinogenesis itself.

Progress in the understanding of the pulp-dentin complex and its formation will require many more experiments to be done before the dental pulp cell and odontoblast are completely understood. This dissertation represents a small step towards that direction. In summary, the work presented here has introduced the importance of MEPE in odontoblast function and opened new pathways of research into its regulation directly or indirectly by the TGF- β superfamily.

As shown in Figure 1, our working model concentrates on the scope of TGF- β signaling on MEPE as a downstream SIBLING target. When dental pulp cells differentiate, cytokines such as TGF- β 1 can influence the content of odontoblast secretory products. Once odontoblasts polarize, apposition of predentin (PD) is followed by establishment of dentin (D). The enamel (E) formation process is initiated after maturation of dentin has begun. With an increase in TGF- β 1 levels in dental pulp cells, we hypothesize that canonical receptor-regulated TGF- β pathway signaling leads to an inverse relationship, a decrease in DECM formation, and concurrently, a decrease in expression of the SIBLINGs DMP1, DSPP, and MEPE. In looking more specifically at how MEPE is involved tooth formation, eliminating expression of MEPE results in increased thickness of predentin, dentin, and enamel though expression levels of ENAM and SIBLINGs also decrease. We hypothesize that the increased tissue content of each tooth layer is a compensation tool in order to try to stimulate mineralization events to begin. There may be an initially increased expression of SIBLINGs with the expanded

tissue layers in the tooth. With greater levels of SIBLINGs comes higher amounts of ASARM peptides which may be released into the DECM. A negative feedback loop with excess ASARM peptides leads to impaired mineralization, possibly by the degradation of SIBLINGs to achieve a normalized balance. Therefore, mineralization density and possibly volume may be observed to have no overall change.

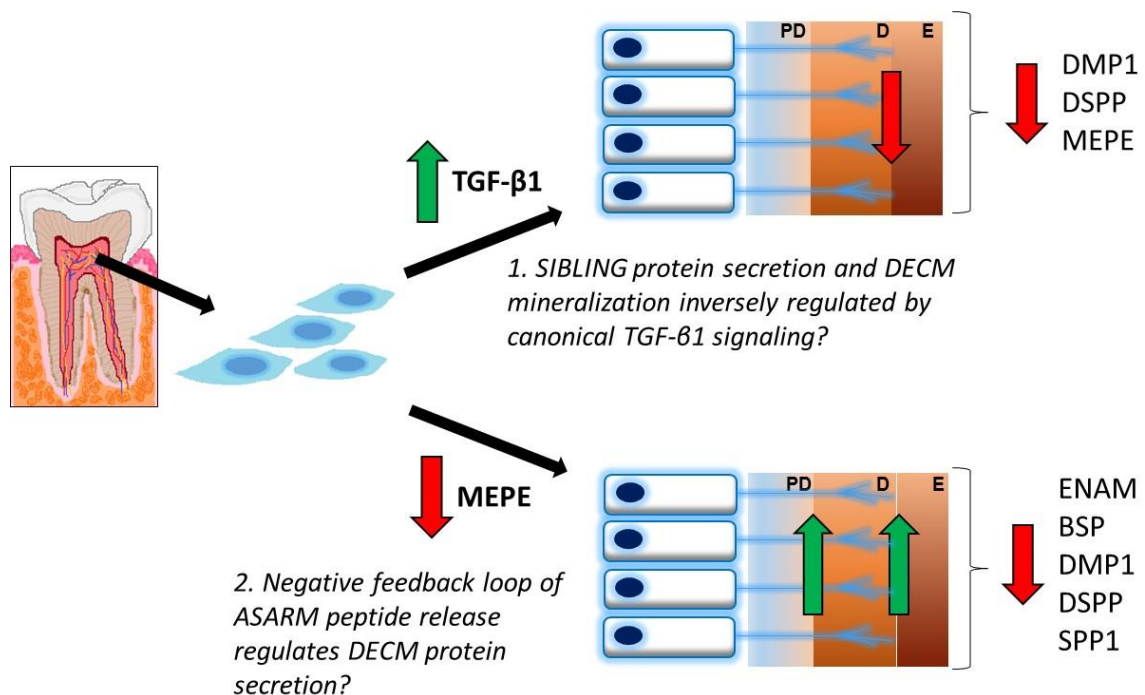


Figure 1. Potential roles for TGF-β1 and MEPE in the dentin-pulp complex

GENERAL LIST OF REFERENCES

1. Mealey BL. Periodontal disease and diabetes. A two-way street. J Am Dent Assoc. 2006;137 Suppl:26S-31S.
2. Demmer RT, Desvarieux M. Periodontal infections and cardiovascular disease: the heart of the matter. J Am Dent Assoc. 2006;137 Suppl:14S-20S.
3. Zoellner H. Dental infection and vascular disease. Semin Thromb Hemost. 2011;37(3):181-92.
4. Nesse W, Dijkstra PU, Abbas F, Spijkervet FK, Stijger A, Tromp JA, van Dijk JL, Vissink A. Increased prevalence of cardiovascular and autoimmune diseases in periodontitis patients: a cross-sectional study. J Periodontol. 2010;81(11):1622-8.
5. Ash MM, Nelson S. Wheeler's dental anatomy, physiology, and occlusion. 3rd ed. Philadelphia: W.B. Saunders; 2003.
6. Torabinejad M, Walton R. Endodontics: Principles and Practice. 4th ed. St. Louis, MO: W.B. Saunders Company; 2009.
7. Parksinon CF. Similarities in resorption patterns of maxillary and mandibular ridges. J Prosthet Dent. 1978;39(6):598-602.
8. Thesleff I, Keränen S, Jernvall J. Enamel knots as signaling centers linking tooth morphogenesis and odontoblast differentiation. Adv Dent Res. 2001;15:14-8.
9. Thesleff I, Mikkola M. The role of growth factors in tooth development. Int Rev Cytol. 2002;217:93-135.
10. Thesleff I, Sharpe P. Signalling networks regulating dental development. Mech Dev. 1997;67(2):111-23.
11. Itoh S, Itoh F, Goumans MJ, Ten Dijke P. Signaling of transforming growth factor-beta family members through Smad proteins. Eur J Biochem. 2000;267(24):6954-67.
12. Nilsen-Hamilton M. Transforming growth factor-beta and its actions on cellular growth and differentiation. Curr Top Dev Biol. 1990;24:95-136.

13. Roberts AB, Flanders KC, Heine UI, Jakowlew S, Kondaiah P, Kim SJ, Sporn MB. Transforming growth factor-beta: multifunctional regulator of differentiation and development. *Philos Trans R Soc Lond B Biol Sci.* 1990;327(1239):145-54.
14. Yamashiro T, Tummers M, Thesleff I. Expression of Bone Morphogenetic Proteins and Msx Genes during Root Formation. *J Dent Res.* 2003;82(3):172-6.
15. Thesleff I. Developmental biology and building a tooth. *Quintessence Int.* 2003.
16. Heikinheim K. Stage-specific expression of decapentaplegic-Vg-related genes 2, 4, and 6 (bone morphogenetic proteins 2, 4, and 6) during human tooth morphogenesis. *J Dent Res.* 1994;73(3):590-7.
17. Ornitz DM, Marie PJ. Fibroblast growth factor signaling in skeletal development and disease. *Genes Dev.* 2015;29(14):1463-86.
18. Bresnick S, Schendel S. Apert's syndrome correlates with low fibroblast growth factor receptor activity in stenosed cranial sutures. *J Craniofac Surg.* 1998;9(1): 92-5.
19. Jackman WR, Draper BW, Stock DW. Fgf signaling is required for zebrafish tooth development. *Dev Biol.* 2004;274(1):139-57.
20. Rao TP, Kühl M. An updated overview on Wnt signaling pathways: a prelude for more. *Circ Res.* 2010;106(12):1798-806.
21. Yin X, Li J, Salmon B, Huang L, Lim WH, Liu B, Hunter DJ, Ransom RC, Singh G, Gillette M, Zou S, Helms JA. Wnt Signaling and Its Contribution to Craniofacial Tissue Homeostasis. *J Dent Res.* 2015. Epub [2015 Aug 18].
22. Lee CS, Fan CM. Embryonic expression patterns of the mouse and chick Gas1 genes. *Mech Dev.* 2001;101:293-7.
23. Claret S, Sanial M, Plessis A. Evidence for a novel feedback loop in the Hedgehog pathway involving Smoothened and Fused. *Curr Biol.* 2007;17:1326-33.
24. Ishida K, Murofushi M, Nakao K, Morita R, Ogawa M, Tsuji T. The regulation of tooth morphogenesis is associated with epithelial cell proliferation and the expression of Sonic hedgehog through epithelial-mesenchymal interactions. *Biochem Biophys Res Commun.* 2011;405(3):455-61.
25. Hu X, Zhang S, Chen G, Lin C, Huang Z, Chen Y, Zhang Y. Expression of SHH signaling molecules in the developing human primary dentition. *BMC Dev Biol.* 2013;13(11).

26. Smith MM, Hall BK. A developmental model for evolution of the vertebrate exoskeleton and teeth: the role of cranial and trunk neural crest. . *Evol Biol.* 1993;27:387–448.
27. Nanci A. *Ten Cate's Oral Histology: Development, Structure, and Function.* 8th ed. St. Louis, MO: Mosby; 2013.
28. Peters H, Neubüser A, Kratochwil K, Balling R. Pax9-deficient mice lack pharyngeal pouch derivatives and teeth and exhibit craniofacial and limb abnormalities. *Genes Dev* 1998;12(17):2735-47.
29. Tziafas D, Kodonas K. Differentiation potential of dental papilla, dental pulp, and apical papilla progenitor cells. *J Endod.* 2010;36(5):781-9.
30. Xiao L, Tsutsui T. Three-dimensional epithelial and mesenchymal cell co-cultures form early tooth epithelium invagination-like structures: expression patterns of relevant molecules. *J Cell Biochem.* 2012;113(6):1875-85.
31. Toyono T, Nakashima M, Kuhara S, Akamine A. Expression of TGF-beta superfamily receptors in dental pulp. *J Dent Res.* 1997;76(9):1555-60.
32. Tai TF, Chan CP, Lin CC, Chen LI, Jeng JH, Chang MC. Transforming growth factor beta2 regulates growth and differentiation of pulp cells via ALK5/Smad2/3. *J Endod.* 2008;34(4):427-32.
33. Nishikawa S, Sasaki F. DNA localization in nuclear fragments of apoptotic ameloblasts using anti-DNA immunoelectron microscopy: programmed cell death of ameloblasts. *Histochem Cell Biol* 1995;104(2):151-9.
34. Joseph BK, Gobé GC, Savage NW, Young WG. Expression and localization of sulphated glycoprotein-2 mRNA in the rat incisor tooth ameloblasts: relationships with apoptosis. *Int J Exp Pathol.* 1994;75(5):313-20.
35. Shibata S, Suzuki S, Tengan T, Yamashita Y. A histochemical study of apoptosis in the reduced ameloblasts of erupting mouse molars. *Arch Oral Biol.* 1995;40(7): 677-80.
36. Toyono T, Nakashima M, Kuhara S, Akamine A. Temporal changes in expression of transforming growth factor-beta superfamily members and their receptors during bovine preodontoblast differentiation in vitro. *Arch Oral Biol.* 1997;42(7): 481-8.
37. Wei X, Ling J, Wu L, Liu L, Xiao Y. Expression of mineralization markers in dental pulp cells. *J Endod.* 2007;33(6):703-8.
38. Shirakawa M, Shiba H, Nakanishi K, Ogawa T, Okamoto H, Nakashima K, Noshiro M, Kato Y. Transforming growth factor-beta-1 reduces alkaline

- phosphatase mRNA and activity and stimulates cell proliferation in cultures of human pulp cells. *J Dent Res*. 1994;73(9):1509-14.
39. Li Y, Lü X, Sun X, Bai S, Li S, Shi J. Odontoblast-like cell differentiation and dentin formation induced with TGF- β 1. *Arch Oral Biol*. 2011;56(11):1221-9.
 40. Lee JH, Lee DS, Choung HW, Shon WJ, Seo BM, Lee EH, Cho JY, Park JC. Odontogenic differentiation of human dental pulp stem cells induced by preameloblast-derived factors. *Biomaterials*. 2011;32(36):9696-706.
 41. Oh HJ, Choung HW, Lee HK, Park SJ, Lee JH, Lee DS, Seo BM, Park JC. CPNE7, a preameloblast-derived factor, regulates odontoblastic differentiation of mesenchymal stem cells. *Biomaterials*. 2015;37:208-17.
 42. Butler W, Brunn J, Qin C. Dentin extracellular matrix (ECM) proteins: comparison to bone ECM and contribution to dynamics of dentinogenesis. *Connect Tissue Res*. 2003;44(Suppl 1):171-8.
 43. Linde A, Goldberg M. Dentinogenesis. *Crit Rev Oral Biol Med*. 1993;4:679-728.
 44. Qin C, Baba O, Butler WT. Post-translational modifications of sibling proteins and their roles in osteogenesis and dentinogenesis. *Crit Rev Oral Biol Med*. 2004;15(3):126-36.
 45. Butler W. Dentin matrix proteins and dentinogenesis. *Connect Tissue Res*. 1995;33(1-3):59-65.
 46. Murayama T, Iwatsubo R, Akiyama S, Amano A, Morisaki I. Familial hypophosphatemic vitamin D-resistant rickets: dental findings and histologic study of teeth. *Oral Surg Oral Med Oral Pathol Oral Radiol Endod*. 2000;90(3):310-6.
 47. Souza AP, Kobayashi TY, Lourenço NN, Silva SM, Machado MA, Oliveira TM. Dental manifestations of patient with vitamin D-resistant rickets. *J Appl Oral Sci*. 2013;21(6):601-6.
 48. Cooper PR, Holder MJ, Smith AJ. Inflammation and regeneration in the dentin-pulp complex: a double-edged sword. *J Endod*. 2014;40(4 Suppl):S46-S51.
 49. Seltzer S. Reparative dentinogenesis. *Oral Surg Oral Med Oral Pathol*. 1959;12(5):595-602.
 50. Devlin H, Ferguson MW. Alveolar ridge resorption and mandibular atrophy. A review of the role of local and systemic factors. *Br Dent J*. 1991;170(3):101-4.

51. Tummers M, Yamashiro T, Thesleff I. Modulation of epithelial cell fate of the root in vitro. *J Dent Res*. 2007;86(11):1063-7.
52. Zeichner-David M, Oishi K, Su Z, Zakartchenko V, Chen LS, Arzate H, Bringas P Jr. Role of Hertwig's epithelial root sheath cells in tooth root development. *Dev Dyn*. 2003;228(4):651-63.
53. Huang X, Xu X, Bringas P Jr, Hung YP, Chai Y. Smad4-Shh-Nfic signaling cascade-mediated epithelial-mesenchymal interaction is crucial in regulating tooth root development. *J Bone Miner Res*. 2010;25(5):1167-78.
54. Liu Y, Feng J, Li J, Zhao H, Ho TV, Chai Y. An Nfic-hedgehog signaling cascade regulates tooth root development. *Development*. 2015. Epub [2015 Aug 20].
55. Newman MG. Carranza's Clinical Periodontology. Saunders Book Company; 2006.
56. Ikezawa K, Hart CE, Williams DC, Narayanan AS. Characterization of cementum derived growth factor as an insulin-like growth factor-I like molecule. *Connect Tissue Res* 1997;36(4):309-19.
57. Han P, Ivanovski S, Crawford R, Xiao Y. Activation of the Canonical Wnt Signaling Pathway Induces Cementum Regeneration. *J Bone Miner Res*. 2015;30(7):1160-74.
58. Murakami S, Takayama S, Ikezawa K, Shimabukuro Y, Kitamura M, Nozaki T, Terashima A, Asano T, Okada H. Regeneration of periodontal tissues by basic fibroblast growth factor. *J Periodontal Res* 1999;34(7):425-30.
59. Fisher L, Fedarko N. Six genes expressed in bones and teeth encode the current members of the SIBLING family of proteins. *Connect Tissue Res*. 2003;44 Suppl 1:33-40.
60. MacDougall M, Simmons D, Gu TT, Dong J. MEPE/OF45, a New Dentin/Bone Matrix Protein and Candidate Gene for Dentin Diseases Mapping to Chromosome 4q21. *Connect Tissue Res*. 2002;43(2&3):320-30.
61. Kim J, Simmer J. Hereditary Dentin Defects. *J Dent Res*. 2007;86:392-99.
62. David V, Martin A, Hedge AM, Rowe PS. Matrix extracellular phosphoglycoprotein (MEPE) is a new bone renal hormone and vascularization modulator. *Endocrinology*. 2009;150(9):4012-23.
63. Petersen D, Tkalecivic G, Mansolf A, Rivera-Gonzalez R, Brown T. Identification of osteoblast/osteocyte factor 45 (OF45), a bone-specific cDNA encoding an RGD-containing protein that is highly expressed in osteoblasts and osteocytes. *J Biol Chem*. 2000;275: 36172–80.

64. Nampei A, Hashimoto J, Hayashida K, Tsuboi H, Shi K, Tsuji I, Miyashita H, Yamada T, Matsukawa N, Matsumoto M, Morimoto S, Ogihara T, Ochi T, Yoshikawa H. Matrix extracellular phosphoglycoprotein (MEPE) is highly expressed in osteocytes in human bone. *J Bone Miner Res.* 2004;22:176-84.
65. Siggelkow H, Schmidt E, Hennies B, Hüfner M. Evidence of downregulation of matrix extracellular phosphoglycoprotein during terminal differentiation in human osteoblasts. *Bone.* 2004;35:570-6.
66. Gowen L, Petersen D, Mansolf A, Qi H, Stock J, Tkalecivic G, Simmons H, Crawford D, Chidsey-Frink K, Ke H, McNeish J, Brown T. Targeted Disruption of the Osteoblast/Osteocyte Factor 45 Gene (OF45) Results in Increased Bone Formation and Bone Mass. *J Biol Chem.* 2003;278(3):1998-2007.
67. Wang H, Kawashima N, Iwata T, Xu J, Takahashi S, Sugiyama T, Suda H. Differentiation of odontoblasts is negatively regulated by MEPE via its C-terminal fragment. *Biochem Biophys Res Commun.* 2010;398(3):406-12.
68. Cho YD, Yoon WJ, Woo KM, Baek JH, Lee G, Cho JY, Ryoo HM. Molecular Regulation of Matrix Extracellular Phosphoglycoprotein Expression by Bone Morphogenetic Protein-2. *J Biol Chem.* 2009;284(37):25230-40.
69. Liu H, Li W, Gao C, Kumagai Y, Blacher R, DenBesten P. Dentonin, a Fragment of MEPE, Enhanced Dental Pulp Stem Cell Proliferation. *J Dent Res.* 2004;83:496-9.
70. Minamizaki T, Yoshiko Y. The bioactive acidic serine- and aspartate-rich motif peptide. *Curr Protein Pept Sci.* 2015;16(3):196-202.
71. Liu S, Rowe PS, Vierthaler L, Zhou J, Quarles LD. Phosphorylated acidic serine-aspartate-rich MEPE-associated motif peptide from matrix extracellular phosphoglycoprotein inhibits phosphate regulating gene with homologies to endopeptidases on the X-chromosome enzyme activity. *J Endocrinol.* 2007;192(1):261-7.
72. Rowe PS. Regulation of bone-renal mineral and energy metabolism: the PHEX, FGF23, DMP1, MEPE ASARM pathway. *Crit Rev Eukaryot Gene Expr.* 2012;22(1):61-86.
73. Unterbrink A, O'Sullivan M, Chen S, MacDougall M. TGF- β 1 downregulates DMP-1 and DSPP in odontoblasts. *Connect Tissue Res.* 2002;43(2&3):254-8.
74. Cohen MM. The new bone biology: Pathologic, molecular, and clinical correlates. *Am J Med Genet Part A.* 2006;140A(23):2646-706.

75. Vaahtokari A, Vainio S, Thesleff I. Associations between transforming growth factor β 1 RNA expression and epithelial-mesenchymal interactions during tooth morphogenesis. *Development*. 1991;113:985-94.
76. Kulkarni A, Huh C, Becker D, Geiser A, Lyght M, Flanders K, Roberts A, Sporn M, Ward J, Karlsson S. Transforming growth factor- β 1 null mutation in mice causes excessive inflammatory response and early death. *Proc Natl Acad Sci USA*. 1993;90:770-4.
77. Kulkarni A, Ward J, Yaswen L, Mackall C, Bauer S, Huh C, Gress R, Karlsson S. Pathology of TGF- β 1 null mice. *Am J Pathol*. 1995;146:264-75.
78. Letterio J, Geiser A, Kulkarni A, Roche N, Sporn M, Roberts A. Maternal rescue of transforming growth factor- β 1 null mice. *Science*. 1994;264:1936-8.
79. D'Souza R, Litz M. Analysis of tooth development in mice bearing a TGF-beta 1 null mutation. *Connect Tissue Res*. 1995;32:41-6.
80. Sloan AJ, Couble ML, Bleicher F, Magloire H, Smith AJ, Farges JC. Expression of TGF-beta receptors I and II in the human dental pulp by in situ hybridization. *Adv Dent Res*. 2001;15:63-7.
81. Pacheco M, Reisa A, Aguiar D, Lyons K, Abreu J. Dynamic Analysis of the Expression of the TGF β /SMAD2 Pathway and CCN2/CTGF during Early Steps of Tooth Development. *Cells Tissues Organs*. 2008;187(3):199-210.
82. He WX, Niu ZY, Zhao SL, Jin WL, Gao J, Smith AJ. TGF-beta activated Smad signalling leads to a Smad3-mediated down-regulation of DSPP in an odontoblast cell line. *Arch Oral Biol*. 2004;49(11):911-8.
83. Wallace SE, Wilcox WR. Camurati-Engelmann Disease. *GeneReviews*. Seattle, WA: University of Washington, Seattle; 1993-2014.
84. Cockayne EA. Case for diagnosis. *Proc R Soc Med*. 1920;13(Sect Study Dis Child):132-6.
85. Campos-Xavier B, Saraiava JM, Savarirayan R, Verloes A, Feingold J, Faivre L, Munnich A, Le Merrer M, Cormier-Daire V. Phenotypic variability at the TGF-beta1 locus in Camurati-Engelmann disease. *Hum Genet*. 2001;109(6):653-8.
86. Kinoshita A, Saito T, Tomita H, Makita Y, Yoshida K, Ghadami M, Yamada K, Kondo S, Ikegawa S, Nishimura G, Fukushima Y, Nakagomi T, Saito H, Sugimoto T, Kamegaya M, Hisa K, Murray JC, Taniguchi N, Niikawa N, Yoshiura K. Domain-specific mutations in TGFB1 result in Camurati-Engelmann disease. *Nat Genet*. 2000;26(1):19-20.

87. Kinoshita A, Fukumaki Y, Shirahama S, Miyahara A, Nishimura G, Haga N, Namba A, Ueda H, Hayashi H, Ikegawa S, Seidel J, Niikawa N, Yoshiura K. TGFB1 mutations in four new families with Camurati-Engelmann disease: confirmation of independently arising LAP-domain-specific mutations. *Am J Med Genet A*. 2004;127A(1):104-7.
88. Bartuseviciene A, Samuilis A, Skucas J. Camurati-Engelmann disease: imaging, clinical features and differential diagnosis. *Skeletal Radiol*. 2009;38(11):1037-43.
89. Carlson ML, Beatty CW, Neff BA, Link MJ, Driscoll CL. Skull base manifestations of Camurati-Engelmann disease. *Arch Otolaryngol Head Neck Surg* 2010;136(6):566-75.
90. Vanhoenacker FM, Janssens K, Van Hul W, Gershoni-Baruch R, Brik R, De Schepper AM. Camurati-Engelmann disease. Review of radioclinical features. *Acta Radiol*. 2003;44(4):430-4.
91. Wang C, Zhang BH, Liu YJ, Hu YQ, He JW, Zhang ZL. Transforming growth factor- β 1 gene mutations and phenotypes in pediatric patients with Camurati-Engelmann disease. *Mol Med Rep*. 2013;7(5):1695-9.
92. McGowan NW, MacPherson H, Janssens K, Van Hul W, Frith JC, Fraser WD, Ralston SH, Helfrich MH. A mutation affecting the latency-associated peptide of TGF β 1 in Camurati-Engelmann disease enhances osteoclast formation in vitro. *J Clin Endocrinol Metab*. 2003;88(7):3321-6.
93. Toumba M, Neocleous V, Shammas C, Anastasiadou V, Allgrove J, Phylactou LA, Skordis N. A family with Camurati-Engelman disease: the role of the missense p.R218C mutation in TGF β 1 in bones and endocrine glands. *J Pediatr Endocrinol Metab* 2013;26(11-12):1189-95.
94. Tang Y, Wu X, Lei W, Pang L, Wan C, Shi Z, Zhao L, Nagy T, Peng X, Hu J, Feng X, Van Hul W, Wan M, Cao X. TGF- β 1-induced migration of bone mesenchymal stem cells couples bone resorption with formation. *Nat Med*. 2009;15(7):757-65.
95. Andujar MB, Couble P, Couble ML, Magloire H. Differential expression of type I and type III collagen genes during tooth development. *Development*. 1991;111(3):691-8.
96. Janssens K, Vanhoenacker F, Bonduelle M, Verbruggen L, Van Maldergem L, Ralston S, Guañabens N, Migone N, Wientroub S, Divizia MT, Bergmann C, Bennett C, Simsek S, Melançon S, Cundy T, Van Hul W. Camurati-Engelmann disease: review of the clinical, radiological, and molecular data of 24 families and implications for diagnosis and treatment. *Med Genet* 2006;43(1):1-11.

97. Ayyavoo A, Cundy T, Derraik J, Hofman PL. Losartan improves clinical outcome in Camurati Engelmann Disease. *Int J Pediatr Endocrinol.* 2013;2013(Suppl 1):O42.
98. Gaucher C, Walrant-Debray O, Nguyen TM, Esterle L, Garabedian M, Jehan F. PHEX analysis in 118 pedigrees reveals new genetic clues in hypophosphatemic rickets. *Hum Genet* 2009;125:401–11.
99. Boukpassi T, Septier D, Bagga S, Garabedian M, Goldberg M, Chaussain-Miller C. Dentin alteration of deciduous teeth in human hypophosphatemic rickets. *Calcif Tissue Int* 2006;79:294–300.
100. Boukpassi T, Gaucher C, Léger T, Salmon B, Le Faouder J, Willig C, Rowe PS, Garabédian M, Meilhac O, Chaussain C. Abnormal presence of the matrix extracellular phosphoglycoprotein-derived acidic serine- and aspartate-rich motif peptide in human hypophosphatemic dentin. *Am J Pathol.* 2010;177(2):803-12.
101. Salmon B, Bardet C, Coyac BR, Baroukh B, Naji J, Rowe PS, Opsahl Vital S, Linglart A, Mckee MD, Chaussain C. Abnormal osteopontin and matrix extracellular phosphoglycoprotein localization, and odontoblast differentiation, in X-linked hypophosphatemic teeth. *Connect Tissue Res.* 2014;55(Suppl 1):79-82.
102. Neville B, Damm D, Allen C, Bouquout J. *Oral and Maxillofacial Pathology.* 3 ed. St. Louis, MO: Elsevier; 2008.
103. Maciejewska I, Chomik E. Hereditary dentine diseases resulting from mutations in DSPP gene. *J Dent.* 2012;40(7):542-8.
104. McKnight DA, Simmer JP, Hart PS, Hart TC, Fisher LW. Overlapping DSPP mutations cause dentin dysplasia and dentinogenesis imperfecta. *J Dent Res.* 2008;87(12):1108-11.
105. de La Dure-Molla M, Philippe Fournier B, Berdal A. Isolated dentinogenesis imperfecta and dentin dysplasia: revision of the classification. *Eur J Hum Genet* 2015;23(4):445-51.
106. Min B, Song JS, Lee JH, Choi BJ, Kim KM, Kim SO. Multiple teeth fractures in dentinogenesis imperfecta: a case report. *J Clin Pediatr Dent.* 2014;38(4):362-5.
107. Barron MJ, McDonnell ST, Mackie I, Dixon MJ. Hereditary dentine disorders: dentinogenesis imperfecta and dentine dysplasia. *Orphanet J Rare Dis.* 2008;3(31):10.
108. Sekerci AE, Etoz M, Sahman H, Sisman Y, Nazlim S. A rare condition affecting the primary and permanent dentition: Dentin dysplasia type I. *Journal of Oral and Maxillofacial Radiology.* 2013;1(1):13-6.

109. Shankly PE, Mackie IC, Sloan P. Dentinal dysplasia type I: report of a case. *Int J Paediatr Dent*. 1999;9(1):37-42.
110. Witkop CJ. Hereditary defects in enamel and dentin. *Acta Genet Stat Med*. 1957;7(1):236-9.
111. Singh A, Gupta S, Yuwanati MB, Mhaske S. Dentin dysplasia type I. *BMJ Case Rep*. 2013; June 1757-790.
112. Cherkaoui Jaouad I, El Alloussi M, Laarabi FZ, Bouhouche A, Ameziane R, Sefiani A. Inhabitual autosomal recessive form of dentin dysplasia type I in a large consanguineous Moroccan family. *Eur J Med Genet*. 2013;56(8):442-4.
113. Bespalez-Filho R, Couto Sde A, Souza PH, Westphalen FH, Jacobs R, Willems G, Tanaka OM. Orthodontic treatment of a patient with dentin dysplasia type I. *Am J Orthod Dentofacial Orthop*. 2013;143(3):421-5.
114. Rocha CT, Nelson-Filho P, Silva LA, Assed S, Queiroz AM. Variation of dentin dysplasia type I: report of atypical findings in the permanent dentition. *Braz Dent J*. 2011;22(1):74-8.
115. Nirmala SV, Sivakumar N, Usha K. Dentin dysplasia type I with pyogenic granuloma in a 12-year-old girl. *J Indian Soc Pedod Prev Dent*. 2009;27(2):131-4.
116. Naik VV, Kale AD. Dentin dysplasia: single-tooth involvement? *Quintessence Int*. 2009;40(3):183-6.
117. Da Rós Gonçalves L, Oliveira CA, Holanda R, Silva-Boghossian CM, Colombo AP, Maia LC, Feres-Filho EJ. Periodontal status of patients with dentin dysplasia type I: report of three cases within a family. *J Periodontol*. 2008;79(7):1304-11.
118. Muñoz-Guerra MF, Naval-Gías L, Escorial V, Sastre-Pérez J. Dentin dysplasia type I treated with onlay bone grafting, sinus augmentation, and osseointegrated implants. *Implant Dent*. 2006;15(3):248-53.
119. Ravanshad S, Khayat A. Endodontic therapy on a dentition exhibiting multiple periapical radiolucencies associated with dentinal dysplasia Type 1. *Aust Endod J* 2006;32(1):40-2.
120. Ozer L, Karasu H, Aras K, Tokman B, Ersoy E. Dentin dysplasia type I: report of atypical cases in the permanent and mixed dentitions. *Oral Surg Oral Med Oral Pathol Oral Radiol Endod*. 2004;98(1):85-90.
121. Comer TL, Gound TG. Hereditary pattern for dentinal dysplasia type Id: a case report. *Oral Surg Oral Med Oral Pathol Oral Radiol Endod*. 2002;94(1):51-3.

122. Kosinski RW, Chaiyawat Y, Rosenberg L. Localized deficient root development associated with taurodontism: case report. *Pediatr Dent*. 1999;21(3):213-5.
123. Neumann F, Würfel F, Mundt T. Dentin dysplasia type I--a case report. *Ann Anat*. 1999;181(1):138-40.
124. Leccisotti S, Eramo S, Palattella P, Dolci G. Dentin dysplasia type I. Report of case and ultrastructural study. *Minerva Stomatol*. 1998;47(10):545-51.
125. Kalk WW, Batenburg RH, Vissink A. Dentin dysplasia type I: five cases within one family. *Oral Surg Oral Med Oral Pathol Oral Radiol Endod*. 1998;86(2):175-8.
126. Vieira AR, Modesto A, Cabral MG. Dentinal dysplasia type I: report of an atypical case in the primary dentition. *ASDC J Dent Child*. 1998;65(2):141-4.
127. Ansari G, Reid JS. Dentinal dysplasia type I: review of the literature and report of a family. *ASDC J Dent Child*. 1997;64(6):429-34.
128. Seow WK, Shusterman S. Spectrum of dentin dysplasia in a family: case report and literature review. *Pediatr Dent*. 1994;16(6):437-42.
129. O'Carroll MK, Duncan WK. Dentin dysplasia type I. Radiologic and genetic perspectives in a six-generation family. *Oral Surg Oral Med Oral Pathol*. 1994;78(3):375-81.
130. Duncan WK, Perkins TM, O Carroll MK, Hill WJ. Type I dentin dysplasia: report of two cases. *Ann Dent*. 1991;50(2):18-21.
131. Brenneise CV, Dwornik RM, Brenneise EE. Clinical, radiographic, and histological manifestations of dentin dysplasia, type I: Report of case. *J Am Dent Assoc*. 1989;119(6):721-3.
132. Van Dis ML, Allen CM. Dentinal dysplasia type I: a report of four cases. *Dentomaxillofac Radiol*. 1989;18(3):128-31.
133. Resta G, Caprioglio D, Brusotti C, Piacentini C. Histological and ultrastructural observations of dentin dysplasia type I. *G Stomatol Ortognatodonzia*. 1989;8(3):46-51.
134. Tongnoi D, Triratana T, Arunakul S. Dentinal dysplasia type I. *J Dent Assoc Thai*. 1988;38(5):202-8.
135. Steidler NE, Radden BG, Reade PC. Dentinal dysplasia: a clinicopathological study of eight cases and review of the literature. *Br J Oral Maxillofac Surg*. 1984;22(4):274-86.

136. Petrone JA, Noble ER. Dentin dysplasia type I: a clinical report. *J Am Dent Assoc.* 1981;103(6):891-3.
137. Melnick M, Levin LS, Brady J. Dentin dysplasia type I: a scanning electron microscopic analysis of the primary dentition. *Oral Surg Oral Med Oral Pathol.* 1980;50(4):335-40.
138. Coke JM, Del Rosso G, Remeikis N, Van Cura JE. Dentinal dysplasia, Type I. Report of a case with endodontic therapy. *Oral Surg Oral Med Oral Pathol.* 1979;48(3):262-8.
139. Ciola B, Bahn SL, Goviea GL. Radiographic manifestations of an unusual combination Types I and Type II dentin dysplasia. *Oral Surg Oral Med Oral Pathol.* 1978;45(2):317-22.
140. Perl T, Farman AG. Radicular (type 1) dentin dysplasia. *Oral Surg Oral Med Oral Pathol.* 1977;43(5):746-53.
141. Morris ME, Augsburger RH. Dentine dysplasia with sclerotic bone and skeletal anomalies inherited as an autosomal dominant trait. A new syndrome. *Oral Surg Oral Med Oral Pathol* 1977;43(2):267-83.
142. Wesley RK, Wysoki GP, Mintz SM, Jackson J. Dentin dysplasia type I. Clinical, morphologic, and genetic studies of a case. *Oral Surg Oral Med Oral Pathol.* 1976;41(4):516-24.
143. Kantaputra PN. A newly recognized syndrome of skeletal dysplasia with opalescent and rootless teeth. *Oral Surg Oral Med Oral Pathol Oral Radiol Endod.* 2001;92(3):303-7.
144. MacDougall M, Dong J, Herrera M, Galindo M, Gu T, Mestrinho HD, Paula LM, Acevedo AC. NFI-C Mutation Associated with Autosomal Recessive Radicular Dentin Dysplasia. *J Dent Res.* 2006;85(B).
145. Vannahme C, Gösling S, Paulsson M, Maurer P, Hartmann U. Characterization of SMOC-2, a modular extracellular calcium-binding protein. *Biochem J* 2003;373 (Pt 3):805-14.
146. Melvin VS, Feng W, Hernandez-Lagunas L, Artinger KB, Williams T. A morpholino-based screen to identify novel genes involved in craniofacial morphogenesis. *Dev Dyn* 2013;242(7):817-31.
147. Alfawaz S, Fong F, Plagnol V, Wong FS, Fearne J, Kelsell DP. Recessive oligodontia linked to a homozygous loss-of-function mutation in the SMOC2 gene. *Arch Oral Biol.* 2013;58(5):462-6.

148. Bloch-Zupan A, Jamet X, Etard C, Laugel V, Muller J, Geoffroy V, Strauss JP, Pelletier V, Marion V, Poch O, Strahle U, Stoetzel C, Dollfus H. Homozygosity mapping and candidate prioritization identify mutations, missed by whole-exome sequencing, in SMOC2, causing major dental developmental defects. *Am J Hum Genet.* 2011;89(6):773-81.
149. Guideline on Dental Management of Heritable Dental Developmental Anomalies [Internet]. AAPD. 2013 [cited 2014].
150. Khandelwal S, Gupta D, Likhyani L. A Case of Dentin Dysplasia with Full Mouth Rehabilitation: A 3-year Longitudinal Study. *Int J Clin Pediatr Dent.* 2014;7(2): 119-24.

APPENDIX


INSTITUTIONAL ANIMAL CARE AND USE COMMITTEE APPROVAL FORMS



THE UNIVERSITY OF ALABAMA AT BIRMINGHAM
Institutional Animal Care and Use Committee (IACUC)

MEMORANDUM

DATE: 13-Oct-2015
TO: MacDougall, Mary J.

FROM: 
Robert A. Kesterson, Ph.D., Chair
Institutional Animal Care and Use Committee (IACUC)

SUBJECT: NOTICE OF APPROVAL

The following application was approved by the University of Alabama at Birmingham Institutional Animal Care and Use Committee (IACUC) on 13-Oct-2015.

Protocol PI: MacDougall, Mary J.

Title: Functional Role of MEPE in Tooth Mineralization: Mediation by TGFbeta-1

Sponsor: UAB DEPARTMENT

Animal Project Number (APN): IACUC-09954

This Institution has an Animal Welfare Assurance on file with the Office of Laboratory Animal Welfare (OLAW), is registered as a Research Facility with the USDA, and is accredited by the Association for Assessment and Accreditation of Laboratory Animal Care International (AAALAC).

Institutional Animal Care and Use Committee (IACUC)		Mailing Address:
CH19 Suite 403		CH19 Suite 403
933 19th Street South		1530 3rd Ave S
(205) 934-7862		Birmingham, AL 35294-0019
FAX (205) 934-1188		



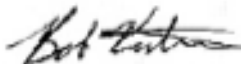
THE UNIVERSITY OF ALABAMA AT BIRMINGHAM

Institutional Animal Care and Use Committee (IACUC)

Notice of Approval for Protocol Modification

DATE: August 4, 2014

TO: MARY J. MACDOUGALL, M.D.
SDB-702A
(205) 996-5122

FROM: 
Robert A. Kesterson, Ph.D., Chair
Institutional Animal Care and Use Committee (IACUC)

SUBJECT: Title: Functional Role of MEPE in Tooth Mineralization: Mediation by TGFbeta-1
Sponsor: Internal
Animal Project_Number: 131009954

On August 4, 2014, the University of Alabama at Birmingham Institutional Animal Care and Use Committee (IACUC) reviewed the animal use proposed in the above referenced application. It approved the modification as described: Personnel- Changming Lu, Agents- P. gingivais, antibiotics, Numbers - 424A. The sponsor for this project may require notification of modification(s) approved by the IACUC but not included in the original grant proposal/experimental plan; please inform the sponsor if necessary.

The following species and numbers of animals reflect this modification.

Species	Use Category	Number In Category
Mice	A	Zero - Procedural modification only

The IACUC is required to conduct continuing review of approved studies. This study is scheduled for annual review on or before October 13, 2014. Approval from the IACUC must be obtained before implementing any changes or modifications in the approved animal use.

Please keep this record for your files.

Refer to Animal Protocol Number (APN) 131009954 when ordering animals or in any correspondence with the IACUC or Animal Resources Program (ARP) offices regarding this study. If you have concerns or questions regarding this notice, please call the IACUC office at (205) 934-7692.

Institutional Animal Care and Use Committee (IACUC)	Mailing Address:
CH19 Suite 403	CH19 Suite 403
933 19th Street South	1530 3rd Ave S
(205) 934-7692	Birmingham AL 35294-0019
FAX (205) 934-1188	



THE UNIVERSITY OF ALABAMA AT BIRMINGHAM

Institutional Animal Care and Use Committee (IACUC)

Notice of Approval for Protocol Modification

DATE: May 15, 2014

TO: MARY J. MACDOUGALL, M.D.
SDB -702A
(205) 996-5122

FROM:

Robert A. Kesterson, Ph.D., Chair
Institutional Animal Care and Use Committee (IACUC)

SUBJECT: Title: Functional Role of MEPE in Tooth Mineralization: Mediation by TGFbeta-1
Sponsor: Internal
Animal Project_Number: 131009954

On May 15, 2014, the University of Alabama at Birmingham Institutional Animal Care and Use Committee (IACUC) reviewed the animal use proposed in the above referenced application. It approved the modification as described: Personnel: Philip Sohn, Samuel Huguley. The sponsor for this project may require notification of modification(s) approved by the IACUC but not included in the original grant proposal/experimental plan; please inform the sponsor if necessary.

The following species and numbers of animals reflect this modification.

Species	Use Category	Number In Category
Mice	A	Zero - Procedural modification only

The IACUC is required to conduct continuing review of approved studies. This study is scheduled for annual review on or before October 13, 2014. Approval from the IACUC must be obtained before implementing any changes or modifications in the approved animal use.

Please keep this record for your files.

Refer to Animal Protocol Number (APN) 131009954 when ordering animals or in any correspondence with the IACUC or Animal Resources Program (ARP) offices regarding this study. If you have concerns or questions regarding this notice, please call the IACUC office at (205) 934-7692.

Institutional Animal Care and Use Committee (IACUC)
CH19 Suite 403
933 19th Street South
(205) 934-7692
FAX (205) 934-1188

Mailing Address:
CH19 Suite 403
1530 3rd Ave S
Birmingham AL 35294-0019



THE UNIVERSITY OF ALABAMA AT BIRMINGHAM

Institutional Animal Care and Use Committee (IACUC)

NOTICE OF APPROVAL

DATE: October 14, 2013

TO: MARY J. MACDOUGALL, M.D.
SDB -702A
(205) 996-5122

FROM:

Robert A. Kesterson, Ph.D., Chair
Institutional Animal Care and Use Committee (IACUC)

SUBJECT: Title: Functional Role of MEPE in Tooth Mineralization: Mediation by TGFbeta-1
Sponsor: Internal
Animal Project_Number: 131009954

As of October 14, 2013 the animal use proposed in the above referenced application is approved. The University of Alabama at Birmingham Institutional Animal Care and Use Committee (IACUC) approves the use of the following species and number of animals:

Species	Use Category	Number In Category
Mice	A	162

Animal use must be renewed by October 13, 2014. Approval from the IACUC must be obtained before implementing any changes or modifications in the approved animal use.

Please keep this record for your files, and forward the attached letter to the appropriate granting agency.

Refer to Animal Protocol Number (APN) 131009954 when ordering animals or in any correspondence with the IACUC or Animal Resources Program (ARP) offices regarding this study. If you have concerns or questions regarding this notice, please call the IACUC office at (205) 934-7692.

Institutional Animal Care and Use Committee (IACUC)
CH19 Suite 403
933 19th Street South
(205) 934-7692
FAX (205) 934-1188

Mailing Address:
CH19 Suite 403
1530 3rd Ave S
Birmingham, AL 35294-0019



THE UNIVERSITY OF ALABAMA AT BIRMINGHAM

Institutional Animal Care and Use Committee (IACUC)

NOTICE OF APPROVAL

DATE: December 1, 2009

TO: MacDougall, Mary
SDB-702 0007
906-5122

FROM: 
Judith A. Kapp, Ph.D., Chair
Institutional Animal Care and Use Committee

SUBJECT: Title: Functional Role of MEPE in Tooth Mineralization: Mediation by TGFbeta-1
(Angela Gullard)
Sponsor: Internal
Animal Project Number: 091108923

On December 1, 2009, the University of Alabama at Birmingham Institutional Animal Care and Use Committee (IACUC) reviewed the animal use proposed in the above referenced application. It approved the use of the following species and numbers of animals:

Species	Use Category	Number in Category
Mice	A	100

Animal use is scheduled for review one year from November 2009. Approval from the IACUC must be obtained before implementing any changes or modifications in the approved animal use.

Please keep this record for your files, and forward the attached letter to the appropriate granting agency.

Refer to Animal Protocol Number (APN) 091108923 when ordering animals or in any correspondence with the IACUC or Animal Resources Program (ARP) offices regarding this study. If you have concerns or questions regarding this notice, please call the IACUC office at 934-7692.

Institutional Animal Care and Use Committee
B10 Volker Hall
1670 University Boulevard
205.934.7692
FAX 205.934.1188

Mailing Address:
VH B10
1530 3RD AVE S
BIRMINGHAM AL 35294-0019



THE UNIVERSITY OF ALABAMA AT BIRMINGHAM

Institutional Animal Care and Use Committee (IACUC)

MEMORANDUM

DATE: December 1, 2009

TO: MacDougall, Mary
SDB-702 0007
996-5122

FROM: 
Judith A. Kapp, Ph.D., Chair
Institutional Animal Care and Use Committee

SUBJECT: NOTICE OF APPROVAL - Please forward this notice to the appropriate granting agency.

The following application was reviewed and approved by the University of Alabama at Birmingham Institutional Animal Care and Use Committee (IACUC) on December 1, 2009.

Title: Functional Role of MEPE in Tooth Mineralization: Mediation by TGFbeta-1 (Angela Gullard)

Sponsor: Internal

This institution has an Animal Welfare Assurance on file with the Office for Protection from Research Risks (Assurance Number A3255-01) and is registered as a Research Facility with the United States Department of Agriculture. The animal care and use program is accredited by the Association for Assessment and Accreditation of Laboratory Animal Care (AAALAC International).

Institutional Animal Care and Use Committee
B10 Volker Hall
1670 University Boulevard
205.934.7692
FAX 205.934.1188

Mailing Address:
VH B10
1530 3RD AVE S
BIRMINGHAM AL 35294-0019